4th CIE Expert Symposium on Colour and Visual Appearance

September 6 - 7, 2016, Prague, Czech Republic

Hotel Don Giovanni

Vinohradská 157a, 13020 Prague, Czech Republic

Metrue

Equipment • Calibration • Test

Total measurement solutions for Light and Color

Metrue, located in the heart of Silicon Valley, supplies high accuracy optoelectronic measurement instruments and customization solutions for industry and laboratories. Metrue Test and Calibration Center, the world model laboratory equipped her own instrument products, has been accredited by NVLAP (Lab Code: 600100-0). Metrue has the capability to supply basic optical and electrical quantities calibration traceable to NIST and also test services (inter lab comparison) for Energy Efficient Lighting Products (EELP).

Calibration traceable to NIST


United States Department of Commerce
National Institute of Standards and Technology
NVLAP
Certificate of Accreditation to ISO/IEC 17025:2005
NVLAP LAB CODE: 600100-0
Metrue Test and Calibration Center
Fremont, CA
Calibration Laboratories

Test laboratory for EELP


United States Department of Commerce
National Institute of Standards and Technology
NVLAP
Certificate of Accreditation to ISO/IEC 17025:2005
NVLAP LAB CODE: 600100-0
Metrue Test and Calibration Center
Fremont, CA
Energy Efficient Lighting Products

More info
www.metrue.com

Metrue, Inc.
3068 Laurelview Court, Fremont, CA 94538
Email: sales@metrue.com Tel: +1-510-770-6900 Cell:+1-510-697-6475

Contents

PROGRAMME

4th CIE Expert Symposium on Colour and Visual Appearance 2016

September 5 - 7, 2016

Hotel Don Giovanni

Vinohradská 157a, 13020 Prague, Czech Republic

Monday, September 5

19:00	**Welcome Reception - Hotel Don Giovanni Bar**	19:00

Tuesday, September 6
Morning

08:00	**REGISTRATION**	08:00
08:45	**OPENING**	08:45
09:10 - 10:30	PA1 Visual Perception - Part 1 (Chair: TBD)	09:10 - 10:30
09:10 - 09:25	OP01 Malgorzata Perz, NL PERCEPTION OF ILLUMINATION WHITENESS	09:10 - 09:25
09:25 - 09:40	OP02 Stijn Hermans, BE BRIGHTNESS PERCEPTION OF RELATED SELF-LUMINOUS STIMULI	09:25 - 09:40
09:40 - 09:55	OP03 Kevin Smet, BE INVESTIGATING CHROMATIC ADAPTATION USING MEMORY COLOURS	09:40 - 09:55
09:55 - 10:10	OP04 Guillaume Ged, FR INTERCOMPARISON OF VISUAL GLOSS PSYCHOMETRIC SCALES	09:55 - 10:10
10:10 - 10:30	**Discussion**	10:10 - 10:30
10:30	**COFFEE BREAK**	10:30
11:00 - 12:20	PA2 BRDF Fundamental Metrology (Chair: TBD)	11:00 - 12:20
11:00 - 11:15	OP05 Pritt Jaanson, FI A REFERENCE MATERIAL WITH CLOSE TO LAMBERTIAN REFLECTANCE AND FLUORESCENCE EMISSION PROFILES	11:00 - 11:15
11:15 - 11:30	OP06 Tatjana Quast, DE POLARIZATION EFFECTS IN DIFFUSE REFLECTANCE MEASUREMENTS - COMPARISON OF WHITE STANDARDS AND SPECIAL-EFFECT PIGMENT SAMPLES	11:15 - 11:30
11:30 - 11:45	OP07 Erkki Ikonen, FI UNCERTAINTY EVALUATION OF FLUORESCENCE QUANTITIES OBTAINED FROM GONIOMETRIC MEASUREMENTS	11:30 - 11:45
11:45 - 12:00	OP08 Noël Richard, FR TOWARD A METROLOGY FOR NON-UNIFORM SURFACE USING THE COMPLEXITY NOTION	11:45 - 12:00
12:00 - 12:20	**Discussion**	12:00 - 12:20
12:20	**LUNCH**	12:20

Tuesday, September 6
Afternoon

13:20 - 13:40	PS1 Presented Posters: Measurement (Chair: TBD)	13:20 - 13:40
13:20 - 13:25	PP01 / PO01 Annette Koo, NZ OPTICAL DETECTION SYSTEM FOR MONOCHRAMATIC BEAM GONIOSPECTROPHOTOMETRY	13:20 - 13:25
13:25 - 13:30	PP02 / PO02 Pierre Boher, FR SPECTRAL BRDF & BTDF MEASUREMENTS USING HIGH RESOLUTION FOURIER OPTICS INTRUMENT	13:25 - 13:30
13:30 - 13:35	PP03 / PO03 Hiroshi Shitomi, JP BRDF MEASUREMENT BASED ON SPECTRAL DIFFUSE REFLECTANCE AND A GONIOREFLECTOMETER	13:30 - 13:35
13:35 - 13:40	PP04 / PO04 Tsung-Hsun Yang, TW EFFICIENT MEASUREMENT OF ANGLE-RESOLVED LUMINANCE DISTRIBUTION WITH IMAGING SENSOR	13:35 - 13:40
13:45 - 15:15	Poster Session 1	13:45 - 15:15
15:15	**COFFEE BREAK**	15:15
15:45 - 17:05	PA3 Measurement of Goniochromatism (Chair: TBD)	15:45 - 17:05
15:45 - 16:00	OP09 Christian Strothkämper, DE TACKLING THE LIGHTNESS AND COLOUR FLOP IN EFFECT-PIGMENTED COATINGS	15:45 - 16:00
16:00 - 16:15	OP10 Alejandro Ferrero, ES MULTI-ANGLE COLOUR CHARACTERIZATION OF COATINGS WITH DIFFRACTION PIGMENTS	16:00 - 16:15
16:15 - 16:30	OP11 Nina Basic, CH MEASURING GONIOAPPARENT SAMPLES USING A BIDIRECTIONAL SPECTROMETER; AN SRGB VISUALIZATION	16:15 - 16:30
16:30 - 16:45	OP12 Paola Iacomussi, IT GONIOCHROMATIC MATERIALS UNDER DIFFERENT LIGHTING CONDITIONS	16:30 - 16:45
16:45 - 17:05	**Discussion**	16:45 - 17:05

18:30	**Symposium Dinner**	18:30

Wednesday, September 7
Morning

09:05 - 10:25	PA4 Visual Perception - Part 2 (Chair: TBD)	09:05 - 10:25
09:05 - 09:20	OP13 Dmitrij Polin, DE VISUAL EXPERIMENTS ON THE STROBOSCOPIC EFFECTS OF PWM-MODULATED WHITE LED INDOOR ILLUMINATIONS AND THEIR CONSEQUENCES	09:05 - 09:20
09:20 - 09:35	OP14 Ute Besenecker, US EXPLORING VISUAL AND VISCERAL QUALITIES OF EQUIVALENT COLOURS UNDER ARCHITECTURAL-SCALE, FULL-FIELD EXPOSURE CONDITIONS	09:20 - 09:35
09:35 - 09:50	OP15 Li-Chen Ou, TW COLOUR CONSPICUITY IN A COMPLEX LAYOUT	09:35 - 09:50
09:50 - 10:05	OP16 Yoshiki Nakamura, JP STUDY ON VISIBILITY ESTIMATON OF OBJECTS IN COMPLICATED LUMIANCE IMAGE	09:50 - 10:05
10:05 - 10:25	**Discussion**	10:05 - 10:25
10:25	**COFFEE BREAK**	10:25
10:55 - 12:15	PA5 Novel Approaches to Measuring Appearance (Chair: TBD)	10:55 - 12:15
10:55 - 11:10	OP17 Colette Turbil, FR BRDF MEASUREMENT AND SIMULATION OF PATTERNED SURFACES TO FORESEE ITS VISUAL RENDERING	10:55 - 11:10
11:10 - 11:25	OP18 Marine Page, FR 3D SURFACE ACQUISITION: COMPARISON OF TWO MICROTOPOGRAPHIC EQUIPMENTS WHEN MEASURING MATERIALS OF CULTURAL HERITAGE	11:10 - 11:25
11:25 - 11:40	OP19 Jiri Filip, CZ CAPTURING MATERIAL VISUALIZATION DATA USING GONIOMETERS	11:25 - 11:40
11:40 - 11:55	OP20 Ming Luo, CN AN LED TUNEABLE SOURCE FOR DISCERNING TEXTURE DETAILS	11:40 - 11:55
11:55 - 12:15	**Discussion**	11:55 - 12:15
12:15	**LUNCH**	12:15

Wednesday, September 7
Afternoon

13:15 - 13:40	PS2 Presented Posters: Perception and Models (Chair: TBD)	13:15 - 13:40
13:15 - 13:20	PP05 / PO28 Yuki Akizuki, JP STUDY ON SPECTRAL CHARACTERISTICS FOR IDENTIFICATION OF SKIN COLOUR OF INJURED JAPANESE PERSONS AT DISASTER SITES	13:15 - 13:20
13:20 - 13:25	PP06 / PO29 Jan Krüger, DE DIRECTIONAL LIGHT OF LED ARRAYS AND ITS INFLUENCE ON SHAPE PERCEPTION	13:20 - 13:25
13:25 - 13:30	PP07 / PO30 Peter Bodrogi, DE COLOUR SURFACE RENDERING: A NEW ASPECT OF LIGHT SOURCE COLOUR QUALITY FOR MUSEUM LIGHTING	13:25 - 13:30
13:30 - 13:35	PP08 / PO31 Yukiko Yoshida, JP COLOUR VISUAL EFFECTS OF STEADY STATE EXPERIMENTS IN DIFFERENT THERMAL ENVIRONMENTS AT AN OFFICE TEST SITE	13:30 - 13:35
13:35 - 13:40	PP09 / PO32 Johannes Mäder, DE COMPREHENSIVE SCATTER MEASUREMENT AND MODELING	13:35 - 13:40
13:45 - 15:15	Poster Session 2	13:45 - 15:15
15:15	**COFFEE BREAK**	15:15
15:45 - 17:05	PA6 Models and Digital Rendering (Chair: TBD)	15:45 - 17:05
15:45 - 16:00	OP21 Martijn Vyncke, BE ACCURATE SIMULATION OF LIGHT DIFFUSION EFFECTS OF STRUCTURED GLAZING BY IMPLEMENTATION OF BIDIRECTIONAL TRANSMITTANCE DISTRIBUTION FUNCTIONS INTO DAYLIGHT CALCULATION SOFTWARE	15:45 - 16:00
16:00 - 16:15	OP22 Shoji Tominaga, JP SPECTRAL IMAGE ANALYSIS AND APPEARANCE RECONSTRUCTION OF FLUORESCENT OBJECTS UNDER DIFFERENT ILLUMINATIONS	16:00 - 16:15
16:15 - 16:30	OP23 Michal Havlicek, CZ TEXTURE SPECTRAL SIMILARITY CRITERIA	16:15 - 16:30
16:30 - 16:45	OP24 Jiri Filip, CZ USING REFLECTORS FOR ANALYSIS AND ACQUISITION OF ANISOTROPIC BRDF	16:30 - 16:45
16:45 - 17:05	**Discussion**	16:45 - 17:05
17:10	**CLOSING**	17:10

Colour Key

DAY
ORAL PRESENTATION
ORAL PRESENTATION
BREAK
SESSION NO./TITLE
PRESENTED POSTER
POSTER
SOCIAL EVENT
OPENING/CLOSING CEREMONY

Poster Session 1

PO01	Annette Koo, NZ	OPTICAL DETECTION SYSTEM FOR MONOCHROMATIC BEAM GONIOSPECTROPHOTOMETRY
PO02	Pierre Boher, FR	SPECTRAL BRDF & BTDF MEASUREMENTS USING HIGH RESOLUTION FOURIER OPTICS INTRUMENT
PO03	Hiroshi Shitomi, JP	BRDF MEASUREMENT BASED ON SPECTRAL DIFFUSE REFLECTANCE AND A GONIOREFLECTOMETER
PO04	Tsung-Hsun Yang, TW	EFFICIENT MEASUREMENT OF ANGLE-RESOLVED LUMINANCE DISTRIBUTION WITH IMAGING SENSOR
PO05	Shino Okuda, JP	PREFERABLE LIGHTING CONDITION TO IMPROVE APPEARANCE OF WOMAN'S FACIAL SKIN WITH COSMETIC FOUNDATION
PO07	Raphael Kirsch, DE	INFLUENCE OF DIFFERENT ROOM SURFACE COLOURS ON THE MELANOPIC FACTOR
PO08	Kees Teunissen, NL	CHARACTERIZING COLOURFULNESS AND GAMUT AREA OF WHITE LIGHT SOURCES, IN ADDITION TO COLOUR FIDELITY
PO09	Leonie Geerdinck, NL	DISCOMFORT GLARE OF NON-UNIFORM LUMINAIRES - A LITERATURE REVIEW
PO10	Tushar Chauhan, FR	DISCRIMINATION THRESHOLDS FOR SKIN IMAGES
PO11	Michico Iwata, JP	STUDY OF VISIBILITY UNDER COMPLEX LUMINANCE CONDITIONS FOR THE VISUALLY CHALLENGED PEOPLE USING LUMINANCE-IMAGE FILTERING
PO12	Marcela Pechová, CZ	INFLUENCE OF LUMINANCE LEVELS OF ILLUMINATION D65 ON EVALUATION OF HIGH CHROMATIC COLOURS
PO13	Markéta Kašparová, CZ	VISUAL EVALUATION HIGH CHROMA SAMPLES UNDER THE TWO TYPES OF DAYLIGHT SIMULATORS
PO14	Manuel Melgosa, ES	USING A STANDARD GREY SCALE FOR COLOUR CHANGE IN A MULTI-ANGLE COLOUR-ASSESSMENT CABINET
PO15	Alejandro Ferrero, ES	IMPACT OF SURFACE CURVATURE ON SPECTRAL BRDF OF EFFECT COATINGS
PO16	Irma Kruger, ZA	INVESTIGATION AND MEASUREMENT OF UNCERTAINTY CONTRIBUTORS FOR COLORIMETRIC CALIBRATIONS
PO17	Petr Bos, CZ	CCT CHANGES OF THE LED'S DEPENDING ON THE ANGLE OF THEIR RADIATION
PO18	Michal Vik, CZ	VISUAL EVALUATION OF WHITE SAMPLES NEAR TO CIE LIMITS
PO19	Michael Marutzky, DE	METHOD FOR THE TREATMENT OF WAVELENGTH-DEPENDENT VOLUME SCATTERING IN A HOMOGENEOUS, ABSORPTIVE MEDIUM
PO21	Aravin Periyasamy, CZ	PROBLEMS IN KINETIC MEASUREMENT OF MASS DYED PHOTOCHROMIC POLYPROPYLENE FILAMENTS WITH RESPECT TO DIFFERENT COLOUR SPACE SYSTEMS
PO26	Nayab Khan, CZ	THE COMPARISON STUDY OF INSTRUMENTAL COLOUR MEASUREMENT AND VISUAL GRADING OF COTTON FIBER
PO27	H.C. Li, TW	OPTIMIZATION OF WHITE LED SPECTRUM UNDER MESOPIC CONDITION BASED ON 3D COLOUR GAMUT

Poster Session 2

PO28	Yuki Akizuki, JP	STUDY ON SPECTRAL CHARACTERISTICS FOR IDENTIFICATION OF SKIN COLOUR OF INJURED JAPANESE PERSONS AT DISASTER SITES
PO29	Jan Krüger, DE	DIRECTIONAL LIGHT OF LED ARRAYS AND ITS INFLUENCE ON SHAPE PERCEPTION
PO30	Peter Bodrogi, DE	COLOUR SURFACE RENDERING: A NEW ASPECT OF LIGHT SOURCE COLOUR QUALITY FOR MUSEUM LIGHTING
PO31	Yukiko Yoshida, JP	COLOUR VISUAL EFFECTS OF STEADY STATE EXPERIMENTS IN DIFFERENT THERMAL ENVIRONMENTS AT AN OFFICE TEST SITE
PO32	Johannes Mäder, DE	COMPREHENSIVE SCATTER MEASUREMENT AND MODELING
PO33	Omar Gomez Lozano, ES	ANALYSIS OF THE INTERPLAY OF THE PIGMENT SHAPE AND SIZE ON SPARKLE DETECTION DISTANCE BY DESIGN OF EXPERIMENTS
PO34	Omar Gomez Lozano, ES	CORRELATIONS BETWEEN CONCENTRATION OF EFFECT PIGMENTS, OPTICAL MEASUREMENTS AND VISUAL ASSESSMENT OF SPARKLE
PO35	Laura Bellia, IT	THE RIGHT LIGHT FOR PAINTINGS: AN AMBITIOUS CHALLENGE
PO36	Tarek Abd El Magid, OM	CREATE COLOUR MODEL INSPIRED BY CONES SPECTRAL SENSITIVITY IN THE RETINA OF THE HUMAN EYE
PO37	Ming Ronnier Luo, CN	APPEARANCE RESEARCH BASED ON SPECTRUM TUNEABLE LIGHTING SYSTEMS
PO38	Takahiko Horiuchi, JP	MEMORY EFFECTS IN GOLD MATERIAL PERCEPTION
PO39	Takahiko Horiuchi, JP	PHYSICAL INDEX FOR JUDGING APPEARANCE HARMONY OF MATERIALS
PO40	Esther Perales, ES	ESTIMATION OF THE SPARKLE TEXTURE EFFECT BY VISUAL AND INSTRUMENTAL ASSESSMENTS
PO41	Shigeko Kitamura, JP	EVALUATION INDEX FOR THE VISUAL APPEARANCE AND THE TACTILE TEXTURE
PO42	Martina Viková, CZ	SPECTROPHOTOMETRY OF DYNAMIC COLOURS
PO43	Kumiko Kikuchi, JP	A CORRECTION METHOD FOR SKIN REFLECTANCE OBTAINED WITH DIFFERENT SPECTROPHOTOMETERS AND ITS APPLICATION: LONG-TERM CHANGES IN THE SKIN COLOUR OF JAPANESE FEMALES
PO44	Jan Audenaert, BE	CONVOLUTION AND DECONVOLUTION OF BSDF DATA TO ENABLE INTER-INSTRUMENT COMPARISON
PO45	Mihai Ivanovici, RO	ENTROPY VERSUS FRACTAL COMPLEXITY FOR COMPUTER-GENERATED COLOUR FRACTAL IMAGES
PO46	Mekbib Amdemeskel, DK	PHOTOMETRIC AND COLORIMETRIC COMPARISON OF HDR AND SPECTRALLY RESOLVED RENDERING IMAGES
PO47	Pedro Pardo, ES	VISUAL FIDELITY ASSESSMENT OF ARTWORKS IN VIRTUAL REALITY
PO48	Quang Vinh Trinh, DE	GENERAL ASPECTS OF THE SPECTRAL OPTIMIZATIONS OF MULTICHANNEL HYBRID LED-LUMINAIRES ON COLOUR FIDELITY, COLOUR PREFERENCE, COLOUR MEMORY AND SATURATION ENHANCEMENTS
PO49	Gertjan Scheir, BE	DEFINING THE EFFECTIVE LUMINOUS SURFACES IN THE UNIFIED GLARE RATING
PO50	Shau-Wei Hsu, TW	COLORIMETRIC PROPERTIES OF LED ILLUMINATED ROADS STUDIED BY IN-FIELD MEASUREMENTS AND SIMULATIONS
PO51	Kazim Hilmi Or, TR	ARTIFICIAL VISION: WHY IS COLOUR HDR VIDEO NEEDED?
PO52	Kazim Hilmi Or, TR	COLOUR VISION PERCEPTION: A TRIAL TO UNDERSTAND HOW THE CHANGE IN COLOUR PERCEPTION HAPPENS IN “#THEDRESS”
PO53	Hiroshi Takahashi, JP	EFFECTS OF CHROMATIC COLOUR LIGHTING ON WORK EFFICIENCY
PO54	Youngshin Kwak, KR	HUE PERCEPTION OF NEAR-WHITE LIGHTINGS AROUND 5000 K

ORAL PRESENTATIONS

Session PA1
Visual Perception - Part 1
Tuesday, September 6, 09:10–10:30

OP01

PERCEPTION OF ILLUMINATION WHITENESS

Perz, M.[1], Baselmans, R.[1], Sekulovski, D.[1]
[1] Philips Research Lighting, Eindhoven, NETHERLANDS
Gosia.perz@philips.com

1 Introduction

LEDs allow for easy control of their emission properties, including their spectral composition. This gives almost arbitrary control over the chromaticity of the emitted light. The communication of the chromaticity to the users of the light sources can be quite challenging. To simplify the communication, the lighting industry uses a quantity called the Correlated Colour Temperature (CCT) of the emitted spectrum or a classification of CCTs using natural language terms (e.g. warm, cold). The Correlated Colour Temperature of a source is the temperature of a black body radiator with a chromaticity that is closest to the chromaticity of the source. Taking all black body radiators for different temperature one gets a line in chromaticity space called the Black Body Line (BBL), that has dominated the characterization of “white” light sources. In LED lighting the points on the BBL are used to specify the chromaticity in the whole production chain, from the LEDs themselves to luminaires. As sources with the same CCT can have widely different appearance it is natural to question if the BBL is the most appropriate reference.

An often heard argument for the choice of the BBL as a reference is that it represents natural light sources or white light sources (usually meaning sources without perceived tint). In recent years, however, a number of studies contested both the perceived whiteness (Rea, 2011) as well as the perceived naturalness (Ohno, 2016) of sources having a chromaticity on the BBL. Rea (2011) found that perception of white illumination is associated with positions of the chromaticity that fall above BBL for high CCTs (above 4000 K) and that fall well below BBL for low CCTs (below 4000 K) and for all CCTs different from 4000 K the points on BBL appeared tinted. Partially agreeing with those results, Ohno (2016) demonstrated that for all CCTs, points below the BBL appear more natural than points on the BBL. These studies show the possibility of adding a “white body line” and a “natural illumination line” in parallel to the BBL to specify the chromaticity of light sources.

The differences in the setups of the above mentioned studies clearly demonstrate the most important aspects of illumination chromaticity perception that have to be taken into account. In the study of Rea, participants were instructed to identify the tint of a large, uniformly illuminated viewing box for a number of stimuli having the same CCT but different chromaticities. Using one stimulus, this study was aimed to define the whitest point in an absolute sense. Contrary to this, the study of Ohno always showed two different stimuli to the participants and asked for the more natural of the two. Even though it is logical that the point of equal choice between the stimuli in the second approach is equivalent to the point of the least tint in the first approach, this equivalence is not necessarily true. Second important difference between the studies is in the way that chromatic adaptation is controlled for. In the study of Rea all the stimuli were presented in a random order and the adaptation state is treated was a nuisance factor and added to the error. In the second study, adaptation was controlled for and participants were given enough time to adapt to a point in between the two stimuli. As adaptation to a specific chromaticity greatly changes the perception of the following light stimulus, this consideration is very important. The last difference important for this work is the inclusion of coloured objects in the experiment. The first study was done in an empty white box, while the second one was done in a more realistic environment having a large number of objects with different colours.

In the present study, we aim to understand the basic perception of whiteness of light sources. Due to large influence of chromatic adaptation, we use a methodology that does not measure absolute whiteness, but a relative one. Instead of answering the question “Which light source with a CCT of x is the whitest when seen in isolation” we aim to answer the question “Which light of CCT x is whiter than any other source with the same CCT when directly compared”. As

a first step in the study, we use only white surfaces and no coloured objects. Lastly, similar to the work of Ohno, we control for adaptation by giving time to the participants to adapt to a point between the stimuli to be compared.

2 Method

2.1 Set-up

A viewing box, with two chambers having dimensions of 75 cm x 75 cm x 45 cm, was painted with diffused, neutral white paint. Two THOUSLITE LEDCubes, with a light emitting surface of 27 cm x 27 cm, were mounted on top and in the centre of each of the chambers. Each cube had 11 different types of LEDs that can be independently controlled with 11 bits of precision. The LEDs included 2 white LEDs: a warm white and a cold white, and 9 coloured LEDs with narrow spectra and a single peak. The chambers were uniformly illuminated.

2.2 Stimuli

As most important CCTs in North European applications, 3000K and 4000K stimuli were used. For each of the CCTs 15 different isotemperature stimuli were generated: 7 positioned above the BBL, 7 positioned below BBL, and 1 positioned on the BBL. The stimuli ranged between -0.021 Δuv (we use a convention where a negative distance means a chromaticity above the BBL) to 0.021 Δuv from the BBL. The distance between all stimuli was equal to 0.003 Δuv. The spectrum of the stimuli was smooth, meaning that it was optimized to be as close as possible to a spectrum of blackbody radiator. The light level in the middle of each chamber was 1645 lux.

2.3 Procedure

Participants were seated 0.5 meter away from the viewing box, in the dark room. For each pair of stimuli, the reference light, having a chromaticity between the two stimuli, was shown in both chambers for 10 seconds. Then the stimuli were shown. In total 13 pairs of stimuli were used. Participants were instructed to indicate on a portable numerical keyboard, which of the two stimuli is whiter; they were instructed to press the right arrow key, if the stimuli in right chamber was whiter and otherwise the left arrow key. Each pair of stimuli was repeated three times. All the stimuli were randomized. The experiment took about 30 minutes per participant. The normal vision of the participants was ensured by Ishihara colour vision test.

2.4 Results

The point where there is an equal probability for the participant to pick the point below the reference and above the reference is taken to be the resulting “whitest” point per CCT. At the moment of writing this abstract a pilot study was carried out and showed results that are below the BBL for both 3000K as well as 4000K. Interestingly, the results for 3000K are closer to the BBL than the results of Rea and Ohno and between the results of Rea and Ohno for 4000K.

The results of the full experiment will be presented in the final version of the paper.

REFERENCES

Rea M.S., Freyssinier J.P., 2011. White Lighting. *Color Research and Application*, 38(2):82-92

Ohno Y., Oh S., 2016. Vision Experiment II on White Light Chromaticity for Lighting. In *Proceedings of CIE 2016 “Lighting Quality and Energy Efficiency”,* March 2016, Melbourne, Australia

OP02

BRIGHTNESS PERCEPTION OF RELATED SELF-LUMINOUS STIMULI

Hermans, S.[1], Smet, K.A.G.[1], Hanselaer, P.[1]
Stijn.hermans@kuleuven.be

Abstract

Colour Appearance Models (CAM) attempt to predict the colour appearance of a stimulus by taking the physical properties of the stimulus and its surroundings into account. The fundamental goal is to look for correlates between the measured optical spectral data of a stimulus and its surrounding and the corresponding perceptual attributes. There are three absolute colour attributes (Brightness, Colourfulness and Hue) and three relative colour attributes (Lightness, Chroma and Saturation).

Most of the existing CAMs are developed to describe the perception of related surface colours which implicitly assume the presence of a light source illuminating the target and one or more other surfaces. Recently, a new CAM (CAM15u) was developed for unrelated light sources (i.e. self-luminous stimuli seen in a completely dark environment). However, at this moment, there is no colour appearance model for light sources seen in a specific luminous context (e.g. a traffic signal at daytime).

An experimental room has been set up. The room is 3 m x 5 m and has a grey ceiling. The walls are covered by black curtains and there is a black carpet on the floor. One wall has been modified for the experiments. This wall is a self-luminous wall (dimensions: 5 m by 4 m) composed of a large diffusor illuminated from the back by a series of dimmable TL-fluorescent lamps. A circular test stimulus (D = 0.35 m) is created in the center of the wall by a RGB-LED light source encased in a cylindrical tube placed behind the diffusor.

The observers are seated in front of the wall at a distance such that the stimulus has a field-of-view of 10°. The self-luminous wall itself has a field-of-view of 70°. Both the background and the stimulus were optically characterized using a telescopic measuring head coupled to a spectroradiometer. The uniformity of the wall and the stimulus are within 10 % of the mean.

In a first series of experiments, the impact of the introduction of a self-luminous background on the colour appearance of the light source, specifically on the brightness, was investigated. The luminance of the background was 28 cd/m^2 at a correlated colour temperature (CCT) of 3880 K. The 30 test stimuli were selected at 6 different hues. For each hue, 5 different stimuli with increasing saturation have been chosen. For comparison purposes and to minimize confounding factors, a luminance level of 50 cd/m^2 was attributed to all the 30 stimuli. In this way, only positive contrasts to the background were used at this stage.

Brightness is one of the absolute attributes of the visual sensation according to which an area appears to emit more or less light. Visual data on the brightness perception of the test stimuli were obtained in a magnitude estimation experiment in which a group of observers were asked to rate, on a half-open scale, the brightness of the test stimulus in comparison to that of a reference stimulus. Thanks to this method, a numerical and scalable result for the observed brightness was obtained. The test panel was composed of 22 observers with normal colour vision, with ages ranging from 20 to 50 years (average age was 30 years old) and with an approximately 50-50 male-to-female ratio (12 males and 10 females).

In a first series of experiments a reference stimulus is shown for 5 seconds before every stimulus. This stimulus has the same chromaticity coordinates and luminance level as the background. To this reference, a fixed brightness value of 100 was attributed. The actual stimulus is then presented for 5 seconds and the observers had to make an estimation for the brightness relative to the reference stimulus. In a second experiment the background itself served as reference. Again, a fixed brightness value of 100 was attributed to it. The 30 stimuli are presented again for 5 seconds and the observers have to rate the brightness relative to the

background. Assessing the brightness in relation to the background can be done simultaneously, which is not the case when using the reference stimulus.

The results of the individual observers were converted to an ‘average observer’ by using the geometric mean. Inter-observer variability were evaluated by the coefficient of variation (CV) and the STandardized-Residual-Sum-of-Squares (STRESS) between each individual observer and the average observer. The inter-observer and intra-observer coefficient of variation using the fixed reference stimulus was 22.3 and 23.3 respectively. These values are in line with earlier experiments and with values mentioned in literature. The inter-observer and intra-observer coefficient of variation using the background as the reference stimulus was 24.2 and 19.4 respectively.

The difference between both intra-observer CV values turned out to be significant. This can be explained by the fact that almost all the male observers (10 of the 12 males) claimed that the brightness estimation was easier when the background was used as reference. Both stimulus and reference were available at the same time and the brightness comparison could be done more accurately. When analyzing only the data of the male observers, a mean intra-observer CV of 15.8 was found when the background was used as reference and a mean intra-observer CV of 21.8 was found when a reference stimulus was presented before the actual stimulus. This difference in mean intra-observer CV value turned out to be again significant.

For each hue series, the brightness increases strongly with saturation although the luminance is identical. This indicates a large contribution of the Helmholtz-Kohlrausch effect (H-K effect). It is also clear that the H-K effect has a much larger contribution for red and blue than for the other hues. Comparing the rank of the perceived brightness with the rank of the brightness prediction of the existing CAM15u model results in a spearman correlation equal to 0.897. Although the CAM15u model was develop for unrelated colours, it seems to be useful to predict related self-luminous colours as well.

OP03

INVESTIGATING CHROMATIC ADAPTATION USING MEMORY COLOURS

Smet, K.A.G.[1], Zhai, Q.[2], Luo, M.R.[2], Hanselaer, P.[1]
[1] ESAT/Light&Lighting Laboratory, KU Leuven, Ghent, BELGIUM, [2] State Key Laboratory of Modern Optical Instrumentation, Zhejiang University, Hangzhou, CHINA
Kevin.Smet@kuleuven.be

Abstract

Chromatic adaptation refers to the ability of the human visual system to (partially) adapt to the intensity and colour of the illumination, producing an approximately colour constant appearance of objects across changes in illumination.

Models that predict the adaptive shift due to chromatic changes in lighting/viewing conditions are referred to as Chromatic Adaptation Transforms (CATs) and are an important part of colour appearance models (CAMs). As an example, the CAT02 transform (CIE160-2004, 2004, CIE159-2004, 2004) is embedded in CIECAM02 (Moroney et al., 2002). CATs are typically based on one or more sets of corresponding colours (CC), which are stimuli that appear similar in colour under different illumination (adaptive) conditions. Corresponding colours are commonly derived using *asymmetric matching* where observers have to match the colour appearance of a stimulus under the test illuminant with that under a reference illuminant. However, for most existing CC sets, the adaptive conditions were limited to (near) neutral illuminants (CIE160-2004, 2004), while new solid-state lighting technologies open up a range of potentially high chroma, coloured illuminants for which the applicability of existing CAT can be questioned as the degree of adaptation tends to decrease as the purity of the adaptive field increases (Kuriki, 2006).

With the aim of testing existing CAT and, if necessary, developing a new model that is able to account for coloured, high chroma, adaptive fields, a set of corresponding colours has been obtained for a variety of neutral and coloured illuminations using a *Memory Colour Matching* (MCM) approach.

MCM involves observers adjusting the *colour appearance* of a familiar object stimulus presented under each adaptive condition until it matches the internal memory colour. Note that observers are asked to make colour appearance matches and not surface matches (Arend and Reeves, 1986). The resultant memory colour chromaticity (and luminance) values under the different adaptive conditions then form a set of corresponding colours.

Memory colours have been used successfully in the past as an internal reference to study the colour rendering of white light sources (Sanders, 1959, Smet et al., 2012) or image colour quality (Bartleson, 1961, Xue et al., 2014, Zeng and Luo, 2010).

MCM is analogous to other approaches based on internal references, such as *achromatic matching* and *unique hue setting*, often used in colour constancy research. However, these approaches only allow for resp.1 and 4 internal references whereby shifts in stimulus lightness and/or chroma are ignored.

The advantages of MCM approach are:

- the substantial increase in the number of possible internal references
- the matches are expected to be more accurate compared to short-term 'learned' memory matching (Smithson, 2005)
- less time consuming than asymmetric matching as no paired presentations are required. Indeed, obtaining all CC sets for N illuminants would require N^2-N asymmetric matching experiments, while it would only require N MCM experiments.

- it has many of the benefits of successive matching: unrestricted eye movements resulting in a more natural viewing conditions and good control of the observer's adaptive state which can be affected by the presence of the reference field in simultaneous (Smithson, 2005) or haploscopic matching (Barbur and Spang, 2008, Vimal and Shevell, 1987), no need for switching back-and-forth between test and reference conditions eliminating numerous observer re-adaptation.
- it requires no extensive training in a colour order system (cfr. magnitude estimation) (CIE160-2004, 2004)

Possible disadvantages are:

- memory colour matches might be less sensitive to changes in viewing conditions and therefore be less representative (Hansen et al., 2006).
- no familiar objects for any desired chromaticity (Blue or magenta familiar objects are difficult to find (Smet et al., 2011)).

In this study, memory colours were obtained for a gray cube, a green apple, a ripe lemon, a ripe tomato and a blue smurf.

Thirteen illumination conditions were investigated with 8 of them having chromaticity values on or near the blackbody or daylight locus: a neutral obtained by (Smet et al., 2015, Smet et al., 2014), EEW, D65, illuminant A and Planckian radiators of 2000K, 4000K, 12000K and infinite K. Furthermore, 5 high chroma illumination conditions (Red, Yellow, Green, Blue and Magenta) were selected. The adaptive field luminance of the spectrally neutral background was approximately 760 cd/m² (~2600 lux). The background scene has approximately a 70° field of view and was populated with various spectrally neutral 3D objects to enhance scene realism by providing depth, parity and illumination cues, which also enhances colour constancy and chromatic adaptation (Foster, 2011). The background illumination was provided by a calibrated data projector. In the experiments, familiar object chromaticity and luminance could be adjusted by the observers using the arrow keys on a keyboard while navigating in the CIE *u'v'* diagram. Each key press only changed the RGB output of the data projector pixels corresponding to the 3D object's projection on the imaging plane, resulting in only a change in the object's colour. Each memory colour setting was spectrally recorded using a telespectroradiometer.

Ten colour-normal observers, as tested by the Ishihara-24-plate test, participated in the experiments.

The memory colour data under each adaptive illuminant were averaged and 156 *(=13²-13*) pair wise corresponding colour data sets were derived. The CC data were used to test the performance of the CAT02 by calculating the minimal colour difference DE (in *u'v'* and CAM02-UCS) between the measured corresponding colours and those predicted by the CAT02 model. Colour differences were minimized by allowing different degrees of adaptation (D) for each of the adaptive conditions. On average, the minimum colour differences obtained for the memory colour based corresponding colour data sets were similar to those obtained for other data sets published in literature (CIE160-2004, 2004). The following trends were observed for the degree of adaptation: D decreases with increasing background purity, and increases as the angle between the background hue and the positive yellow-blue axis increases. As a chromaticity dependent degree of chromatic adaptation is currently missing in many CATs and colour appearance models, the results of the current study could be used to provide further improvements to these models. Future research will extend the data sets to other illuminance levels and more objects.

Acknowledgments

Author KS was supported through a Postdoctoral Fellowship of the Research Foundation Flanders (FWO) (12B4916N).

References

AREND, L. & REEVES, A. 1986. SIMULTANEOUS COLOR CONSTANCY. *Journal of the Optical Society of America a-Optics Image Science and Vision,* 3**,** 1743-1751.

BARTLESON, C. J. 1961. Color in memory in relation to photographic reproduction. *Phot. Sci. Eng.,* 5**,** 327–331.

CIE159-2004 2004. A Colour Apperance Model for Color Management System: CIECAM02. *In:* REPORT, C. T.-T. (ed.). Vienna: CIE.

CIE160-2004 2004. A review of chromatic adaptation transforms Vienna: Commission Internationale de L'Eclairage.

FOSTER, D. H. 2011. Color constancy. *Vision Research,* 51**,** 674-700.

HANSEN, T., OLKKONEN, M., WALTER, S. & GEGENFURTNER, K. R. 2006. Memory modulates color appearance. *Nature Neuroscience,* 9**,** 1367-1368.

KURIKI, I. 2006. The loci of achromatic points in a real environment under various illuminant chromaticities. *Vision Research,* 46**,** 3055-3066.

MORONEY, N., FAIRCHILD, M. D., HUNT, R. W. G., LI, C., LUO, M. R. & NEWMAN, T. 2002. The CIECAM02 color appearance model. *IS&T/SID Tenth Color Imaging Conference.*

SANDERS, C. L. 1959. Assessment of color rendition under an illluminant using color tolerances for natural objects. *Illum. Eng.,* 54**,** 640-646.

SMET, K. A. G., DECONINCK, G. & HANSELAER, P. 2014. Chromaticity of unique white in object mode. *Optics Express,* 22**,** 25830-25841.

SMET, K. A. G., DECONINCK, G. & HANSELAER, P. 2015. Chromaticity of unique white in illumination mode. *Optics Express,* 23**,** 12488-12495.

SMET, K. A. G., RYCKAERT, W. R., POINTER, M. R., DECONINCK, G. & HANSELAER, P. 2011. Colour appearance rating of familiar real objects. *Color Research and Application,* 36**,** 192-200.

SMET, K. A. G., RYCKAERT, W. R., POINTER, M. R., DECONINCK, G. & HANSELAER, P. 2012. A memory colour quality metric for white light sources. *Energy and Buildings,* 49**,** 216-225.

SMITHSON, H. E. 2005. Sensory, computational and cognitive components of human colour constancy. *Philosophical Transactions of the Royal Society B-Biological Sciences,* 360**,** 1329-1346.

XUE, S., TAN, M., MCNAMARA, A., DORSEY, J. & RUSHMEIER, H. Exploring the use of memory colors for image enhancement. SPIE: Human Vision and Electronic Imaging XIX, 2014. 901411-901411-10.

ZENG, H. & LUO, R. Modelling memory colour region for preference colour reproduction. SPIE: Color Imaging XV: Displaying, Processing, Hardcopy, and Applications, 2010. 752808-752808-11.

OP04

INTERCOMPARISON OF VISUAL GLOSS PSYCHOMETRIC SCALES

Ged, G.[1], Leloup, F.B.[2], De Wit, Y.[2], Obein, G.[1]
[1] LNE-Cnam, Trappes, FRANCE, [2] Light&Lighting Laboratory – KU LEUVEN, Gent, BELGIUM
guillaume.ged@lecnam.net

Abstract

The total visual appearance of a surface is a concern in a wide panel of industrial sectors. In many manufacturing processes, more than instruments, the visual system has the last word when quality of the finished product is at stake. Psychophysical studies aim to produce scales describing our perception of stimuli. In the field of gloss appraisal, such techniques are used since Hunter early works and many scales describing this quantity have been produced. However, to our knowledge, no metrological assessment of scales constructed from a same set of samples through different protocols has ever been carried out.

We use two sets of seven dark grey gloss samples from a commercially available scale. The samples are made from coated paper. Their 60° specular gloss levels range between 2 gloss units and 95 gloss units. The size of the samples is fixed to 50 mm by 80 mm. Both laboratories are free to choose a psychophysical protocol to produce the perceptual functions for these artefacts, using in-house light booths.

LNE-Cnam designs a pair comparison, the results of which are processed by a Maximum Likelihood Difference Scaling algorithm [1]. 16 observers below 40 years old (5 male, 5 female), twice evaluate 35 key-sample quadruples in two directions (permutation between left and right). The paradigm they have to answer is “which pair exhibits the higher differences among its samples?” The experiment lasts from 30 to 40 minutes per observer. Measurement are carried out in a black light booth under a uniform D65 illumination produced by fluorescent tubes behind a double diffuser. In order to ease the samples assessment, a grid of mesh size 5 cm by 5 cm was superimposed below the last diffuser. The illumination level in the cabin is 1850 lux. The output from the measurement is a psychometric function defined between 0 and 1, corresponding respectively to the extremal samples form the scale.

KU Leuven uses a paired comparison technique according to the method described by Scheffé [2]. 16 observers (8 male, 8 female), aged between 18 and 40, are asked to rate the difference in visual gloss between each pair of two samples, on a -3 to 3 scale, in both orders of presentation (left vs. right). The presentation order is defined by a Digram-balanced Latin square. For each observer, the experiment takes between 30 and 40 minutes. Two different light conditions are installed. For both test conditions, the resulting visual gloss scale is derived, and the consistency among observers is evaluated.

In order to provide guidelines and recommendations for visual evaluation of surface gloss, the functions produced by the two methods and under the 3 different lighting conditions are compared.

[1] K. Knoblauch and L. T. Maloney, *Modeling Psychophysical Data in R*. New York, NY: Springer New York, 2012.

[2] H. Scheffé, "An analysis of variance for paired comparisons," J. Am. Stat. Assoc. 47, 381-400 (1952).

Session PA2
BRDF Fundamental Metrology
Tuesday, September 6, 11:00–12:20

OP05

A REFERENCE MATERIAL WITH CLOSE TO LAMBERTIAN REFLECTANCE AND FLUORESCENCE EMISSION PROFILES

Jaanson, P.[1,2], Pulli, T.[2], Manoocheri, F.[2], Ikonen, E.[1,2]
[1] Centre for Metrology MIKES, VTT Technical Research Centre of Finland Ltd, Espoo, FINLAND; [2] Metrology Research Institute, Aalto University, Espoo, FINLAND
priit.jaanson@aalto.fi

Abstract

Fluorescence is a process in which light is absorbed by a molecule and re-emitted at longer wavelengths. Various scientific and industrial applications make use of fluorescent brightening agents to enhance the appearance of materials (e.g. textiles, paper and plastics). For accurate characterisation and reproduction of appearance, relative and absolute measurements of fluorescence characteristics are needed. The angular emission and reflectance of fluorescent surfaces have earlier been shown to deviate from Lambertian behaviour, however in industry and calibration facilities single geometry measurements are often used, which requires assumptions to be made on the angular distributions. In addition, the measurement geometry of the calibration of the reference sample is often different from that of the routine measurements.

The objective of this study was to investigate whether confining the fluorophore into a thin layer on the surface of the sample will result in more Lambertian angular reflectance and fluorescence emission profiles than when the fluorophore is in the bulk of a translucent material as in the conventional commercially available polytetrafluoroethylen (PTFE) based samples. Furthermore, the spectral dependences of relative angular emission and reflectance profiles were studied.

The bispectral luminescent radiance factors and the reflected radiance factors of three samples were measured. Two of the samples were commercially available PTFE based fluorescent diffuse reflectance standard materials with the fluorophores added in the bulk. The third sample was a ceramic panel with a fluorescent coating. That way the fluorophores were confined in a layer on the surface of the panel with a thickness of 0.18 mm.

The measurement results indicate that the novel sample has more Lambertian reflectance and emission angular profiles than the conventional samples. The deviations of the reflectance and emission profiles were up to 13 % from Lambertian for the novel sample and up to 35 % for the PTFE based samples. In addition, spectral dependence of the angular reflectance profiles was measured in all the samples, and it was the smallest for the novel sample. The spectral dependence is caused by the spectral change of the absorbance of the sample and is therefore dependent on the type and concentration of the fluorophore. The dependence on the absorbance can be explained qualitatively and is reproduced by a quantitative Monte-Carlo ray-tracing model. The aforementioned effects are minimal at 45°/0° and 0°/45° geometries and remain within 1 %–3 % with the best results for the novel sample. However, the errors of conventional samples can increase by an order of magnitude at other geometries.

The novel sample can be useful for improved uncertainties for single geometry measurements where 45°/0° and 0°/45° geometries are not available e.g. commercial instruments with fixed angle of 90° between the irradiation and viewing angles. Furthermore, the smaller dependence of angular reflectance on the absorbance of the sample can reduce the cost of calibration where extensive characterisation of the sample is needed. The new knowledge on the spectral dependence of angular reflectance profiles can be useful for reducing measurement uncertainties when the reference sample and the sample under measurement contain different types and concentrations of fluorophores, are measured at different geometries or when measurements are performed with different UV contents of the irradiance spectra.

OP06

POLARIZATION EFFECTS IN DIFFUSE REFLECTANCE MEASUREMENTS – COMPARISON OF WHITE STANDARDS AND SPECIAL-EFFECT PIGMENT SAMPLES

Quast, T.[1], Hauer, K.-O.[1], Schirmacher, A.[1]
[1] Physikalisch-Technische Bundesanstalt, Braunschweig and Berlin, GERMANY
tatjana.quast@ptb.de

Abstract

To precisely characterize the bidirectional reflectance distribution function (BRDF) of any sample under test, the polarisation of the incident and reflected light has to be taken into account. While the influence of polarization is expected to be small in standard geometries in the case of white standards, the polarisation dependence is especially interesting for special-effect pigments. Such pigments are widely used in a number of different branches of industry (e.g. automobile, printing, cosmetics) due to their different visual effects like sparkle or goniochromatism. However, these effects in turn make it challenging to characterize the pigments because the BRDF depends strongly on the geometry investigated so that a large number of geometries deviating from standard cases have to be sampled.

For the measurement of BRDF of radiance factor PTB uses a robot-based gonioreflectometer in which the angles of illumination and detection can be chosen. As also the orientation of the sample can be controlled many different in-plane and out-of-plane geometries can be realized. By using a broadband light source and different detectors, the wavelength range of 250 nm to 1750 nm is available for measurements. With this experimental setup it is possible to determine the spectral radiance factor as an absolute quantity.

The gonioreflectometer has been equipped with a polarization-analyzer unit. It consists of a quarter-wave plate whose fast axis can be rotated perpendicular to the direction of detection by computer control, and a linear polarizer behind with fixed transmission axis. By measuring the spectral radiance factor at different angles of the wave plate, it is possible to determine the Stokes parameters *I*, *M*, *C* and *S* of the reflected beam. This set of parameters fully describes the polarization state of the reflected beam of light in terms of linear (parameter *M* for s/p and *C* for +/-45 degrees orientation of the fast axis, respectively) and circular polarization (parameter *S*) and intensity *I*. In this way one can gain a quick overview of the polarization dependence of the spectral radiance factor.

However, determining the Stokes parameters for each geometry would increase the measurement time by a factor of eight, since an eight-step technique is used in our experiments. In order to measure the spectral radiance factor efficiently one has to discriminate between geometries which exhibit a strong polarization dependence and those where polarization only plays a minor role. In the former case it is advisable to determine the Stokes parameters whereas in the latter case the polarization dependence can be omitted. Also in most cases it is expected that circular polarization is close to zero in the reflection process and therefore its determination could be avoided.

In this study, the polarization properties of the gonioreflectometer setup itself and of a variety of samples have been examined. It could be shown that the incident light can be considered unpolarized as is expected from an isotropically emitting integrating sphere source. Thus, any detected polarization dependence is caused by the sample under test.

Different kinds of samples have been studied, among them special-effect pigments which exhibit a strong goniochromatism, interference pigments, monochrome samples with glossy surface and white standards with matte surface. The geometries range from “typical” measurement geometries (e.g. illumination under 45 °, detection under 0 ° relative to the surface normal of the sample) to more unusual ones. In this way it is possible to evaluate the

influence of the polarization on the spectral radiance factor for a variety of experimental situations.

The results of this study are supposed to give an overview to which extent a polarization dependence exists, which parameters have the most pronounced effect and to supply information on parameter dependence, e.g. with respect to sample type, surface finish, measurement geometry and wavelength. It will give information on such cases where it is most pronounced and therefore should be taken into account and in which cases it may be neglected.

OP07

UNCERTAINTY EVALUATION OF FLUORESCENCE QUANTITIES OBTAINED FROM GONIOMETRIC MEASUREMENTS

Ikonen, E.[1,2], Jaanson, P.[1,2], Pulli, T.[1] and Manoocheri, F.[1]
[1] Metrology Research Institute, Aalto University, Espoo, FINLAND,
[2] MIKES Metrology, VTT Technical Research Centre of Finland Ltd, Espoo, FINLAND
erkki.ikonen@aalto.fi

Abstract

Fluorescence quantities are important in characterizing the appearance of materials. Bispectral luminescent radiance factor at a varying viewing angle describes the relative fluorescent spectral flux from a sample when irradiated at a certain wavelength. Spectral quantum efficiency of the fluorescent sample depends on the excitation wavelength and it is calculated as a spectral and angular integral of the bispectral luminescent radiance factor. In addition, spectral fluorescence quantum yield describes the conversion efficiency of the fluorophore and it is obtained as the ratio of the number of emitted and absorbed photons. The uncertainty evaluation for the two latter quantities needs to take into account possible unknown spectral and angular correlations between the luminescent radiance factors at different measurement settings, because those quantities depend on spectral and angular integrals. Such unknown correlations have been earlier analyzed with spectral integrals with the result that they can produce surprisingly large effects. Here the analysis method is extended to angular integrals.

The uncertainty budget of the bispectral luminescent radiance factor contains such components as measurement repeatability, detection system responsivity, wavelength settings and grating dispersion. To get realistic uncertainty estimates for spectral and angular integrals, we have to account for possible correlations between the values at different wavelength and viewing angle settings. One problem is that we typically know the uncertainties at each setting, but we do not know the correlations between the values at different settings. If we assume that the values are uncorrelated, we obtain very low uncertainties of the integrated quantities. Uncorrelated uncertainties behave like noise and largely average out in the integration. On the other hand, if we assume full correlation of the relative values, the relative deviation is the same at each setting and a cumulative effect on spectral or angular integrals results.

In practice, the situation typically varies between the two extremes presented above. The majority of the uncertainty components are partly correlated. It is typically so that the expected deviations at neighbouring setting values are close to each other but the correlation of unknown effects reduces as we move further away on the viewing angle or wavelength scale. For a reliable uncertainty analysis, we produce a mathematically consistent set of deviated data in the Monte Carlo analysis that sufficiently covers all possible correlations and is in agreement with the uncertainty estimate at each single setting. The disturbed data are then used to evaluate the uncertainties of the spectral and angular integrals.

The relative uncertainty for measuring bispectral luminescent radiance factors for 0°:45° geometry is between 2 % and 3 % (k = 2) for s- and p-polarisation, respectively. The values of spectral quantum efficiencies of a Spectralon sample are in agreement with measurements of another institute. The expanded uncertainties were obtained by the methods described above and they were between 3 % and 7 %. The corresponding quantum yield values were also calculated from goniometrical measurements with expanded uncertainties ranging from 4 % to 8 %. We can conclude that our uncertainty analysis method allows to address the effect of correlations on spectral and angular integrals of fluorescence quantities in a practical and cost-effective way.

OP08

TOWARD A METROLOGY FOR NON-UNIFORM SURFACE USING THE COMPLEXITY NOTION

Richard, N.[1], Ivanovici, M.[2], Bony, A.[1]
[1] XLIM laboratory JRU CNRS 6852, University of Poitiers, 86962 Futuroscope, FRANCE,
[2] MIV Laboratory, Department of Electronics and Computers, Transilvania University, Braşov, ROMANIA
noel.richard@univ-poitiers.fr

Abstract

Since more than 50 years ago, the texture aspect of surface takes an important place in image processing [1, 2, 3, 4]. In the case of grey-level images, features like granulometry or, more generally, pattern spectra from Mathematical Morphology offer metrological solutions to assess the textured aspect of surfaces [5, 6, 7]. Nevertheless, there exists actually no metrological solution for the physical or perceptual assessment of colour surfaces. In the last decades, many authors proposed solutions to characterize or discriminate colour textures using mathematical constructions which unfortunately cannot be linked to the perception or the physical content of surfaces [8, 9, 10]. We can ask ourselves also about the possible correlation between a texture characterization performed in the colorimetric domain in front of the physical domain when hyperspectral images are used.

Two questions are to solve to progress towards a valid texture feature for colour images. Firstly, how to define a colour or spectral texture feature adapted for metrological purpose? And secondly, how to assess its performances in front of the metrological requirements? In this work, we address the second question that induces the validation criterion for colour texture feature. Then we show on an existing colour texture features proposed recently how to adapt it for the validation.

As the only one operations validated in the colour domain are colour distances (in colorimetric and photometric level), we argue that a texture feature based on colour or spectral distance can solve the first constraint. In addition, we develop in the framework of CIE TC 8-14, the notion of spatio-chromatic complexity as a generic notion in the vision domain, as well in Mathematics, Physics, Computer-graphics and Signal/Image processing [11, 12]. Such concept is not entirely new, as a plethora of research has proven the sensitivity of the human perception to a complexity change in scene or image [13, 14]. Inside the existing definitions, some are based on the multiscale relationship between a measured or perceived property and the spatial evolutions. Inside this group of models, the fractal models based on fractional Brownian movement propose a relationship based on a power function between the spatial distance and the colour or spectral distance [11, 15].

So our hypothesis it that it is possible to develop a metrological validation of texture features using fractal surfaces where the theoretical fractal dimension is known by construction. This initial validation based on synthetic surfaces allows assessing the stability and bias of a texture feature in a high range of case, not reachable in real conditions. In CIE TC 8-14, experimental validations are planned in addition to this first level to complete the validation process in real cases.

In this work, we firstly recall the fractal model used to synthetized the test image [16]. In particular, we develop the relationship between the spatial construction linked to the contrast variations and the contrast sensitivity functions [12].

Then, we present the selected texture feature for the demonstration. We selected to work using the Colour Contrast Occurrence (C_2O) matrix [16]. Due to distance-based construction the C_2O is well adapted for metrological purpose when retained distances are selected from the perceptual ones. Nevertheless, the C_2O is a mono-scale texture feature, inspired by the first Julesz's conjecture [18] and the Haralick works [19].

In the third section, we show how to estimate the fractal dimension of colour surfaces from the C_2O matrix. And finally, we present the correlation results (direct correlation and rank-correlation) between the generated fractals and the measured fractal dimensions. We comment the results, and the obtained limits due to the quantization level of the generated images.

Then we conclude on the limits and interests of the proposed approach of criterion for texture feature validation. Firstly, the notion of complexity presents a great interest in its multi-disciplinary genericity with very similar definitions. Several models are often cited as being correlated to the human vision or physical variations, as entropic and fractal models. In this work, the fractal model was proposed as a possible criterion for texture feature validation. Using a vector texture feature coming from concept inspired by the human vision models, we shown that the required adaptation to process the criterion is direct. Then the results on synthetic images have proven the great interest of this feature for the texture aspect assessment. These results complete the obtained ones on texture classification contests on existing data-bases in the ability of this texture feature to preserve the spatio-chromaticity of images.

Bibliographie

[1] M. Cotte et A. Brazan Albu, «Robust texture classification by aggregating Pixel-based LBP statistics,» *IEEE Signal processing letters,* pp. 2102-2105, 2015.

[2] M. Mojki et S. Bakar, «Gray-level cooccurrence matrix computation based on haar wavelet,» chez *IEEE Computer Graphics, Imaging and Visualization (CGIV)*, Bangkok (Thailand), 2007.

[3] A. Dixit et N. Hedge, «Image Texture Analysis - Survey,» chez *IEEE Advanced Computing and Communication Technologies (ACCT)*, 2013.

[4] R. Mehta et K. Egiazarian, «Dominant Rotated Local Binary Patterns (DRLBP) for texture classification,» *Pattern Recognition Letters,* vol. 71, pp. 16-22, February 2016.

[5] P. Kuzas, D. Gailius, V. Augustis et A. Dumcius, «Sampling problems in granulometry,» chez *IEEE International Instrumentation and Measurement Technology Conference (I2MTC)*, 2012.

[6] E. Aptoula, «Extending morphological covariance,» *Pattern recognition,* vol. 45, n° %112, pp. 4524-4535, 2012.

[7] G. K. Ouzounis et M. H. Wilkinson, «Partition-induced connections and operators for pattern analysis,» *Pattern recognition,* vol. 43, n° %110, pp. 3193-3207, 2010.

[8] E. Aptoula et S. Lefèvre, «A comparative study on multivariate mathematical morphology,» *Pattern recognition,* vol. 40, n° %111, pp. 2914-2929, 2007.

[9] V. Arvis, C. Debain, M. Berducat et A. Benassi, «Generalization of the cooccurrence matrix for colour images : application to colour texture segmentation,» *Image Analysis and Stereologie,* vol. 23, n° %11, pp. 63-72, 2004.

[10] F. Bianconi, R. Harvey, P. Southam et A. Fernandez, «Theoretical and experimental comparison of different approaches for color texture classification,» *Journal of Electronic Imaging,* vol. 20, n° %14, November 2011.

[11] R. Voss, Chapter Fractals in nature : from characterization to simulation, vol. The Science of Fractal Images, Springer-Verlag, 1988, pp. 21-70.

[12] A. Coninx, G. Bonneau, J. Droulez et G. Thibault, «Visualization of uncertain scaar data fields using color scales and perceptually adapted noise,» chez *SIGGRAPH- Symposium of Applied Perception in Graphics and Visualization (APGV)*, 2011.

[13] G. Ciocca, S. Corchs, F. Gasparini, E. Bricolo et R. Tebano, «Does color influence image complexity perception ?,» *Computation color Imaging, Lecture Notes in Computer Science,* vol. 9016, pp. 139-148, 2015.

[14] A. Forsythe, M. Nadal, N. Sheehy, C. Cela-Conde et M. Sawey, «Predicting beauty: fractal dimension and visual complexity,» *British Journal of Psychology,* vol. 102, pp. 49-70, 2011.

[15] D. Saupe, Point evaluation of multi-variable random fractals, vol. Visualisierung in Mathematik und Naturwissenschaften, e. Hartmunt Jurgens and Dietmar Saupe, Éd.,

Springer Berlin Heidelberg, 1989, pp. 114-126.

[16] M. Ivanovici, N. Richard et C. Fernandez-Maloigne, «Fractal Dimension of colour Fractal Images,» *IEEE Transactions on Image Processing,* vol. 20, n° %11, pp. 227-235, 2011.

[17] A. Martinez, N. Richard et C. Fernandez, «Alternative to colour feature classification using colour contrast occurrence matrix,» chez *Quality Control by Active Vision (QCAV)*, Dijon, 2015.

[18] B. Julesz, "Experiments in the visual perception of texture," *Scientific American,* pp. 20-30, 1975.

[19] R. Haralick, S. K. and H. Dinstein, "Textural features for image classification," *IEEE Transactions on systems, man and cybernetics,* 1973.

Session PA3
Measurement of Goniochromatism
Tuesday, September 6, 15:45–17:05

OP09

TACKLING THE LIGHTNESS AND COLOUR FLOP IN EFFECT-PIGMENTED COATINGS

Strothkämper, C.[1], Schirmacher, A.[1]
[1] Physikalisch-Technische Bundesanstalt, Bundesallee 100, 38116 Braunschweig, GERMANY
christian.strothkaemper@ptb.de

Abstract

The looks of products are an important topic in the industry. Apart from the design, i.e. the shape of the product, there are numerous visual effects that significantly contribute to the overall appearance of a product like gloss or colour. Regarding the latter, effect-pigmented coatings are a way for manufacturers to realize particularly eye-catching visual effects for their products. For this purpose, a variety of different types of effect pigments has been developed. There are, for instance, metallic pigments, which are mostly aluminium micro platelets that, in essence, act as little micro-mirrors because they specularly reflect light. Another example that is also very relevant from a commercial perspective are interference pigments. These are micro-platelets with a layered structure of (semi) transparent materials. As a result, the reflectance spectrum can be tuned to have a very colourful appearance.

The effect pigments are dispersed randomly in a coating, regarding their position and the angle relative to the surface. So each ray of light that hits a group of effect pigments is split up and reflected into different directions. In addition, the spectral reflectance at each of the illuminated pigments will be different due to a different angle of incidence on each pigment. So in general, the appearance of an effect pigmented coating depends on the illumination and the observation direction. Especially coatings with metallic effect pigments show a strong angular variation of the lightness and coatings with interference pigments can exhibit a so called colour flop, i.e. large variations in hue.

Standards like ASTM E2539-14 “Standard Test Method for Multiangle Color Measurement of Interference Pigments” or DIN 6175-2 “Color Tolerances in Automotive Lacquerings” propose measurement geometries, i.e. configurations of illumination and observation directions. Several commercial colour measuring instruments derive e.g. L*a*b* colour coordinates at these and/or other geometries. However, these results are just a small excerpt of the abundance of colour impressions an effect pigmented surface can exhibit, especially if pigments with a strong colour flop are used. For practical applications in quality control, the number of measurement geometries has to stay on a reasonable level. Therefore, it seems desirable to use measurement geometries that deliver a maximum amount of information on the colour appearance of a given lacquering.

Within the EMRP Project “Multidimensional reflectometry for industry”, we developed a methodology that allows for a relatively easy assessment of the hue, chroma and lightness variations of an effect pigmented coating. It is based on the conclusion that not the illumination and observation direction themselves determine the colour of an effect-pigmented coating but rather two corresponding parameters of the ensemble of pigments that partakes in the given measurement geometry. These parameters are the angle of incidence on the pigments themselves and the tilting angle of the pigments surface normal with respect to the surface of the lacquering layer it is embedded into. While the former determines the spectral shape of the reflectance, the latter controls the amplitude of the reflectance. This allows for an uncomplicated modelling of the appearance and a prediction of the colour at arbitrary geometries based on the data from just a small number of base geometries. With as little as 10 base geometries the deviations ΔE_{ab} between the predicted and the measured colour coordinates are usually in the lower single figure range. This method thus presents a promising step towards an optimal characterization of special effect models since the underlying physical model offers potential for further accuracy enhancements. Apart from that, making use of the flake based parameters for colour measurements, it offers a sound way to select geometries that are superior in terms of the information that can be obtained to those currently used.

OP10

MULTI-ANGLE COLOUR CHARACTERIZATION OF COATINGS WITH DIFFRACTION PIGMENTS

Ferrero, A.[1], Bernad, B.[1], Campos, J.[1], Perales, E.[2], Velázquez, J.L.[1], Martínez-Verdú, F.M.[2]
[1] Instituto de Óptica, Consejo Superior de Investigaciones Científicas (CSIC), Madrid, SPAIN,
[2] Department of Optics, Pharmacology and Anatomy, University of Alicante, Carretera de San Vicente del Raspeig s/n 03690, Alicante, SPAIN
alejandro.ferrero@csic.es

Abstract

The complex reflectance properties of coatings with effect pigments result in quite strange colour sensation for humans, because our sense has evolved to perceive colours from absorption pigments. As a consequence of their appealing appearances, they have become very popular in the automotive industry, and they are also widely used in other markets, such as packaging or cosmetics industry. The complexity of their spectral reflectance also allows them to be used for more functional purposes, as anti-counterfeiting. The colour of effect pigments is caused by anisotropic optical processes like low-order scattering, interference, or diffraction. This work specifically deals with the reflectance characterization of coatings with diffraction pigments. Its main purpose is to determine the most adequate illumination/observation geometries to characterize the variation of its colour gamut.

Waves are diffracted when they interact with structures of dimensions of the same order of magnitude as their wavelength. This way, light is split up into spectral components by diffractive gratings. Among them, reflective diffraction pigments are the sorts of special interest in industrial colour physics, though they are also present in natural structural colours. They basically consist of a metal substrate with a grating of embossed parallel grooves. This substrate is coated by inorganic substances. The spectral reflectance of diffraction pigments depends on the geometry, because for every pair of illumination and observation directions the optical path difference introduced by the diffraction pigment is different.

In the effect coatings with diffraction pigments, these pigments are embedded in a transparent medium or binder with a refractive index. Within this medium, the flake pigments are randomly oriented and, therefore, the observed diffraction corresponds to the superposition of diffraction patterns produced by the different orientation of the grooves. In addition, the flake pigments are not perfectly parallel to the surface of the coatings, but they are tilted, what should cause a slight blurring in the diffraction pattern. In order to describe the diffraction of these coatings, we will consider this lack of parallelism to the surface as a second-order effect.

The spectral bidirectional reflectance distribution functions (BRDF) of five coatings with SpectraFlair diffraction pigments have been measured using the robot-arm-based goniospectrophotometerer GEFE, designed and developed at CSIC. Principal Components Analysis (PCA) has been applied to study the BRDF data of the studied coatings. From the data evaluation and based in theoretical considerations, we propose a relevant geometrical variable to study the spectral reflectance and colour variation of coatings with diffraction pigments. At fixed values of this geometrical variable, the spectral BRDF due to diffraction is constant. Our measurements and analysis have revealed that commercially-available portable goniospectrophotometers, extensively used in several industries (automotive and others), are not adequate to characterize goniochromatic coatings based on diffraction pigments, because assessment at more aspecular angles than available (according to current ASTM and DIN normatives) is required.

OP11

MEASURING GONIOAPPARENT SAMPLES USING A BIDIRECTIONAL SPECTROMETER; AN sRGB VISUALIZATION

Basic, N.[1], Penttinen, N.[2], Urbas, R.[3], Klanjšek Gunde, M.[4]
[1] Institute of Photonics, University of Eastern Finland, P.O. Box 111, 80101 Joensuu, FINLAND (currently at Federal Institute of Metrology METAS, Lindenweg 50, 3003 Bern-Wabern, SWITZERLAND), [2] Focus Action Ltd, P.O. Box 71, 33471 Ylöjärvi, FINLAND, [3] University of Ljubljana, Faculty of Natural Sciences and Engineering, Snežniška 5, Ljubljana, SLOVENIA, [4] National Institute of Chemistry, Hajdrihova 19, Ljubljana, SLOVENIA
nina.basic@metas.ch

Gonioapparent targets, whose appearance depends on illumination and viewing angles, are used in many industrial applications within the printing, cosmetic, automotive and clothing sectors. These targets require control of their sophisticated appearance, as the appearance is one of the most valuable acceptability criteria. The complexity of gonioapparent effects are often represented using the bidirectional reflectance distribution function (i.e. BRDF), which describes spectral reflectance coefficient for illumination and viewing directions. The BRDF can be measured using a bidirectional spectrometer with an independently movable light source and detector. Measured BRDF data can be presented as a matrix of spectral reflectance coefficients or using a goniocolorimetric space as the bidirectional colour distribution function (i.e. BCDF). Representing the BRDF data has in general always been a challenge. Thus, the feasibility and usefulness of such representation was the goal of this study.

Two types of samples were used; 3 diffraction gratings and 3 gonioapparent textiles. One of the diffraction gratings was a semi-transparent overlay, which was measured on top of a black cardboard. Its diffraction period was 900 nm, which was created by altering between a high refractive index material and a polymer. Other two diffraction gratings were an ordinary CD and a DVD, both measured as blank and recorded. Two gonioapparent textiles had the same structure – both were knitted with a basic black thread in combination with differently coloured metallic thread. One sample had a silver metallic thread, giving the textile silver/black appearance. The second sample had a metallic thread, which was on one side coloured magenta and on the other cyan. This textile sample gave a magenta/cyan/black appearance. The third gonioapparent textile was a woven multicolour scarf, weaved with silk warp and weft threads, wherein the weft threads were twice thicker than the warp. The colours of both warp and weft changed along both sides of the scarf, creating a multi-coloured pattern. Thus measurements on the scarf were performed at 6 different areas.

All samples were measured with a bidirectional spectrometer, presented in more detail in *Rogelj et.al. 2015.* The device uses a halogen lamp at an incident angle of 45°, its detector covers polar angles from 0° to 60°, and azimuthal angles from 0° to 360°, with a 2° angle step in both directions. In order to provide maximum signal dynamics, the bidirectional spectrometer uses automatically adjusting exposure time. Although the spectrometer is capable of measuring signal from 200 to 1160 nm with resolution of 0.6 nm, only the visible wavelength range was used (380 – 780 nm) for the purpose of this study. Detector and environmental noise were subtracted from the measurements; normalization was done according to angle and wavelength using a 99 % reflecting Spectralon as a white reference.

BRDF for each sample were used to create a polar coordinate sRGB image, under D65 illumination. This was done because the samples were visually interesting, and sRGB image for a single illumination angle is easy to understand. Each sRGB image presents a circle, where the polar coordinates are displayed from the centre of the image to its edge (linearly from 0° to 60°), and azimuthal coordinates go linearly around the circle from -180° to 180°.

Using the samples described above, this study focuses on how the sRGB images change depending on the sample. Diffraction grating was rotated around its axes to verify how the rainbow diffraction pattern also rotates. CD and DVD samples were measured to establish how the signal changes depending on whether the sample is blank or recorded. They were also

compared with a diffraction grating; here, the influence of diffraction grooves being straight or slightly curved were analysed. At the same time, three different sized measurement areas were used; circles with diameter of 14, 20 and 24 mm. This allowed us to investigate how the size of the sample affects the measurements. Measurement area for all gonioapparent textiles was larger and kept the same for all samples; a circle with diameter of 38 mm. The selection of gonioapparent sample allowed us to systematically verify how the sRGB images, which represents the BRDF, change when the sample gets more and more optically complex. The silver/black textile had the simplest pattern, while the magenta/cyan/black textile had a more complex pattern on the sRGB image, which also changed depending on how the sample was rotated regarding to the light source. The gonioapparent scarf was measured to establish how the warp and the weft affect the sRGB images; some of the measurement areas were selected in which firstly the sample had the same coloured warp with different colour of weft, and secondly vice versa.

This study shows that the sRGB images, which are generated from the polar coordinates, can be a visually appealing representation of gonioapparent samples measured in visual range of wavelengths. While sRGB images of samples differ as soon as they are differently structured, such presentation provides distinguishable and understanding image, which could be used by non-experts as well as by experts for a quick visual comparison.

References

N. Rogelj, N. Penttinen, and M. K. Gunde, “Evaluation of complex gonioapparent samples using a bidirectional spectrometer,” Opt. Express 23, 22004–22011 (2015).

OP12

GONIOCHROMATIC MATERIALS UNDER DIFFERENT LIGHTING CONDITIONS

Iacomussi, P.[1], Radis, M.[1], Rossi, G.[1]
[1] INRIM, Torino, ITALY
p.iacomussi@inrim.it

Abstract

In 2013 the European Metrology Research Program (EMRP) funded a research project about the measurement of quantities related to visual appearance: seven European NMI (National Metrological Institute) plus New Zealand NMI, two Universities and one private research partner, were co-funded in the research, while some thirty international industrial stakeholders supported the “xD-reflect - Multidimensional Reflectometry for industry” project.

The main scope of the project was to improve the measurement methods of optical characteristics and their traceability to SI through multidimensional reflection measurements to meet new demands and needs of industries for new and advanced materials.

The measured quantities involved in the project, Radiometric Bidirectional Reflectance Distribution Function (BRDF), gloss, sparkle and colour, are all related to the visual appearance of the objects: so one additional goal of the project is to investigate about the visual appearance of modern surfaces and materials with innovative effects and their relationship with the measured quantities. In the project several subjective tests on visual descriptors of gloss, sparkle, graininess, colour and their combined influences with condition of observation and lighting were arranged and performed by NMI and Universities.

INRIM, the Italian NMI, performed investigations on subjective descriptors of brightness and sparkling and their relationship with geometrical conditions of view, illuminating source characteristics, radiometric BRDF, colorimetric attributes (CIE L*a*b*, CIE L*C*h) and sparkle.

The paper presents the results obtained by INRIM in several subjective tests that involved about 130 subjects that evaluated sparkling and brightness perceived qualities in different condition of observations using SSL (Solid State Lighting) sources and fluorescent sources, at the same CCT (Correlated Colour Temperature) in different viewing conditions.

The materials, goniochromatics with different mica and rutile particles size distributions and aluminium particles shapes, were metrologically characterized among the project partners using NMI multi-angles measuring devices and portable multi-angles measuring devices, for radiometric BRDF and Sparkle quantities.

Indeed portable multi-angles instruments respond to industrial needs of characterising materials on site for few fixed directions, at low cost minimizing time consuming, but having spectral BRDF and sparkle analysis only for the most interesting geometrical conditions.

INRIM used the measured spectral BRDF values to calculate Lightness (L*) and Chroma (C*) for the different viewing conditions used in the subjective tests (four angular conditions of observation, two condition of lighting and six different lighting sources spectrum) used in the subjective experiment. While the values Sparkle Area, Sparkle Intensity, measured with the only commercial device able to measure it, are photometric quantities related only to geometry of measure and were used only to define a ranking between samples.

The subjective experiments were performed using commercial lighting booth and ad-hoc made lighting observation boxes, both equipped with SSL and Fluorescent sources.

The ad-hoc observation boxes reproduce the angular measurement conditions of portable multi-angle devices to compare measured quantities with perceived quantities in the same angular conditions: 45° incidence direction and 0°, 20° 30° observation (plus a free condition).

Indeed commercial lighting booths are able to provide a diffuse lighting condition with sources closed to CIE reference illuminants (CIE D65, CIE D50, CIE A and shop source TL84).

INRIM has two different lighting booths one equipped with fluorescent tubes and one with LED sources. The lighting booth with LED sources has also the interesting feature of being able to provide a light spectral distribution of a desired CCT. In the subjective experiments both lighting booths were used, considering D65 illuminating source in diffuse incidence condition.

The measured ranking was then compared with the ranking provided by subjects for the same perceived quantities, i.e. sparkling and Brightness, in the same geometrical condition of observation and lighting.

Keys points of the study are:

1. to compare portable device measured results and perceived results, considering the same geometrical conditions: considering ranking uniformities for perceived and measured quantities;

2. to compare perception under SSL lighting and Fluorescent lighting at the same CCT.

The results showed a different behaviour of the two different lighting sources (LED vs Fluo) and also of the two different CCT (cold vs warm). But not only: depending on the lighting conditions (LED vs Fluo) the perceived ranking it is not always uniform with the measured ranking of quantities related to spectral BRDF, i.e. L* vs Brightness, C* vs Saturation. This is mostly due the measurement method: using “integral” detectors, i.e. detector without spatial resolution of incoming radiation like photocells, photodiodes etc., that kind of detectors is not able to discriminate in spectral BRDF measurement the reflected radiation due to sparkling particles from the material mass. With these detectors the whole reflected radiation is measured for the spectral BRDF calculations. Instead a CCD camera (with optical system) is able to discriminate the behaviour related to sparkling particles and to material mass. After all the discrepancies between measured and perceived quantities arrive mostly for quantities measured with “integral” detectors; sparkling ranking is coherent between perceived and measured especially when LED sources are considered.

The analysis of the results involves also the study of the occurrence of equivalence in the perceived quantities: some lighting and observation conditions are more subjected to a lower capacity of subject discrimination among the samples.

Session PA4
Visual Perception - Part 2
Wednesday, September 7, 09:05–10:25

OP13

VISUAL EXPERIMENTS ON THE STROBOSCOPIC EFFECTS OF PWM-MODULATED WHITE LED INDOOR ILLUMINATIONS AND THEIR CONSEQUENCES

Polin, D., Tran, Quoc Khanh
Technische Universität Darmstadt, Laboratory of Lighting Technology, Darmstadt, GERMANY
polin@lichttechnik.tu-darmstadt.de

Abstract

Recently, light emitting diodes have become an increasingly important light source. A huge advantage of LED lighting is the easy implementation of dimming. One of the dimming methods is constant current reduction (CCR method). Due to its high cost and the undesirable effect that the current affects the emitted spectrum, in most applications the pulse-width modulation (PWM method) is preferred to regulate the amount of LED power. Turning the LED on and off at frequencies beyond the visual flicker fusion threshold prevents the perception of single light pulses and allows to control the brightness by varying the on-time of the LED. In some dynamic situations, the flicker of PWM dimmed LED lighting can be perceived indirectly through stroboscopic effects like beads effect, phantom array or wagon-wheel effect.

To assess the ability of individuals to perceive stroboscopic effects, and to understand the role of flicker characteristics on comfort, we conducted laboratory studies under flickering patterns differing in frequency and duty cycle. Different methods to provoke stroboscopic effects were also compared. Building on results from the first study, a method was developed which allows to reduce stroboscopic effects by using low-frequency PWM. This method was examined in the second study.

Methods, first study

Using a controllable LED luminaire in a laboratory environment, 38 healthy observers performed visual assessments of the environment while performing five different tasks at a desk:

1. Taking place at the desk;
2. Fast moving of the cable of a computer mouse while connecting to a laptop;
3. Counting words in a printed text;
4. Hatching a square on a sheet of paper; and
5. Waving of a hand.

The noticeability and disturbance of the stroboscopic effect was rated after each task at several lighting conditions with different flicker characteristics, summarized as follows:

- Frequency (100, 200, 300, 400 and 1000 Hz);
- Duty cycle (20 %, 50 %, 100 %).

Findings, first study

Consistent with published literature, flicker was not directly visible under the examined lighting conditions (frequencies of 100 Hz and higher). Indirect perception of flicker through stroboscopic effects was strongest when performing tasks which require fast movements: moving of the mouse cable, hatching a square and waving one's hand. Performing these tasks, multiple object patterns (cable, pen, hand) were strongly evident to most people. About 30 %

of the participants were able to perceive stroboscopic effects even at 1000 Hz. On average, men were more sensitive than women.

Conclusions, first study

The results demonstrate that when LED light sources flicker at frequencies of at least 100 Hz then direct perception of flicker is not visible, but stroboscopic effects can be detected indirectly at frequencies of 400 Hz and by some people even at 1000 Hz. According to the results, a modulation frequency of about 700 Hz is necessary to avoid stroboscopic effects in typical interior-lighting applications. Furthermore, there are significant flicker and stroboscopic perception differences depending on the factors age, gender or the current mental state of the subject. Also the time of day influences the perception of the stroboscopic effect.

Methods, second study

Building on the results of the first study, mitigation of stroboscopic effects can be accomplished through decreasing flicker frequency and/or through increasing duty cycles. In many lighting applications, several LEDs are used for the illumination. By temporal shifting of their modulation signals, the resulting (i.e. composed) flicker characteristics can be decisively influenced: the frequency and duty cycle of composed flicker can be multiplied, whereas the frequency and duty cycle of modulation signals remain unchanged. We examined this approach in the second study.

In a laboratory environment, the single LED units of four luminaires (consisting four LED units) were controlled by PWM at 100 Hz. Four duty cycles of control-signals were examined: 1, 5, 10 and 20 %. The shifting of control-signals was performed in three ways, as summarized below:

1. No shifting → all LED units flicker synchronously at 100 Hz;
2. No shifting within a luminaire, uniform shifting between luminaires by one quarter of PWM-period → composed flicker frequency at 400 Hz; and
3. Uniform shifting between all LED units → composed flicker frequency at 1600 Hz.

Additionally, five constant light conditions at 1, 5, 10 and 20 % of maximal intensity were used. Each condition was repeated three times in randomised order.

Under each lighting condition, 13 subjects were sitting at a desk and were asked to wave a hand back and forth and to report whether they could detect any flicker or any stroboscopic effect. After that, the test was repeated to examine stroboscopic effects on a rotating black disk with a white dot at the border.

Findings, second study

Consistent with the results of the first study, all participants were able to perceive stroboscopic effects by shifting modes 1 and 2 with small duty cycles (1, 5 and 10 %). At the shifting mode 3 for all duty cycles and mode 2 with 20 %, stroboscopic effects did not occur. This is consistent with the results of constant lighting conditions.

Conclusions, second study

In this study, we showed that our approach reduced the stroboscopic effects significantly. Using temporal shifting it became possible to design lighting systems with low PWM frequencies which do not cause unwanted effects such as electromagnetic interference. Because of possible local effects, we recommend nevertheless to operate at 200 Hz with PWM.

OP14

EXPLORING VISUAL AND VISCERAL QUALITIES OF EQUIVALENT COLOURS UNDER ARCHITECTURAL-SCALE, FULL-FIELD EXPOSURE CONDITIONS

Besenecker, U.C.[1], Pearson, Z.[1], Krueger, T.[1], Bullough, J.D.[2], Walf, A.[3], Gerlach, R.[4]
[1] School of Architecture, Rensselaer Polytechnic Institute, Troy, NY, USA; [2] Lighting Research Center, Rensselaer Polytechnic Institute, Troy, NY, USA; [3] Cognitive Science Department, Rensselaer Polytechnic Institute, Troy, NY, USA; [4] Pantochrome, Salt Lake City, UT, USA
besenu@rpi.edu

Abstract

Colour used in architectural settings impacts our perception of form, space, and ambiance. The increased availability of light-emitting diodes (LEDs) significantly eases the incorporation of luminous colour into the built environment.

LED lighting technology introduces opportunities to mix and match luminous colours in various ways. Using colour matching models (chromaticity), nearly-identical-appearing colours (metamers) can be created that have different spectral compositions depending upon the specific technologies used to create them.

Current work in the perception sciences demonstrates that such colours do not necessarily match in saturation and brightness when viewed with the full-field of view (including the periphery). In addition, health related sciences suggest that different spectra can have distinct physiological and neurological effects even when matched for chromaticity.

We conducted experimental sessions at architectural scale to explore possible differences in visual and emotional qualities for nearly equivalent stimuli, matched very closely for chromaticity and light level.

Two different colour series were tested, amber and cyan, with seven conditions each: colour-filtered tungsten, distinct narrowband LED, RGB source LED, 7-colour source LED, video projector, coloured paint illuminated by white tungsten, and coloured paint illuminated by white LED.

The conditions were visible in four semi-cylindrical spaces (denoted ‘tubicles’) that were 14’ (height) x 9’ (diameter) and allowed for complete immersion into each light and colour condition.

These ‘tubicles’ were installed in a 50’ x 60’ x 32’ black box studio space of the Experimental Media and Performing Arts Center (EMPAC) at Rensselaer Polytechnic Institute (RPI), which made it possible to closely control the lighting conditions as well as the surrounding environment.

We conducted three sets of experiments. About half of the participants were professionals working with light and colour as artists, designers or scientists; the other half were recruited from the general public.

The first study (Study 1) used qualitative research methods; 17 participants completed the study. The participants were free to walk from one ‘tubicle’ to another and compare each condition to a reference from close-up and from afar (two tubicles were illuminated at a time). They were asked to express any comments they had either in writing (note pad) or by speaking aloud. All comments were recorded and subsequently transcribed.

Based on the responses we also conducted a quantitative follow-up study (Study 2) with 12 participants that used a fixed viewing location and a questionnaire. The questionnaire was designed based on the findings from Study 1 with the objective of replicating and reinforcing the findings from Study 1.

Most subjects also participated in a third session (Study 3) where blood pressure was measured in response to all conditions, one after the other, in randomized order.

The results showed that participants perceived reliable differences in the visual qualities of brightness and saturation between the conditions in both Study 1 and Study 2, larger than predicted by the luminance and chromaticity. A provisional brightness model matched the brightness results better in both studies. The results from both studies also suggest consistent differences between the conditions, matched for luminance and chromaticity, in emotional and spatial quality.

In addition, there were statistically significant correlations between the visual qualities of brightness and saturation with spatial and emotional qualities, as well as with measured blood pressure.

The results suggest that methods like those used in these studies may be beneficial for identifying combinations of light level and colour that reinforce certain perceptions about a space using coloured light as a medium.

OP15

COLOUR CONSPICUITY IN A COMPLEX LAYOUT

Ou, L.[1], Liu, M.[1]
[1] National Taiwan University of Science and Technology, Taipei, CHINESE TAIPEI
lichenou@mail.ntust.edu.tw

Abstract

There is an increasing need to enhance visual conspicuity for data visualisation within a complex layout such as showing specific data in a map or a chart. Factors affecting conspicuity in such scenarios include colour, shape, location, orientation and contrast. Little is known, however, about how these factors can be quantified and how to predict their effects on visual conspicuity. The present study aims to investigate the impact of colour on visual conspicuity in a complex array.

METHODS

To address the issues described above, a visual search experiment was carried out using the reaction time technique. A total of 30 observers took part in the study. All observers were university students, and have passed Ishihara's test for colour deficiency.

During the experiment, each observer was first presented with a target colour at the centre of screen of an LCD display. After the observer clicked on the target colour, a full screen of neutral grey was presented for one second, and then a page of 24 colour chips, including the target colour and 23 surrounding colours, i.e. the distractors, were immediately presented. The observer's task was to locate the target colour using a computer mouse, and this needed to be done as fast as possible.

Colours for the target and distractors were selected to cover a reasonable range of hue, chroma and lightness in CIELAB uniform colour space. For each observer, there were 242 trials (including 20 replicated) to complete.

The experimental LCD display was situated in a darkened room, with the only light source coming from the display. The viewing distance was around 500mm between the observer and the display.

A number of assumptions regarding this experiment were made on the basis of our observations of a feasibility study previously conducted:

- The reaction time for locating a target colour among a panel of colours is influenced by the mean CIELAB colour difference between the target and the distractors; the larger CIELAB colour difference, the shorter reaction time.
- The reaction time is influenced by the variation in colour between the distractors; the smaller colour variation between the distractors, the shorter reaction time.
- The reaction time is influenced by the location of the target on the screen; the closer the target is located to the centre of the screen, the shorter reaction time.

RESULTS

To see whether and how colour difference between target and surrounding colours might affect the reaction time, we first calculated the mean CIELAB colour difference between target and distractors, denoted as ΔE_{target}. We also calculated the colour difference among the distractors, denoted as $\Delta E_{distractors}$. Then we divided the former (ΔE_{target}) by the latter ($\Delta E_{distractors}$), denoted as ($\Delta E_{target}/\Delta E_{distractors}$). The reaction time was then plotted against the ($\Delta E_{target}/\Delta E_{distractors}$) variable, indicating that the reaction time increases when the ($\Delta E_{target}/\Delta E_{distractors}$) value becomes smaller.

To see whether the distance between the centre of the screen (i.e. the initial location where visual search was started) and the target when shown among the distractors might affect the reaction time, the experimental data (i.e. reaction time) was plotted against such distance, in terms of the viewing angle. As a result, reaction time is shortest at the smallest viewing angle for both gender groups. However, the longest reaction time was obtained for a viewing angle of about 16°, rather than at a location furthest away from the centre of screen. This tendency seems to be more significant for male than for female. At the smallest viewing angle (measured from the screen centre), the reaction time is the shortest – this may be due to the fact that the area close to the screen centre is the easiest to see. It is interesting to note that for the target colour located at the largest viewing angle, i.e. when the target colour is located at one of the four screen corners, the target did not seem to be difficult to identify. This may be due to the relatively smaller number of distractors in such areas, which may help weaken the effect of distraction caused by the surrounding colours.

CONCLUSION

The experimental results show that the reaction time for locating a target colour among a panel of 24 colours was influenced by the mean CIELAB colour difference between the target and the 23 distractors; the larger CIELAB colour difference, the shorter reaction time. The reaction time was also found to be influenced by the variation in colour between the 23 distractors; the smaller colour variation between the 23 distractors, the shorter reaction time.

Regarding the location of the target colour, the closer the target colour was located to the centre of the screen, the shorter reaction time. It is interesting to note that when the target colour is located at one of the four screen corners, the target did not seem to be difficult to identify.

These findings can be used as guidelines in visual communication design to enhance visual conspicuity for data visualisation in a complex layout.

OP16

STUDY ON VISIBILITY ESTIMATON OF OBJECTS IN COMPLICATED LUMIANCE IMAGE

Nakamura, Y.[1], Kato, Y.[1], Iwata, M.[2]
[1] Tokyo Institute of Technology, Yokohama, JAPAN, [2]Setsunan University, Osaka, JAPAN
nakamura.y.af@m.titech.ac.jp

Abstract

BACKGROUND: In order to maintain visual safety, especially for low-vision people, it is quite important to estimate visibility of miscellaneous objects in the real lit environment. Because it is not so difficult to obtain a luminance image of the real lit environment, it would be reasonable to try to establish a method to predict visibility of those objects by use of such a luminance image. Visibility of objects, as well known, can be estimated by a function of object size, contrast and the background luminance, but as those objects often vary in size and shape and sometimes have very complicated background, it is often difficult to extract those parameters from the luminance image. Contrast profile method would be a possible way to resolve this problem, because it uses image-filtering technique and so is applicable even to a quite complicated luminance image. The authors tried to suggest its possibility.

OBJECTIVE: Two experiments were conducted to obtain threshold conditions of objects in various luminance images displayed on a PC screen, and the result was analysed to examine whether the parameters extracted from those luminance images by use of contrast profile method could estimate visibility of the objects in those luminance images.

METHOD OF LUMINANCE IMAGE ANALYSIS: Contrast profile method[1)] was used to analyse luminance images. In this method, luminance contrast is obtained by convolution of 9 by 9 matrix called n-filter into a logarithmic image of luminance, which is a kind of the Mexican hat filter adjusted as the sum of the central area equals to one and the sum of other areas equals to minus one. A luminance contrast profile of an object was obtained by changing detection size of the filter, and the peak contrast in the profile was defined as the contrast between the object and the background and its detection size was defined as the size of the object. Then the average of the object and the immediate background was obtained by the same size averaging filter as the n-filter in the logarithmic image of luminance. The hypothesis was those three parameters could explain the threshold of the object. This hypothesis was examined by plotting the contrast and the average of the object in a figure called C-A graph, the vertical and horizontal axes of which represented contrast and average respectively.

EXPERIMENT 1: ANALYSIS OF THRESHOLD OF LANDOLT RING GAPS.

The parameters adopted in this experiment were the background luminance varying from 2.5 to 160 cd/m^2, luminance ratio between the Landolt ring and the background, and the gap size. 10 subjects, aged around 23, participated in the experiment. The stimulus was displayed on a PC screen as a luminance image. The result was first compared to several famous previous researches and ensured to correspond well. Then luminance images of the result were analysed by contrast profile and combinations of the contrasts and the averages of the result were examined in the C-A graph. It was found that the thresholds of Landolt rings with various gap sizes could be represented as simple lines in the figure.

EXPERIMENT 2: ANALYSIS OF THRESHOLD OF CIRCULAR OBJECTS IN UNIFORM BACKGROUND AND COMPLICATED BACKGROUND.

Uniform-luminance circular objects, sized from 0.67 to 20 minutes, were presented in the centre of uniform-luminance background on the same PC screen and the thresholds of the object were first obtained. The same 10 subjects as the previous experiment participated in the experiments. After examination of correspondence of the result to several previous studies, 2.5 minutes-sized uniform-luminance circles were displayed on the PC screen with various complicated background and the thresholds were obtained. The luminance images of the

background were a sheet of paper with small folds, a wall paper with several prints, a surface of concrete wall, and three pictures of dense leaves. The threshold luminance images with a simple circle in the centre and complicated luminance distribution in the background were analysed in the same method. The threshold conditions were examined in the C-A graph and were found represented as very simple lines as previous Landolt ring result, although some difference were found between them.

CONCLUSIONS: Three values, namely object size, contrast, logarithmic average, extracted from complicated luminance image by use of contrast profile method could be possible parameters for visibility prediction of objects in a complicated real lit environment.

1) Yoshiki Nakamura and Yukio Akashi: The Effect of Immediate Background Size on Target Detection, Volume 32, No. 2, pp. 74-87, Journal of the Illuminating Engineering Society, Summer 2003

Session PA5
Novel Approaches to Measuring Appearance
Wednesday, September 7, 10:55–12:15

OP17

BRDF MEASUREMENT AND SIMULATION OF PATTERNED SURFACES TO FORESEE ITS VISUAL RENDERING

Turbil, C.[1], Gozhyk, I.[1], Teisseire, J.[1], Obein, G.[2], Ged, G.[2]
[1] Saint-Gobain Recherche/CNRS (UMR125), Aubervilliers, France, [2] LNE-CNAM, Trappes, FRANCE
colette.turbil@saint-gobain.com

Abstract

Surface patterning is a very convenient way to modify the properties of the surface in order to give new function to the substrate as for wetting, haptic, friction or optics. Potential scalability of surface patterning processes gives them a high potential for industrial applications. However, patterning of surface can also impact the macroscopic rendering of the final product. Visual appearance being one of the major criteria for customers, the final aspect of surface can be a limiting factor for the surface patterning.

We focus here on particular patterns that confer to treated surfaces superhydrophobic property. These surfaces are covered with micrometric cylindrical pillars obtained by Micro Imprint process [1]. The spatial organization of pillars (surface coverage rate and spatial organization of the pattern) plays a key role on superhydrophobic property [2]. However, this surface patterning has a visual impact on the surface appearance, which must be fully understood in order to optimize the superhydrophobic properties, while keeping a high level of visual quality. The objective of our study is to bring first pieces of knowledge in the comprehension of the relations between surface patterning, BRDF (Bidirectional Reflectance Distribution Function) and visual appearance. With this aim in mind, we design a large panel of functionalized surfaces to evaluate the impact of each controllable parameter, like pillar covering rate (7 different rates from 1.4 % to 22.7 %) and pillar spatial organization (square and hexagonal lattice organization), on visual aspects.

A full optical characterization of the BRDF of the surfaces has been performed, combining a set of complementary tools. We used a glossmeter of evaluate the specular gloss, a commercial goniospectrophotometer to assess the full BRDF of surface and an ultra-high resolution goniospectrophotometer to investigate the shape of the specular peak according to pattern. In parallel to these optical measurements, visual evaluation has been done in a light booth.

Thanks to those different experimental data, we established a strong link between the BRDF and the variable parameters of the patterned surfaces studied. We find that each parameter is linked to the optical response of the sample, in terms of gloss level and regarding to the spatial distribution of the reflected light around the specular direction.

Moreover this particular spatial distribution of light was confirmed by calculations of light diffraction from periodic structures. Reticolo simulation routine based on rigorous coupled wavelength analysis was used to forecast the spatial distribution of light diffracted from these surfaces.

Finally, given the very specific optical response of our patterned surfaces and taking into account their highly reproducible fabrication process, we suggest the usage of such model samples as reference for the alignment of optical measurement setups.

References

[1] Dubov, A L, K Perez-Toralla, A Letailleur, E Barthel, and J Teisseire. “Superhydrophobic Silica Surfaces: Fabrication and Stability.” Journal of Micromechanics and

Microengineering 23, no. 12 (December 1, 2013): 125013. doi:10.1088/0960-1317/23/12/125013.

[2] Rivetti, M., J. Teisseire, and E. Barthel. “Surface Fraction Dependence of Contact Angles Induced by Kinks in the Triple Line.” Physical Review Letters 115, no. 1 (June 30, 2015). doi:10.1103/PhysRevLett.115.016101.

OP18

3D SURFACE ACQUISITION: COMPARISON OF TWO MICROTOPOGRAPHIC EQUIPMENTS WHEN MEASURING MATERIALS OF CULTURAL HERITAGE

Page, M.J.[1,2,3], Boust, C.[2], Mélard, N.[2], Robcis, D.[2], Obein, G.[3], Ortiz Segovia, M.V.[1]
[1] Océ Print Logic Technologies, Créteil, FRANCE, [2] Centre de Recherche et de Restauration des Musées de France, Paris, FRANCE, [3] Conservatoire National des Arts et Métiers, Saint-Denis, FRANCE
marine.page@oce.com

Abstract

Introduction

Acquisition of information on the 3D topography of material is a well-known tool for monitoring the quality of a product in several industries like mechanics, optics or aeronautics. But surface micro-topography can also be linked to visual attributes of materials like colour, gloss and texture. In the field of cultural heritage, recording the topography of a surface of a fragile art piece at a specific moment offers new possibilities for archeologists and curators, as a tool to establish comparisons before and after restoration works, study materials and techniques, or measure specific features, among others.

The Centre de Recherche et de Restauration des Musées de France (C2RMF), a laboratory entirely devoted to cultural heritage, has two topographical devices which can perform 3D surface acquisitions. They can both record surfaces or profiles on a considered object and extract roughness information, but their working principles are different. One uses chromatic optical aberrations, where the other uses multifocal reconstruction. None of them is conceived to study cultural heritage materials, which present a wild range of gloss and colours, are randomly misshapen, heterogeneous and anisotropic. Now, both are only used for qualitative work on the aspect of surfaces or lengths and depths measurements. Therefore we had to face the following questions: are roughness results from both devices comparable? What are the limits of the instruments on cultural heritage materials? The following study aims to answer these questions by performing a metrological comparison of both devices using a large collection of cultural heritage materials.

Devices

The first 3D surface device of the C2RMF is a micro-topographical station from the Stil © brand (CHR 150N model). Inside the sensor, a chromatic optic decomposes the incident white light into all its coloured wavelengths. The object, placed on a (X, Y) motorized platform, reflects one – supposed calibrated – wavelength, which should provide absolute information in Z. Sensors have a scale of accessible heights: we used mostly the 0-300 µm sensor. Recorded surfaces or profiles are processed with Mountains Map 6.2 or 7.2 software of Digital Surf © (ISO norms).The second instrument is an Hirox © KH-8700 numerical microscope. 3D information is obtained thanks to the Z shifting of the device between selected bounds: multiple captures are merged and contribute to the topographical information. Lighting angles are modifiable, from coaxial to side-lighting. Files are exploited using directly Hirox internal software (JIS norms) or with Mountains Map 7.2 (ISO norms), which allows to obtain more information.

Results

We divide this work in two major parts. First, we did a metrological comparison using standard roughness artefacts. Second, we tested the limits of the devices on cultural heritage materials.

For the metrological study, we work with two types of metallic calibrated test samples: the Mahr © PGN3 and the Flexbar © 16008-CAL standards. Performances of both devices for the computation of roughness have been studied on those targets. Results show that roughness

parameters are equal on both devices. However, our study reveals that this promising result is strongly dependent on the ability of the operator to adjust the height, choose appropriate lighting, tune focalization and magnification, and select the adequate choice of acquisition parameters. We conclude that beyond the software processing, the user's ability to handle the instrument represents the quality of the texture acquisition.

For the test of the limitation of the devices, we selected cultural heritage materials with different appearance properties and representative of different artistic fields: among graphic arts materials, albumin, illustrations and papers; among decorative arts materials, woods, brass, aluminum and lacquer; and others such as varnish, bones, glass and oil paint samples. They have diverse appearance properties: dark and pale colours, rough and flat textures, glossy and non-glossy reflections, translucent and opaque media. At the end, we examined 35 different samples under both Stil micro-topography and Hirox microscope. When possible, roughness measurements were also performed and compared.

As we expected, results show that glossy surfaces create optical aberrations on Hirox microscope and can't be measured properly. Flat and smooth surfaces that do not present the right relief to allow depth of field to decrease with magnification can't be 3D reconstructed by the software. In turn, lacquer, paper or aluminum didn't give any 3D Hirox results. On its side, the micro-topographical device performs well on a large range of materials. But dark surfaces profiles (like lacquer) can't be fully characterized with this device, since they absorb too much of the signal. Just as the Hirox microscope, high gloss surfaces can't be reconstructed because they reflect too much light and saturate the sensor.

For both devices, when they are calculable, roughness parameters showed to provide useful information and to be a really discriminant parameter.

Perspectives

Our conclusions on devices capabilities open new applications for cultural heritage, such as quantitative analysis before and after restoration treatment. This preliminary work is also a first step to explore the links between roughness and others appearance properties, particularly between roughness and gloss. Having the roughness and topographical measurements, we are now planning to acquire the BRDF of the materials studied. Analysis will be done using micro-facets based models. We expect determining an adequate model for different kinds of cultural heritage surfaces.

OP19

CAPTURING MATERIAL VISUALIZATION DATA USING GONIOMETERS

Filip, J., Vavra, R., Haindl, M.
Institute of Information Theory and Automation of the CAS, CZECH REPUBLIC
filipj@utia.cas.cz

Abstract

Reproduction of the appearance of real-world materials in virtual environments has been one of the ultimate challenges of computer graphics. The required material representations depend on the complexity of the material's appearance. They start with a bidirectional reflectance distribution function (BRDF) describing distribution of energy reflected in the viewing direction when illuminated from a specific direction. As the BRDF cannot capture a material's spatial structure, it has been extended to a more general bidirectional texture function (BTF) capturing non-local effects in rough material structures, such as occlusions, masking, sub-surface scattering, or inter-reflections. A monospectral BTF is a six-dimensional function representing the material appearance at each surface point for variable illumination and view directions, parameterized by elevation and azimuthal angles. As the BTF data achieves photo-realistic visualization of material appearance it has high application potential mainly in areas requiring physically correct visualizations ranging from computer-aided interior design, visual safety simulations and medical visualizations in dermatology, to digitization of cultural heritage objects.

The measurement of BTF is, due to its high dimensionality, very time- and storage-space-demanding. A majority of the current BTF acquisition setups are based on either expensive hardware or specialized equipment demanding laboratory assembly and calibration. As such setups are usually composed of research and custom build devices, the resulting measured data will reflect their high development and purchase costs. This consequently limits the number of publicly available BTF samples as well as their usage in real applications.

To evaluate any novel BTF measurement approaches, we need a reference device. For this purpose we use UTIA gonioreflectometer. This state-of-the-art setup consists of the measured sample held by a rotating stage and two independently controlled arms with camera (one axis) and light (two axes). It allows for flexible and adaptive measurements of nearly arbitrary combinations of illumination and viewing directions. Although camera view occlusion by arm with light may occur, it can be analytically detected, and in most cases alternative positioning is possible. Verified illumination and camera arms positioning angular accuracy across all axes is 0.03 degree. The inner arm holds LED light source 1.1m from sample producing a narrow and uniform beam of light. The outer arm holds an industrial full-frame 16Mpix RGB camera AVT Pike 1600C. The sensor's distance from the sample is 2m. Using different optics we can achieved spatial resolution up to 1071 DPI (i.e., 24um/pixel), which constrained maximal sample's size to 44x44 mm. Samples of size up to 139x139 mm can be measured in resolution 350 DPI. A typical uniform measurement procedure capture 81 illumination and 81 viewing directions over hemisphere resulting in 6561 captured HDR images of the material. Although this reference setup allows very accurate positioning and high-resolution data capture its main limitation is that mechanical positioning, exposure, and data transfer of 6561 measurements typically take around 20 hours.

Therefore, we look for faster and more flexible measurement solutions for less demanding applications. One of them relies on sparse capturing of images of material surface for fixed elevations angles and variable azimuthal angles. One set of images is measured using rotation of the mutually fixed light and sensor around the sample, while the other set is obtained by mutually opposite movements of the light and sensor with respect to the sample. In both cases, the camera and light travel full circle around the sample and return to their initial positions.

First, we developed a proof of concept device consisting of a mechanical gantry holding two arms rotating synchronously in either the same or opposite direction. The gantry was built using a toy construction set. We used a single DC motor run at a constant speed and manually

switchable gears. One of the arms holds two LED Cree XM-L with 20 degree optics. The second arm has two positions for attachment of a Panasonic FT3 compact camera. Elevations of the LEDs and camera in both positions are fixed at 30 and 65 degrees. The setup's dimensions are 0.6x0.6x0.4m, and weight of 6kg. The measurement process takes 5 minutes. However, as only a subset of BTF was captured using 200 images the remaining data were linearly interpolated. In total image registration and interpolation takes around 20 minutes.

The promising results of this setup resulted in building an automatic BTF capturing device based on similar concept. Its current configuration uses two independent arms holding three LED lights and three USB cameras of resolution 1.3Mpix. Similarly to the initial setup, it captures sample of size up to 3x3cm with resolution 400DPI. Setup’s automatic calibration, movement of the arms, and capturing of images is controlled remotely from PC and the measurement time is 20 minutes. In contrast to the initial setup, we do not capture video sequence but individual photos of the surface for variable exposures allowing us to capture HDR data. This results in much sharper recorded images and sub-pixel registration accuracy. The setup is portable of weight 20kg and thus can be used for field measurements. Due to a modular concept of the device, one can use up to six lights and cameras and thus adapt the speed of measurement procedure and captured data fidelity to application needs.

We compared performance of these setups with the reference one on a set of materials ranging from leather, fabrics to wood and sandpaper. We rendered the measured BTF on a 3D object. To objectively evaluate our results we ran a psychophysical study on eight naive subjects comparing the measured specimen with the rendered data. We found that the average subject was able to recognize differences between complete and sparse measurements as well as distinction between data from reference and proposed setups. However, high standard deviations in both experiments suggest that feedback significantly depends on personal preference. We assume, that even though the BTF reconstruction from sparse samples is not always physically accurate, the performed perceptual study confirmed our setup captures the overall look-and-feel of a given material's appearance.

We consider that speed, simplicity, and portability of the presented capturing methods will make these approximate BTF measurements accessible even to such applications for which the standard BTF acquisition methods are time-consuming and too expensive.

OP20

AN LED SPECTRUM FOR DISCERNING TEXTURE DETAILS

Xu, L.[1], Luo, M.R.[1,2*]
[1] State Key Laboratory of Modern Optical Instrumentation, Zhejiang University, CHINA,
[2] School of Design, University of Leeds, UNITED KINGDOM
*m.r.luo@leeds.ac.uk

1 Introduction

Appearance perception typically includes components such as colour, texture, gloss and translucency. Texture perception is investigated here. The aim is to understand the LED spectra which can maximise the texture visibility for different real objects. It can be applied to the applications such as industrial inspection, medical imaging, surgical lighting, and fine art textures.

In this paper, a multispectral imaging system (MSIS) was used to identify a set of spectral reflectance representing an object. These were used to design spectral power distribution (SPD) based on a LED tuneable source to maximise the visibility of texture details. Two psychophysical experiments were conducted using simulated samples on a display and using real samples in a cabinet. The results showed that a universal spectrum for all materials to reveal texture is possible.

2 The Design of SPD

2.1 Obtaining spectral reflectance from objects

Here, the 'texture' refers to the visual appearance of a surface, and not to the degree of its physical smoothness. Visual texture of a surface is considered as the non-uniformity of the surface colours. So a hypothesis was proposed that larger mean colour difference of the surface colours will lead to a higher visibility. Based on this hypothesis, a method to design SPD was developed and is described below.

Initially, reflectance images of real materials were captured using a MSIS, which describes each pixel in terms of spectral reflectance from 400-700 nm at a 10nm interval. There were 3 types of real materials in this study, including 3 stone samples, 2 wood samples, and 2 organ samples. Then the k-mean method was implemented to perform colour clustering. Each cluster expresses a group of colours representing the whole real material. Finally, the representative colours of the real material studied could be obtained by averaging all the pixels in each cluster and grouped up according to their categories (stone, wood or organ). Thus 3 reflectance datasets were generated.

2.2 Design SPD of illumination

A tuneable LED lighting system called LEDCube® was adopted here. It contained 11 channels consisting of 9 narrow band LEDs and two white LEDs, covering the whole visible spectrum well. Optimization measures were designed to maximise the mean colour difference of all colour combinations from the spectral reflectance functions as described in the last section. It was calculated in CIECAM02-UCS colour space with constraint (CCT of 6500K and Duv less than 0.0054[1]) and without constraint.

Each SPD was optimised by the 11-channel LEDCube system for different types of materials. It was found that the LEDs peaked at 425, 505 and 660nm[2] are needed regardless of what samples used when CCT and Duv are constrained. Hence, in a constraint condition, different datasets will produce a similar spectrum. While if there is no constraint in CCT and Duv, peaks remained the same for organ samples but changes to 480 and 660nm for stone and wood samples.

3 Psychophysical experiments

Three SPDs were optimized. One was obtained in the constraint condition discussed before. Another 2 were optimized with no constraints in CCT and Duv. At this time, stone and wood

will produce the same SPD (8984K) and organ produced another one (5216K). In addition, four sources closely simulated CIE standard illuminants at 2850K, 4000K, 5000K, and 6500K were also included. In total, all the samples and seven optimized SPDs were included in the display experiment while a wood and 2 organ samples as well as the optimized SPD using organ samples were removed in the physical experiment for the perishability of organs. Twenty normal colour vision observers participated in the experiment according to the Ishihara test. Each sample was assessed twice. In total, 9240 judgements were made.

The display experiment was conducted on a well calibrated monitor, EIZO CG243W, in sRGB mode. All the images were accurately reproduced on the display in a darkened room. Background of the display was set to black to ensure full adaption to the displayed images.

Paired comparison method was adopted in this experiment. For each phase, a pair of images of the same material under different SPD of illumination were displayed side by side. Observers were asked to judge which image in a pair to have higher visibility. Due to different types of samples used, the questions asked were different as listed below:

1) Organ images: Which image in the pair shows larger colour difference between muscle and vessel?
2) Wood and Stone images: Which image in the pair shows more texture details?

For the physical experiment, the real materials were assessed against a black background in a viewing cabinet. Observers were asked to answer the same questions as in the display experiment. They looked at the same sample by exchanging between two sources. A short-memory comparison method is used here with an adaptation period of 60 seconds

4 Results

The results showed that the two sets of experimental results agreed with each other well. This implies that the display experiment based on multispectral imaging technique can accurately represent the results. It was found that the optimized SPDs especially for those with high CCT performed the best, surpassing all the CIE standard illuminants. Overall, it can be concluded that the LED tuneable system is effective to find the desired SPD for different applications. When comparing with the 4 CIE illuminants, those with higher CCT gave a better visibility, which means CCT probably has an impact on discrimination. Most importantly, scores of the SPDs studied showed a similar trend on different samples. This implies that a universal spectrum for all materials to reveal texture is a possibility.

5. Conclusions

A method for designing SPD based on a tuneable LED source was successfully developed for discerning texture details. Three wavelength regions at around 425nm, 480-505 and 660nm were found sufficient to form a white illuminant at arbitrary CCT that can largely improve the visibility of texture, which is independent from sample types. Besides, this study also shows consistency of results between experiments using simulated samples and using real physical ones, indicating the experiment can be easily done on display with a more flexible control of the SPD studied.

References

[1] CIE (13.3-1995) Method of Measuring and Specifying Colour Rendering Properties of Light Sources.

[2] HUNG, P. C., & PAPAMICHAEL, K. Application-Specific Spectral Power Distributions of White Light.

Session PA6
Models and Digital Rendering
Wednesday, September 7, 15:45–17:05

OP21

ACCURATE SIMULATION OF LIGHT DIFFUSION EFFECTS OF STRUCTURED GLAZING BY IMPLEMENTATION OF BIDIRECTIONAL TRANSMITTANCE DISTRIBUTION FUNCTIONS INTO DAYLIGHT CALCULATION SOFTWARE

Vyncke, M.[1], Meulenbergs, M.[1], Moens, J.[1], Leloup, F.B.[2]
[1] Bureau Bouwtechniek, Antwerp, BELGIUM, [2] Light&Lighting Laboratory, KU Leuven, Ghent, BELGIUM
martijn.vyncke@b-b.be

Abstract

There is a general trend towards low-energy retrofits with U-values in glazing ranging from 1.1 to 0.5 W/m²K. These types of glazing typically reduce daylight factors in buildings due to lower Light Transmission Aggregometry (LTA)-values of the glass. Having been confronted with a project where huge overhangs were used, solutions were needed to obtain better daylight factors indoors. Creative, low tech solutions were needed to lower the excessive daylight factor near the windowsill, and to redirect the light further towards the back of the office room.

A first study and inquiry on the usage of cathedral glass showed that these types of glass were used in the past to soften the light and to create a more diffuse light distribution throughout the room. Similar usage has been established in greenhouses. However, while light transmission properties of sun shading fabric and the visual comfort of sunscreens can be quantified according to EN 410 and EN 14501, no recommendations exist for the quantification of visual parameters in relation to structured glazing.

Bureau Bouwtechniek and the Light&Lighting Laboratory of KU Leuven engaged in a research that investigates ways to evaluate the use of (existing) structured glazing in projects where better daylighting properties are required. By redirecting light to the ceiling an overall better daylight factor can be obtained.

An inventory of existing structured glazing of four manufacturers has been made and submitted to lab-tests. The total and specular/regular reflectance and transmittance of 12 samples with 21 possible patterns of light distribution were measured by use of a Hunterlab UltraScan PRO spectrophotometer (d:8° geometry) as a pre assessment of the reflection, absorption, direct and diffuse light transmission properties of the samples. Four samples were considered for further evaluation. Of these samples the Bidirectional Transmittance Distribution Function (BTDF) was recorded for two incidence angles, i.e. 0° (normal incident light) and 30°.The resulting BTDF data were transformed into an appropriate format for implementation in light simulation software, i.e. Relux and Dialux. As a result, daylight simulations of buildings can be performed with accurate input data. As an example, the implementation of the four characterized glazing samples in a public office will be presented and evaluated.

OP22

SPECTRAL IMAGE ANALYSIS AND APPEARANCE RECONSTRUCTION OF FLUORESCENT OBJECTS UNDER DIFFERENT ILLUMINATIONS

Tominaga, S., Kato, K., Hirai, K., and Horiuchi, T.
Graduate School of Advanced Integration Science, Chiba University, Chiba, JAPAN

Abstract

In these days, objects containing fluorescence are widely available in our daily life. Fluorescent materials are used in painted objects, papers, plastics, clothes, and all sorts of things that we may come across each day. Fluorescence is a luminosity phenomenon where a material is first excited by light radiation in a specific wavelength region, and then the excited state relaxation emits light radiation in another longer wavelength region. This wavelength shift causes a compelling visual effect. Many fluorescent objects appear brighter and more vivid than the original object colour based on a non-fluorescent light reflection. When two or more fluorescent objects are located closely, an object surface is illuminated by fluorescence emitted from the nearby object surfaces as an indirect illumination, which causes light reflection and fluorescence excitation on the target object.

In this paper we propose a method for analyzing spectral components from the observed images of fluorescent objects and reconstructing realistic appearances of the fluorescent objects under different illuminations. First, we describe the estimation of bispectral characteristics of fluorescent objects in a scene. The bispectral radiance factor is a function of two wavelength variables: the excitation wavelength of incident light and the emission/reflection wavelength. The two-dimensional characteristics of the bispectral radiance factor are summarized as a Donaldson matrix [1],[2]. We show that the Donaldson matrix at each pixel point on object surfaces can be estimated by the two-illuminant projection method [3] using a spectral imaging system in the visible wavelength range (400, 700 nm). The diagonal in each matrix represents the surface-spectral reflectance, and the lower half of the off-diagonal represents the luminescent component by fluorescent emission. The surface appearance of a fluorescent object consists of both reflected and luminescent components. Therefore, realistic images of the fluorescent objects under arbitrary illuminations can be constructed using the estimated Donaldson matrix at each pixel and the illuminant vector of a target light source.

Next, we consider the mutual illumination phenomenon between the fluorescent objects [4]. When multiple objects are located closely, the phenomenon called interreflection or mutual illumination is observed on the object surfaces. In such a case, the illumination consists of at least two distinct parts: the direct illumination from a primary light source, and the indirect mutual illumination created by light coming from the other object surfaces. The mutual illumination affects the appearance of the object surfaces. The problems of mutual illumination analysis, detection, and estimation were studied in a variety of field such as colour science, imaging technology, computer vision, and computer graphics [5]-[7]. However, in most of the previous studies, non-fluorescent objects were used, but not the fluorescent objects. It should be noted that the mutual illumination phenomenon between the fluorescent objects is composed by two types of mutual illumination, the light reflection and the fluorescence emission.

In this paper, we assume that the mutual illumination is based on only one reflection/emission between two surfaces. Then the spectral composition of the mutual illumination is determined by the multiplication of the two Donaldson matrices of two objects. We show that the spectral composition of the observed image is composed with four components of (1) diffuse reflection, (2) diffuse-diffuse interreflection, (3) fluorescent self-luminescence, and (4) interreflection by mutual fluorescent illumination. The observed image of mutual illumination is then modeled by the sum of multiplication of the spectral component functions and their location weights on the surfaces.

We develop an estimation algorithm of spectral image components from the observed images influenced by the mutual illumination. When the Donaldson matrix of each object surface is estimated by the previous method, the algorithm for component estimation is reduced to the standard solution of a linear least squares estimation. We present an effective algorithm to minimize the residual error of the observed images. We also consider the case that the limited knowledge of the Donaldson matrices is available because of strong mutual illumination influence. The estimated component images are used to construct the images of the same fluorescent objects under different light source. Therefore, the realistic appearances of the fluorescent objects with interreflection effects can be constructed by combining the four component images based on the Donaldson matrices and the location weights.

In experiments, we used a variety of fluorescent object samples made of paints and boards. The spectral images are captured using a spectral imaging system at 5 nm intervals in the visible range (400, 700 nm) under an incandescent lamp and a sunlight lump. We compare the appearances of the reconstructed images on a display device to the observations under real light sources. The feasibility of the proposed method is proved in appearance reconstruction of fluorescent objects with/without mutual illumination effects under different light sources.

1. R. Donaldson, Spectrophotometry of fluorescent pigments, British J. of Applied Physics, Vol.5, pp.210-214, 1954.
2. CIE, Calibration Methods and Photo-Luminescent Standards for Total Radiance Factor Measurements, CIE 182, 2007.
3. S. Tominaga, K. Hirai, and T. Horiuchi, Estimation of bispectral Donaldson matrices of fluorescent objects by using two illuminant projections, JOSA-A, Vol. 32, No. 6, **pp.**1068-1078, 2015
4. S. Tominaga, K. Kato, K. Hirai, and T. Horiuchi, Bispectral interreflection estimation of fluorescent objects, Proceedings CIC23, 2015.
5. J. J. Koenderink and A. J. van Doorn, Geometrical modes as a general method to treat diffuse interreflections in radiometry, JOSA, Vol. 73, No. 6, pp. 843-850, 1983.
6. M.S. Drew and B.V. Funt, Variational approach to interreflection in color images, JOSA-A, Vol. 9, No. 8, pp.1255-1265, 1992.
7. S. Tominaga, Separation of reflection components from a color image, Proceedings CIC5, pp.254-257, 1997.

OP23

TEXTURE SPECTRAL SIMILARITY CRITERIA

Havlíček, M., Haindl, M.
Institute of Information Theory and Automation, Czech Academy of Sciences, Prague, CZECH REPUBLIC
havlimi2@utia.cas.cz

Abstract

A fully automatic texture, or more generally image, quality assessment, and mutual-similarity evaluation of two or more of them, presents a very important but still unsolved complex problem. There is still a pressing need for a reliable criterion for such a validation, e.g., to support texture model development (i.e., a comparison of the original measured texture with a synthesized or reconstructed one, evaluation of optimal parameter settings for such a model) or texture database retrieval. Such similarity metrics also play an important role in efficient content-based image retrieval (e.g., from digital libraries, or multimedia databases). Surprisingly, many already developed approaches are limited to mono-spectral images, which is clearly a major disadvantage as colour is arguably the most significant visual feature.

Three novel spectral similarity criteria capable of assessing spectral modelling plausibility of synthetic Bidirectional Texture Functions (BTF), static colours or hyperspectral textures are presented. The criteria credibly compare the spectral contents of two visual textures. It allows support of the optimal modelling or acquisition setup development by comparing the originally measured target texture with its synthetic simulations. The suggested spectral similarity criterion together with its two perception-relevant modifications, are extensively tested on measured natural BTF textures and an artificial distinctly coloured texture, and favourably compared with twelve alternative spectral similarity criteria. The performance quality of the proposed criteria is demonstrated on a long series of specially designed monotonically spectrally degrading experiments. The validation experiments show that it is possible to conduct spectral similarity checking using our criteria on any image from the synthetic BTF space, and this validation performance also holds for the remaining -- and possibly infinite -- number of synthetic images in the corresponding tested BTF space. Unlike many existing approaches, the criterion is not based on three-dimensional histograms, instead representing the estimate of the image spectral distribution, and requiring a sufficiently large data set, which is seldom available. Our criteria neither require the same size of the compared images, nor do they have any limit on the number of spectral bands. The proposed criterion is the only one to rank flawlessly on all deteriorated textures in all controlled degradation experiments. The presented criteria propose a reliable fully automatic alternative to psycho-physical experiments, which are, moreover, extremely impractical due to their cost and strict demands on design setup, conditions control, human resources, and time.

OP24

USING REFLECTORS FOR ANALYSIS AND ACQUISITION OF ANISOTROPIC BRDF

Filip, J., Vavra, R.
Institute of Information Theory and Automation of the CAS, CZECH REPUBLIC
filipj@utia.cas.cz

Abstract

The most accurate representations of material appearance rely on view and illumination dependent reflectance. If we assume homogeneous and opaque materials we can focus on anisotropic BRDF; a four-dimensional function for each spectral channel. One can simplify this representation to three-dimensional isotropic BRDF by relying only on a relative value between azimuthal angles of light and camera. We focus in our work on anisotropic BRDF, which enormously expands measurement state space due to one more dimension when compared to isotropic BRDF. Therefore, it is time demanding to sample this space uniformly using goniometrs while still maintaining visual quality comparable to isotropic measurements.

In general, anisotropy is the property of being directionally dependent, as opposed to isotropy, which implies identical properties in all directions. In the context of our work, when a material's reflectance is not constant for mutually fixed view and illumination with respect to the rotation of the material around its normal, the material is considered anisotropic. Anisotropic materials are, due to their atypical attractive appearance, often used in achieving an eye-catching look of many man-made products. Fabric, metals and their imitations are probably the most typical examples. In this work we discuss using reflectors for rapid and affordable analysis and measurement of anisotropic BRDFs.

Previous anisotropic BRDF measurement approaches used kaleidoscopically arranged flat mirrors, hemispherical mirrors, off-axis parabolic mirrors, ellipsoidal mirrors, or a combination of concave parabolic and custom-built mirrors. All these setups place the measured material into the focal point of the mirror, share the optical and illumination axis using coaxial pair of camera and projector, and thus allow the recording of multiple illumination or view directions in a single image. The main advantages of such an arrangement are the elimination of any mechanical component in the measurement setup, and capturing of retro-reflections which is impossible by goniometric acquisition techniques due to physical conflict of light and sensor. Disadvantages are a limited range of recorded elevation angles, variable reflectance attenuation across the elevations, or a low dynamic range of the measurements due to using a projector as illumination.

However, the common alignment of the material with the optical axis of the mirror is not ideal as it requires a material sample extraction and positioning inside the mirror. Therefore, we aligned the mirror axis with the surface normal. Our methods use standard reflectors, with an opening at the narrowest part attached to the measured material. This extremely simplifies the material handling process.

Depending on application we use two different approaches. For anisotropic behaviour analysis we use ellipsoidal reflector and uncontrolled omni-azimuthal illumination using flash from the sourcing camera. The reflector is photographed by a compact camera having an optical axis aligned with the reflector axis also representing normal of the measured surface. We do not use any special gantry and the image is taken from a distance 1.5 meters. This is done in order to capture the reflector (diameter 100 mm) approximately symmetrically. As the material sample is not positioned in the mirror's focal point, illumination elevations angles vary across its surface. This allows for the capturing of anisotropic behaviour in the image of material at the mirror opening (25 mm wide) taken by the camera. Each surface location is illuminated from two elevations at azimuths 180 degrees apart. Contributions of these directions are averaged in the captured photo. Mean illumination elevation angle across entire material plane is 50 degrees. When an isotropic material is analysed, the captured image contains a circularly shaped peak in the centre. However, for an anisotropic material we additionally observe a

couple of triangle shaped highlighted areas running symmetrically from the centre to the edges of the opening. Their azimuthal orientation coincides with the direction of the main anisotropy axes, while their width corresponds to width of the anisotropic highlight. The introduced method allows for a very convenient and fast detection of material's anisotropy strength, main anisotropy axes, and corresponding highlights shape in only 3 seconds. This information is beneficial for variety of tasks, ranging from material appearance acquisition to its automatic classification or image-based material retrieval. We validated our detection method on eight complex anisotropic fabric materials and compared their microstructure scans with the detected anisotropy direction recorded by our method. Two of the materials exhibited distinct anisotropy highlights corresponding to two anisotropy axes. Our method reliably detected anisotropy axis (azimuth of anisotropic highlights) as well as their typical profile at elevation 50 degrees.

For BRDF measurement we use a parabolic reflector having a focal point in the centre of the opening. Instead of the flash illumination from the camera, we used a digital projector illuminating the reflector by a controlled ray of light. To guarantee camera, projector, and reflector alignment, we attached them to optical bench. The camera lens is positioned closely to projector emitting window to achieve almost identical optical paths. Distance of camera and projector from the reflector is 1.5 meters. The projector circularly sweeps interior of the reflector by ray of light at various elevations. The light reflects from the material in the reflector opening and from its inner body back in direction of illumination. For each location of the ray a photo of reflector is captured, exhibiting appearance of the measured material for many viewing directions.

Our capturing experiments using parabolilic reflector allowed BRDF acquisition for a range of illumination and viewing elevation angles 25-70 degrees. We tested both of-the-shelf and a custom 3D printed parabollic reflector and obtained promising BRDF results. As the visual, fidelity of captured BRDF is dependent on careful alignment of mirror axis with the projector and camera, one can use a beam-splitter at the cost of losing some illumination intensity. Main advantage of our technique is short BRDF acquisition time (12 seconds), which depends purely on camera frame-rate and the required azimuthal resolution.

Our work shows that ellipsoidal and parabolic reflector mirrors can be used for fast, convenient, and affordable BRDF analysis and measurement of real-world materials.

PRESENTED POSTERS

Session PS1
Presented Posters: Measurement
Tuesday, September 6, 13:20–13:40

PP01

OPTICAL DETECTION SYSTEM FOR MONOCHRAMATIC BEAM GONIOSPECTROPHOTOMETRY

Koo, A.[1], Porrovecchio, G.[2], Smid, M.[2]
[1] MSL, Lower Hutt, NEW ZEALAND, [2] Czech Metrology Institute Okruzni 31, 63800 Brno, CZECH REPUBLIC
annette.koo@callaghaninnovation.govt.nz

Abstract

The design and manufacture of a detection system suitable for an 'underfilled sample' goniospectrophotometer system illuminated by a quasi-monochromatic beam is described and assessed. The detection system is designed to measure light reflected by a sample illuminated by a collimated, linearly polarized output beam of a scanning Czerny Turner double monochromator in conjunction with a Laser Driven Light Source (LDLS). The detection system images an area of 70 mm diameter at a distance of 800 mm into a 25 mm inner diameter integrating sphere on which two sensors are mounted. Several apertures are available to vary the angular resolution of the measured BRDF. Photon detection is performed by a combination of a state-of-the-art small factor photon counter and a Si based detector in conjunction with custom made switch integrator low noise electronics. This hybrid detector covers ten orders of magnitude of linear operation.

Optical design of the detection system was optimised to ensure equal efficiency for both vertically and horizontally polarized light. A mirror rather than a lens was used to avoid inter-reflections and was tilted about both the horizontal and vertical axes by 5.5°. Total reflectance of unpolarised light is therefore obtained by making two measurements with vertically and horizontally polarized incident light. The integrating sphere is machined from sintered halon with three ports – one 10 mm diameter input port for the focussed light from the mirror, and two recessed ports for the sensors. The two sensors, of different surface areas, are positioned so as to maximise the fraction of the interior surface within their field of view while ensuring that they are shielded from the first reflection of the beam in the sphere, and so that they each view a similar portion of the sphere.

The hybrid photon detection system is composed of the latest generation VIS-optimized USB driven photon counter from Hamamatsu H11890 in conjunction with a low photon flux detector (LOFD) [1,2]. The LOFD comprises a state-of-the art Silicon photodiode with custom made high sensitive electronics based on the switched integrator principle [3].

The linearity of the Hamamatsu photon counter was measured to be linear up to 800 000 counts per second, well in agreement with a model based on 20 ns dead time, while the LOFD was has been shown to be linear in the range from about 1 pW to about 10 µW [4]. The power level range from 1pW to 8pW, where the two linear sensors 'dynamic ranges overlap, is used to account for the hysteresis effect in the photon counter. The hybrid photon detection system provides 10 orders of magnitude of dynamic range in the visible spectrum (from few fW to tens of µW) that may be required by the illuminating beam irradiance levels and by sample reflectivity values expected to be measured in different goniometric configurations.

References:

[1] J Y Cheung, C J Chunnilall, G Porrovecchio, M. Smid and E Theocharous (2011) Optics Express **19**(21):20347-63

[2] G. Porrovecchio, M. Šmid, M. López, H. Hofer, B. Rodiek, S. Kück, Comparison down to sub-100-fW optical power level …, Submitted for publication in Metrologia

[3] J Mountford, G Porrovecchio, M Smid and R Smid (2008) Applied Optics **47**(31):5821—5828

[4] K M Nield, G Porrovecchio and M Smid, (2010) CIE x036:2010, Bern

PP02

SPECTRAL BRDF & BTDF MEASUREMENTS USING HIGH RESOLUTION FOURIER OPTICS INTRUMENT

Boher, P., Leroux, T., Bignon, T., Collomb-Patton, V.
ELDIM, 1185 rue d'Epron, 14200 Hérouville St. Clair, FRANCE
pboher@eldim.fr

Abstract

The proposed paper intends to present the last developments of a specific technique for fast BRDF and BTDF measurements. This technique is based on one Fourier optics which is designed in order to convert angular field map into a planar one allowing very rapid measurements of the full viewing cone with an imaging detector. The first commercial version of such type of instrument dedicated to viewing angle measurements of displays was publicly introduced by ELDIM at Eurodisplay'1993 [1]. A multispectral version EZContrastMS to measure the emissive properties of displays was also introduced in 2008 [2]. Since then, the capacity to illuminate the sample and to measure spectral BRDF with this type of instrument has been developed. The first practical application examined by ELDIM was the physico-realistic simulation of displays under external illumination [3-5]. In this case, the intrinsic emissive properties and the spectral BRDF of the display surface are successively measured in order to simulate the aspect of the display under any type of illumination environment. For ray tracing simulation, different algorithms to compress the BRDF data and to interpolate them have also been developed [6]. The specific case of anisotropic surfaces has also been examined [7].

Recently we have presented a new generation of Fourier optics system more compact in terms of size and with excellent specifications in terms of angular aperture, angular resolution and speed [8]. In the proposed paper, we intend to present the new system in details with new results obtained on various type of surfaces: practical examples concerning metallic painting, cosmetic and anisotropic metallic and plastic surfaces will be presented and the best measuring conditions adapted to each case will be discussed. Some of the data will be used for spectral ray-tracing simulations in relation to the different applications.

BRDF of metallic paintings is generally the superposition of an intense specular reflection and low diffusion contribution that give the colour to the painting. Measurement are then very demanding in terms of signal over noise ratio. It is why a new measurement procedure combining the use of various densities and multi-exposures have been developed in this case to allow very realistic ray tracing simulation of cars under any type of outdoor environments.

For characterize of cosmetic foundations and their components it is important to measure the backscattering properties. Our instrument has the unique property to allow illumination and measurement along the same angular direction and is then very useful for that purpose. The backscattering properties of light diffusers will be quantified in relation to their morphology.

Anisotropic surfaces are generally tedious to characterize using standard goniometer because of the great number of measurements required for a realistic simulation. In addition on metallic surfaces with transparent protection layers a complex pattern of interferences fringes can be superposed to the diffusion of the metallic layer and a very high angular resolution is required for the measurements. Different examples of application in this field will be presented. Plastic surfaces are also very often anisotropic. In addition it also necessary to measure the BTDF when thin films are used. Some examples in the field of packaging will be presented.

[1] T. Leroux, "Fast contrast vs. viewing angle measurements for LCDs," Proceedings 13th Int. Display Research Conference (Eurodisplay 93), 447 (1993)

[2] P. Boher, T. Leroux, T. Bignon, D. Glinel, "New multispectral Fourier optics viewing angle instrument for full characterization of LCDs and their components", SID, Los Angeles, USA, May 18-23, P89 (2008)

[3] P. Boher, T. Leroux, T. Bignon, V., Leroux, “Optical measurements for comparison of displays under ambient illumination and simulation of physico-realistic rendering,” Vehicle Display Symposium, Dearborn, Michigan, October 20-21 (2011)

[4] P. Boher, T. Leroux, V. Collomb-Patton, V., Leroux, “Physico-realistic simulation of displays,” Vehicle Display Symposium, Dearborn, October 18-19 (2012)

[5] P. Boher, T. Leroux, V. Collomb-Patton, T. Bignon, “Display Aspect Simulation using Measured Emissive and Reflective Display Imperfections,” SID Int. Symp. Digest Tech. Papers, P44 (2013)

[6] V. Collomb-Patton, P. Boher, T. Leroux, “Wavelet based processing of angular measurements: application to realistic aspect simulation,” 3th International Conference on Appearance, Edinburgh, UK, 17-19 (2012)

[7] P. Boher, T. Leroux, V. Collomb Patton, T. Bignon, “Multispectral BRDF measurements on anisotropic samples: application to metallic surfaces and OLED displays”, Electronic Imaging, San Francisco, USA, 14-18 February, MMRMA-359 (2016)

[8] P. Boher, T. Leroux, V. Collomb Patton, T. Bignon, “New generation of Fourier optics instruments for fast multispectral BRDF characterization”, SPIE Imaging, San Francisco, USA, February, 9398, 16 (2015)

PP03

BRDF MEASUREMENT BASED ON SPECTRAL DIFFUSE REFLECTANCE AND A GONIOREFLECTOMETER

Shitomi, H.
National Metrology Institute of Japan (NMIJ, AIST), Tsukuba, JAPAN
h-shitomi@aist.go.jp

Abstract

Appearance of an object is quite important aspect that gives us the basis to determine our preference or impression to it and that, in many cases, has a certain level of controlling effect on customer's choice of products. Recently, new materials that show prominent visual effect such as goniochromatism, sparkle effects and gloss have been developed and applied in many industries. Rapid growth of the development for such material and their prevalence in various kinds of products have aroused the strong need for metrology to precisely characterize their optical properties and to provide knowledge about the parameters governing their visual appearance, which become the basis to ensure quality control as well as further innovation in material technology. So reflectance colorimetry, especially, the measurement of bidirectional reflectance distribution function (BRDF) and its derivatives, plays a major role in characterizing the optical properties of such new generation materials.

To meet demands from related industries for traceability of BRDF and related measurements, a new gonioreflectometer facility for measuring BRDF, radiance factor and derived visual appearance-related quantities has been built up at National Metrology Institute of Japan (NMIJ). The facility is based on the combination of two mounting stages, each of which is used to mount photo-detector(s) and a devise under test (mainly diffusely reflecting samples for calibration purposes), respectively. The detector stage has a diameter of 1200 mm and revolves 360º around the sample. It is equipped with a disk-shaped optical table that can mount multiple detectors and optical systems to fit for various application, e.g. simultaneous multi-angle measurement etc. The sample stage has six degrees of freedom (x, y, z, θ_x, θ_y and θ_z). Among them, θ_x and θ_z axes revolve 360º that enables us to align the sample to arbitrary direction with respect to an incident angle and an in-plane angle. This basic setup enables us to perform measurements of the directional reflection characteristics of materials with arbitrary angles of irradiation and detection relative to the surface normal. The facility is also equipped with a double-grating monochromator-based light source that emits highly-uniform collimated monochromatic radiation of around 10 mm in diameter from the UV to near IR region, and a detector system that consists of apertures, focusing optics and devices such as TE-cooled Si and PMT detectors with an I-V amplifier, an array spectroradiometer, spot and imaging luminance meter and illuminance meter that can be arranged according to application. The system can measure the reflected radiation from the sample at high grazing angles up to 85º.

In general, determination of BRDF requires the measurement of both direct irradiance on and radiance at specified reflection direction from the sample in absolute scale, which is one of the technical challenges when it comes to achieving the measurement with lower uncertainty. There are two major technical issues attributable to the difficulty. One is the accuracy of radiance measurement that generally done with the combination of a precision aperture on a detector and the measurement distance between the surface of the sample and the reference plane of the detector, that is necessary to define the solid angle. The other is the requirement of high dynamic range measurement between the irradiance on the sample and the radiance corresponded to a reflected component at a specified angle, which generally shows the difference in power level with 3 or 4 orders of magnitude. As a practical solution on these issues, in this study, BRDF has been derived from the spectral diffuse reflectance standard. First, a standard diffusing plate is calibrated against the spectral diffuse reflectance standard. NMIJ has the capability to calibrate the spectral diffuse reflectance in the wavelength range from 250 nm to 2500 nm, which was traceable to the national standard realized based on its own integrating sphere-based absolute reflectance measurements. Then, the monochromatic

radiation is irradiated on the standard diffusing plate, and the spatial distribution of spectral radiant intensity corresponded to the reflected radiation is measured from -85º to 85º with 5º intervals for two orthogonal in-plane angles (0º and 90º). Its spatial integration weighted by the zonal constant can be related to the spectral diffuse reflectance calibrated for the standard diffusing plate, which cancels out geometrical factors such as aperture area and measurement distance, and is used as substitute for direct comparison between incident and reflected radiation. BRDF at a specified incident and reflected geometry can generally be converted to spectral radiance factor by using the coefficient of π.

The current measurement wavelength range is only from 360 nm to 830 nm and the measurement geometry is limited to a few typical ones with specific incident and receiving angles such as 0º:45ºx. The relative expanded uncertainty (k=2) for the 0º:45ºx radiance factor measurement of the standard diffusing plate is 0.52 % to 0.76 % depending on the wavelength. As the next step toward establishing versatile multi-geometry spectrophotometery, it is planned to upgrade the system to cover recommended measurement geometries for metallic and interference samples such as DIN 6175-2 and ASTM E2194. Extending the wavelength range in the UV and near IR range is also planned in the near future.

PP04

EFFICIENT MEASUREMENT OF ANGLE-RESOLVED LUMINANCE DISTRIBUTION WITH IMAGING SENSOR

Yang, T.-H., Yu, Y.-W., Lin, C.-C., Le, M., Lin, Y.-H., and Sun, C.-C.
Department of Optics and Photonics/National Central University, Chungli, CHINESE TAIPEI
thyang@dop.ncu.edu.tw

Abstract

In this work, one efficient measuring scheme is proposed for the measurement of angle-resolved luminance with imaging sensors. Mainly, a Lambertian diffuser transmitting screen is introduced to highly reduce the measuring time. In addition to the light sources, the measuring scheme can be also easily expanded for the measurement on the BRDF and the BTDF of the diffuse surface materials. Finally, some testing examples are also presented in our experiments.

Specific objective -- As the more and more novel lighting applications being brought to the world, the angular luminance distribution provides with solid and complete information in design and in simulation. Actually, the angle-resolved luminance distribution is one of the basic quantities of the light sources/luminaires. Conventionally, the goniometer is the only one solution to collect the whole angular luminance distribution. However, the 4pi angular scanning makes it very time-consuming. Besides, the goniometer also requires a very large space for the 4pi angular scanning. Recently, the imaging luminance measuring devices (ILMDs) have been introduced to improve the above drawbacks of the goniometers. On the other hand, the field of view of ILMD is restricted for better accuracy of angle-resolved luminance. Therefore, there will be more images to capture for collecting the complete 4pi luminance distribution. So, how to efficiently measure the angular luminance distribution becomes an urgent and practical subject.

Method – To extend the field of view, a diffusive transmitting screen is accordingly introduced in the measuring scheme. In our measuring scheme, the light source first illuminate on the screen on a wide area. Then, an image sensor captures the diffuse transmission image on the screen. With the aid of the diffusive transmitting screen, the imaging sensor is able to detect the luminance in the as large angles as possible, and to greatly reduce the number of the images to capture for the whole sphere measurement.

Under such a circumstance, the mapping between the angle-resolved luminance of the light source and the position-dependent illuminance on the screen can be easily formularized. Besides, the BSTF of the diffusive transmitting screen is also characterized. Finally, the image sensor with a macro lens to mapping the transmitting luminance of the screen is also characterized. Then, the angle-resolved luminance distribution can be well recovered from the captured images by the image sensor.

Furthermore, when the tested light sources are replaced with a diffuse material, the BTDF and the BRDF of the diffusive material can be measured almost in the same procedure with appending an extra angle scanning collimating illuminating light source.

Result – The proposed measuring scheme is successfully established. First, the mapping between the angular luminance of the measured light source and the position-dependent illuminance has been analysed and derived. Also, the mapping between the luminance of the diffusive transmitting image and the pixel intensity of the image sensor is analysed and characterized. The BTDF of the Lambertian transmitting screen is also taken into the consideration. In a summary, an efficient measuring system is well analysed and characterized for the measurement of the angle-resolved luminance distribution of a light source.

Except for the exploitation and characterization on the measuring system, we also show the measurement on some characterized samples for the verification. The first example is a Lambertian-like LED chip. The second example is a side-emitting LED chip. The last example

is a diffusive plate. All the examples show the high efficiency and the good accuracy of the proposed measuring scheme.

Conclusion - In this work, one efficient measuring scheme is proposed for the measurement of angle-resolved luminance with imaging sensors. With a Lambertian diffuser transmitting screen is introduced to highly reduce the measuring time. In addition to the light sources, the measuring scheme can be also easily expanded for the measurement on the BRDF and the BTDF of the diffuse surface materials. Finally, three testing examples prove the success of the measuring scheme. This measurement scheme with image sensor does enhance the detection efficiency and reduce the requiring space of the system.

Session PS2
Presented Posters: Perception and Models
Wednesday, September 7, 13:15–13:40

PP05

STUDY ON SPECTRAL CHARACTERISTICS FOR IDENTIFICATION OF SKIN COLOUR OF INJURED JAPANESE PERSONS AT DISASTER SITES

Akizuki, Y.[1], Ohno, Y.[2]
[1] University of Toyama, Toyama, JAPAN, [2] National Institute of Standards and Technology, Gaithersburg, MD USA,
akizuki@edu.u-toyama.ac.jp

Abstract

We have many disasters in Japan every year. It is widely known that response time for saving injured persons alive is within 72 hours, so rescue and medical teams operate whole day through midnight. Limited light source makes rescuers' observing situations significantly more difficult, especially night time and in confined spaces. Recent LED technology can support rescue works, but some medical relief workers warn LED lights make it difficult to observe injured person's skin colour, as LED has distinct spectral distribution from incandescent or florescent lamps. At the relief efforts in confined spaces after earthquake disaster, it is important to diagnose injured persons as a case of crush syndrome or not, based on their skin colour. In order to develop suitable lighting equipment for disaster relief works, we should determine the colour information of skin under various health conditions such as shocked or congested state. Our research aims to extract problems of lighting and visual environment for relief works, and to create more effective lighting equipment in the disaster areas.

In preceding research, we carried out an experiment to collecting skin's spectral reflectance data which were artificially-produced shocked/congested state of healthy subjects. Because the skin colour of the critical patient in shock changes over time widely, therefore we artificially produced the injured skin colour which was the most prominent symptom in shock with the distal ischemia portion of healthy subjects. Subjects were all Japanese: 22 young female (average age of 22.0±4.4 y/o), 15 young male (20.7±2.7 y/o), 15 elderly female (69.3±2.8 y/o) and 15 elderly male (71.7±2.6 y/o). Before an experiment, a subject sits a chair quietly for 60 seconds. Then he put his hand on a table and the skin colour of part of the back of his hand between first metacarpal and second metacarpal was measured as "healthy skin state" by a spectrophotometric colorimeter (CM-2600d, Konica Minolta). After the experiment started (t=0), the subject raised his upper arm, kept the pose for 90 seconds in order not to flow the blood in peripheral part such as hand. The upper arm was wrapped a sphygmomanometer cuff (UM-101, AND). After 90 seconds with keeping the pose (t=90), the upper arm was brought to 200mHg pressure by the sphygmomanometer cuff, and kept the pressure for 60 seconds. The internal bleeding was not appeared. After that (t=150), the subject slowly pulled his arm down on the table, and kept the pose for 60 seconds. And then (t=210), the skin colour of the same part was measured as "ischemia-shocked skin state" by the spectrophotometric colorimeter. The experimental time marked the 240 seconds since its beginning (t=240), the pressure of the sphygmomanometer cuff was reduced to 0mmHg, and the skin colour of same part was measured as "the reperfusion-congested skin state" at 10 seconds intervals for 240 seconds. In this experiment, we set three skin states: healthy skin, shocked skin, and congested skin. As compared with the healthy skin, the shocked skin tended to be more yellowish and to have higher brightness, and the congested skin tended to be more reddish and to have higher saturation. These tendencies were found in most subjects.

According to a typical result of a young female in our previous study, the spectral reflectance of the shocked skin was whitened and higher as compared with healthy skin, especially within a range of 500-600nm. On the other hand, the spectral reflectance of the congested skin was wholly lower than other skin states. This tendency was applicable to many subjects, but we confirmed gender difference and age difference. Thus, we selected four typical subjects' skin data for each subject group.

Unlike the real skin colour, Skin Color Sample (Nihon Shikiken) available in Japan has spectral reflectance distribution with lower reflectance than real skin colour at 600nm and more, even

with same tristimulus values (Yxy) as metamerism. So we used four typical subjects' skin data for each subject group directly instead of Skin Color Sample, in order to examine illuminant spectral characteristics able to distinguish three kinds of skin states (healthy, shocked and congested).

In order to extract a theoretical and ideal illuminant spectral power distributions (SPD) which produces the maximum colour difference ∆E*ab between healthy skin and the shocked skin or the congested skin, we use the RGB white LED Model of the Excel Program NIST CQS ver.9.0.1. In our simulation, the spectral width is fixed at 20nm, and the correlated colour temperature (CCT) is fixed at 6500K and 2700K. The peak wavelengths of RGB LEDs are set up at every 5nm within the range of 450-660nm, and Duv is set up at every 0.01 within the range of -0.02 and +0.02. We found the theoretical and ideal SPD which **produced** the highest ∆E*ab by simulation results; R=660nm, G=555nm, B=460nm CCT=6500K and Duv=-0.02. And the relationship was indicated that lower Duv and higher Qg, produced higher ∆E*ab.

There is no Green LED with 20nm narrow band, therefore we cannot evaluate lighting environment same as the ideal SPD we extracted. So we used NIST Spectrally Tunable Lighting Facility to set up lighting environment similar to the ideal SPD, and conduct the evaluation experiment with one subject with normal chromatic vision. Under the condition of CCT=6500K and Duv=-0.01, skin colour and entire room are looked natural, and ∆E*ab between healthy and shocked skin of typical young female is 0.89 higher than ∆E*ab of reference Daylight 6500K. But, in case of the ideal SPD, ∆E*ab is 3.00 higher than ∆E*ab of reference Daylight 6500K, therefore it is desirable to develop new Green LED with narrow band to distinguish colour of human skin colour.

PP06

DIRECTIONAL LIGHT OF LED ARRAYS AND ITS INFLUENCE ON SHAPE PERCEPTION

Krüger, J.
Federal Institute for Occupational Safety and Health, Dresden, GERMANY
krueger.jan@baua.bund.de

Abstract

Objective:

When looking at a three-dimensional object, the combination of directional light and the surface angle produces luminance variations (luminance distribution) on the object surface, which are referred to as shading. Take for example, parallel light rays of a known direction and a body with Lambertian reflection properties, then the luminance changes on the object surface define the changes of the surface geometry (Horn and Brooks, 1989). In addition to stimuli such as binocularity, object motion, cast shadows and texture (Todd, 2004), the visual system uses the shading to perceive the object shape (shape from shading). From "shape from shading" experiments with circular disks filled with a monotonic gradient on an uniform surround (cups and caps) it is known, that an observer has to make assumptions about the light field and the light direction to perceive the form correctly (van Doorn et al., 2011).

Due to LED technology and the use of LED arrays, light fields are becoming increasingly complex. Directional light, generated using LED arrays is built of from multiple light sources. The spatial separation of the many points of light in the light source produces a variety of light incident directions on the target object, this makes it difficult to estimate the light direction that can lead to a false perception of the object. Our study shows the extent to which the complexity of the light field has an influence on the shape perception. It is hypothesized that more complex light fields are associated with a larger error in shape perception.

Methods:

The influence of the illumination on shape perception was examined on a complexly shaped object (dimensions 18x18x18 cm) with nearly Lambertian reflectance characteristics. In order to compare the shape perception in different lighting conditions with the real geometrical shape, the 3D object was created with 3D printer from a CAD Model.

The object was presented to 48 observers (20-33 years) at a distance of 1.5 m under three different lighting situations. In a balanced repeated measurement plan with two repetitions each subject looked at the object shape twice under two different lighting conditions. To reduce memory effect, the object was rotated by 90 degrees between the two viewings. The lighting situations included a direct / simple lighting situation (separate LED point light source), a diffused lighting situation (fluorescent tubes) and a direct / complex lighting situation (spatially separated LED point light sources). The average luminance were kept constant at the object and the background and were measured with a luminance camera. The lights were turned away from the observer, so that no glare would occur.

The method for the estimation of object shape is originally used in the field of "Computer Vision" (Todd et al., 1996) and has been adapted for use in real lighting scenes (Krüger, 2014). The participants had to estimate the angle of the surface at 68 different points (gauge figure task after Todd et al.). With the data gathered using two different lighting situations, internal representations of the perceived object shape could be recreated (Wijntjes, 2012). After the reconstruction of the perceived object shapes we calculated the root mean square error (RMSE) as a quality criteria for the match to compare the subject data with the real dimensions of the CAD model. For the statistical analysis, a linear mixed model (GEE-regression model with fixed and random trend components) was used. In addition to shape perception we asked the subjects about the effort they needed to apply to obtain a result.

Results:

In the statistical analysis, the following model effects were considered: pass (first pass, second pass), lighting (direct / simple, diffuse, direct / complex) and object rotation (upright, rotated 90°). Significant effects on shape perception were observed in pass and lighting. The object rotation had no measurable effect on the shape perception ($p = 0.748$). The significant effect of the pass ($p = 0.000$) indicates a learning effect during the evaluation of the object.

Furthermore, illumination had a significant effect ($p = 0.0007$) on shape perception. The pairwise comparisons between the illumination conditions show a significantly worse shape perception in direct / complex lighting. Shape perception in direct and diffuse / simple lighting revealed no significant difference but the regression coefficients point to a better shape perception in direct / simple lighting.

The analyzes showed no difference in effort values in regard to lighting, pass or object rotation.

Conclusions:

The results are therefore surprising, since direct lighting conditions usually improve plasticity and perceived depth of the object. In this experiment the assumption, that direct light improves plasticity was confirmed only for the direct illumination by a single light source. The direct light of several spatially separated light sources led however, to a significant deterioration in the perception of form. Thereof the depth compression of the diffuse illumination is reflected in the test results, but showed no significant effect. The results suggest that complex, inconsistent light fields affect the shape perception, whereas consistent, simple light fields promote the correct shape perception.

The experimental results could have significance for the lighting of workplaces, in particular when it comes to the recognition of expression on faces (modelling of faces). Good modelling facilitates communication and the interpretation of facial features. In the CIE "Review of Lighting Quality Measures for Interior Lighting with LED Lighting Systems" (CIE 205:2013) it is pointed out that for modelling a new quality standard is required. With this method shape perception can be investigated, depending on different modelling indices. Finally, these results may also be important for assembly workers. For example, it is known that the visual system uses shape information of objects in the grasping process in order to control motor actions (Keefe et al., 2011).

Literature:

CIE 205:2013 (2013) Review of Lighting Quality Measures for Interior Lighting with LED Lighting Systems. In, pp 1-26, International Commission on Illumination, Wien.

Horn B, K. P. , and Brooks M, J., Eds. (1989) Shape from shading. pp 577, MIT Press.

Keefe BD, Hibbard PB, and Watt SJ (2011) Depth-cue integration in grasp programming: no evidence for a binocular specialism. Neuropsychologia 49:1246-1257.

Krüger J (2014) Untersuchungsansatz zur Feststellung der Auswirkungen von LED-Mehrfachschatten auf die Formwahrnehmung. 60Frühjahrskongress der GfA - Gestaltung der Arbeitswelt der Zukunft:714-716.

Todd JT (2004) The visual perception of 3D shape. Trends in Cognitive Sciences 8:115-121.

Todd JT, Koenderink JJ, van Doorn AJ, and Kappers AML (1996) Effects of Changing Viewing Conditions on the Perceived Structure of Smoothly Curved Surfaces. Journal of Experimental Psychology: Human Perception and Performance 22:695-706.

van Doorn AJ, Koenderink JJ, and Wagemans J (2011) Light fields and shape from shading. Journal of Vision 11(3):1-21.

Wijntjes MWA (2012) Probing pictorial relief: from experimental design to surface reconstruction. Behavior Research Methods 44:135-143.

PP07

COLOUR SURFACE RENDERING: A NEW ASPECT OF LIGHT SOURCE COLOUR QUALITY FOR MUSEUM LIGHTING

Bodrogi, P.[1], Stojanovic, D.[1,] Tran, Quoc Khanh[1],
[1] Technische Universität Darmstadt, Laboratory of Lighting Technology, Darmstadt, GERMANY
bodrogi@lichttechnik.tu-darmstadt.de

1. Objective

The objective is to investigate in visual experiments how the visual colour quality attributes including the impression of coloured surfaces vary with the illuminant's relative spectral power distribution and the level of (over-)saturation for paintings in the context of museum lighting. In the experiment, a wide range of different spectra generated by a multi-LED light engine was used. The painting selected had delicate colour shadings of the paintbrush work of the artist. It was illuminated at 750 lx with different CCTs and different amounts of object over-saturation. Subjects had to assess four main visual attributes about the colour appearance of the objects on a questionnaire: general colour preference, naturalness, vividness and the perceived quality of spatial colour (continuity of colour transitions, colour shadings) under the given light source.

2. Hypotheses

To predict the above visual attributes by different colour quality metrics, we are working with the following hypotheses:

1. CCT and the amount of object oversaturation are important predictor variables;

2. Visual attributes can be predicted by suitable (linear) combinations of at least two colour quality metrics including a new colour surface rendering index (CSRI), see below;

3. Distortions of the chroma histograms of the coloured object surfaces of the painting captured by an imaging colorimeter (a pixel-resolving CCD camera with filters matching the colour matching functions of CIE 1931) and caused by discontinuous (highly oversaturating) multi-LED spectra deteriorate spatial colour impression and influence the visual attributes. E.g. if the painting depicts a pink rose with delicate surface shadings and it is illuminated by a multi-LED spectrum with a very high red LED peak then the shadings of the rose become invisible and the visual spatial colour attribute (and also the other attributes) tend to decrease. To quantify this effect, a "colour surface rendering index (CSRI)" derived from the chroma histograms of selected regions of the painting is used to characterise the spectral power distribution of the light source.

3. Chroma histograms of coloured surfaces and their distortions

The above mentioned chroma histograms of the coloured surfaces of the painting change with the type of the illuminating spectrum in a characteristic manner. If the colour rendering index is the highest at the given CCT (which corresponds to approximately zero over-saturation of the painting compared to the reference illuminant) then broad and smooth chroma histograms can be obtained which makes the colour shadings, colour transitions more visible. A moderate oversaturation does not distort the chroma histogram very much so that the perceived quality of spatial colour remains good but it increases the colour preference, naturalness and vividness attributes scaled by the observers. A too high degree of oversaturation, however, distorts the perception of colour transitions (the painting becomes rather decorative with certain regions looking homogeneously). This effect can be predicted from the distortion of the chroma histogram of the painting: the histogram shifts toward higher chroma so that lower chroma values disappear. The consequence is a deterioration of perception.

4. The colour surface rendering index (CSRI)

To describe the above effect, a colour surface rendering index (CSRI) was defined in the following way: the absolute value of the difference of the CIELAB chroma (C^*) histograms of the selected region of the painting under the test and the reference light sources is computed at every chroma value (with a resolution of $\Delta C^*=1.0$) and these differences are summed up (Δn) and then CSRI = 100 – k Δn. In the conference, results of the above described visual attributes from 20 observers, 1 painting, 4 CCTs (2700 K, 3100 K, 4000 K, 5600 K) x 6 levels of oversaturation will be presented. These results will be predicted in terms of suitable predictor quantities: linear combinations from the new CSRI, IES Rf, CCT and the amount of oversaturation of the painting colours caused by the test light source. The resulting equation can be used to optimise the illuminating spectrum for museum lighting for every painting separately in order to render its spatial colour distributions optimally - provided that the painting is captured by an imaging colorimeter so that its histogram distortions can be analysed. From the semantic scale for visual attributes (e.g. very good, good, tolerable, not tolerable) a corresponding semantic scale for CSRI will be determined and analysed in the final paper to be presented at the conference.

PP08

COLOUR VISUAL EFFECTS OF STEADY STATE EXPERIMENTS IN DIFFERENT THERMAL ENVIRONMENTS AT AN OFFICE TEST SITE

Yoshida, Y.[1]*, Kuno, S.[2], Takahashi, H.[3], Nakayama, H.[3], Kato, N.[3], Miyaoka, Y.[3], Noguchi, Y.[4], Nakagawa, T.[4]
[1] Osaka University, Osaka, JAPAN, [2] Nagoya University, Nagoya, JAPAN, [3] CHUBU Electric Power, Nagoya, JAPAN, [4] TOSHIBA Lighting & Technology Corporation, Tokyo, JAPAN
* yoshida.yukiko@mail.osaka-u.ac.jp

Abstract

Light-emitting diode (LED) lighting can be used for spectral control, and through the use of this technology, real-time illuminance and colour temperature modification is possible. Preferred illuminance and colour temperature were related to each other which Kruithof said in 1941.

We experimentally adjusted the predicted mean vote (PMV) values and lighting environment at a test site located at CHUBU Electric Power Co., Nagoya, where the thermal environment could be controlled with a high degree of precision and accuracy. This office test site was 3.45 m in length, 3.3 m in width, and 2.4 m in height. In addition, it contained two LED lights and workspaces for four people in Japan. Partitions were placed on each desk to prevent each participant from being able to see the answers provided by the others during the experiment. The illuminance and colour temperature settings were adjusted at each desk, and the areas shaded from the lights were not included in the adjustment. Participants wore clothing (white shirts and black pants to simulate common office styles) adjusted to suit each season.

In each test scenario, we questioned at least six people about their perceptions of the comfort of their working environment. We then examined the relationship between the physical environment and subjects' psychological perceptions. Steady state experiments were performed four times (in the summer and fall of 2014, and in the winter and spring of 2015), and the colour temperature was varied from 5000 K via 4000 K to 3000 K. Each colour temperature lasted for thirty minutes and continuously varied by 1000 K in ten minutes, while the thermal environment remained constant. Before the experiment, each participant was kept in a state of rest for 1 h. During the test, we gave the subjects instructions via a transceiver while answering in the questionnaire.

We assessed the illumination value intensity that the people's eyes received from the light source indirectly; its unit is lx. And, we evaluated relationship between lighting space concerning comforts and energy saving.

Moreover, we adjusted the physical quantity effect on "hot-cold"," warm-cool" and "comfortable-uncomfortable", and brightness at the same eyes view. Then, the brightness and colour rendering properties indicated the same value physically by measurement. From the point of an optical parameter, brightness reflects the internal relation between direct (light directly irradiates to people's eyes) and illuminating quality.

In each colour temperature, psychological evaluations were conducted four times by using a personal computer typing test and the Uchida-Kraepelin test. The estimated metabolic rate was 1.1 MET. The air in the room moved horizontally at a speed of approximately 0.2 m/s. In the office space, we examined the optimal comfort range for enabling ideal physiological responses, energy reduction savings, and enhanced workplace productivity. By referencing the PMV meters, we could monitor the room environment.

Participants answered questions about their comfort and working efficiency in terms of "writing by hand," "reading hard copy," "typing on a computer," "talking," and "resting." Phrases such as "hot," "feel air flow," and "acceptable" were presented for response under each scenario during the questioning.

In the spring experiment, we changed the order of the colour temperature from 3000 K to 5000 K. Others were the same experimental protocol.

Photos from eyes view in each case of different colour temperature show that it made at equal illuminance and brightness when preference judgements are not same. The differences may be explained only by preferred appearance.

Consider the judgements of the space from an office test site; at equal illuminance and equal colour rendering properties, preferred brightness has a certain range when colour temperature changes and for different thermal environments. Even if it was equal brightness where LED illuminance and colour temperature were same, the physical quantities were tended to be higher preferred brightness.

In steady state experiments, especially in the interim periods such as autumn and spring, we could observe a change corresponding to the hue-heat effect on hot-cold, warm-cool, and comfortable-uncomfortable feelings of the subjects based on the colour temperature. It means that we could not find the hue-heat effect in winter and summer.

At that time, the physical quantities of luminance, illumination, and colour rendering properties were almost same. Therefore, psychological evaluations such as “hot-cold”,” warm-cool” and “comfortable-uncomfortable” effect from colour temperature difference and thermal environment in physical quality of indoor environment.

Further, same physical quality of lightings felt different psychological evaluations under the same colour temperature in different thermal environments. The conception of thermal environment brings comfort and pleasure to people’s feeling, both physical and mental.

Then, we evaluated the comfort zone of Kruithof; hotter or colder thermal environments were associated with different comfort values under the same lighting conditions.

The comfort range was affected by not only the colour temperature, but also the thermal environment.

Thus, these data will be valuable for designing office lighting for optimal comfort and energy control. Additionally, when we design an office room, we should consider the room humour and the physical quantity from eyes view in each season. Thermal comfort and preferred brightness should be matched when we design an office room.

PP09

COMPREHENSIVE SCATTER MEASUREMENT AND MODELING

Mäder, J.[1], Schumacher, V.[1], Weißhaar, J.[1], Steidle, J.[1]
[1] opsira GmbH, Weingarten, GERMANY
info@opsira.de

Abstract

Surface and volume scattering models based on measured data obtain realistic simulation results of optical systems. Unfortunately, the required measurement data (resolution, size, coordinate system and format) differ between every single simulation tool, so a conversion between the different formats is only possible by reservations. Further, the interpolation between different measured angles of incidence, which is done in the optic simulation tools at the moment, results in different simulated scatter characteristics.

opsira is engaged in a long-term research project focusing on the simplification and reduction of the extensive measurement efforts and the development of a uniform definition of those scatter models.

The measurement effort can be minimized by sampling the scattering distribution of a probe with a reduced number of measurement points. A higher resolution is chosen for areas of scattering distributions with an important slope than for areas with a low angular variation.

An additional reduction of the measurement time can be reached by using modern state of the art measurement techniques, i.e. the opsira goniophotometer robogonio, allowing the measurement of the BSDF “on the fly”. This technique allows the measurement of a BSDF within a few minutes, reaching the angular resolution, repeatability and dynamics of conventional BSDF measurement systems.

The measurement results are mathematically fitted on an algorithm so that the measurement data can be reduced to a limited set of parameters or functions. These algorithms describe the complete scatter distribution of a sample at every angle of incidence.

POSTERS

Poster Session 1

Tuesday, September 6, 13:45–15:15

PO05

PREFERABLE LIGHTING CONDITION TO IMPROVE APPEARANCE OF WOMAN'S FACIAL SKIN WITH COSMETIC FOUNDATION

Okuda, S.[1], Komai, K.[1], Tanigawa, Y.[1] and Okajima, K.[2]
[1] Doshisha Women's College of Liberal Arts, Kyoto, JAPAN,
[2] Yokohama National University, Yokohama, JAPAN
sokuda@dwc.doshisha.ac.jp

Abstract

The appearance of women's facial skin with make-up is one of the important factors for their own fashion and self-expression in daily lives. The colour appearance of the skin depends on the spectral distribution of the luminaires. This study aims to clarify the preferable lighting conditions for the improvement of the appearance of woman's facial skin with cosmetic foundation. We conducted an experiment under some lighting conditions differing in the spectral power distribution.

We set up the lighting conditions using a wavelength programmable light source (One Light Spectra, One Light Corporation) which enable to create arbitrary spectral power distributions. First, we set three types of spectral power distribution, linearly increasing distribution (2895K), flat distribution (5656K) and linearly decreasing distribution (9177K) ranging from 435nm to 637nm. A specific wavelength's component from 424nm to 636nm was added on these three types of spectral power distribution in 8 or 9nm pitch. In total, we set up 78 kinds of lighting condition with different spectral distributions.

We prepared a female model, who was 22 years old and with make-up as usual. We measured the chromaticity values of her face using a 2D colorimeter (UA-1000, Topcon Co.Ltd.) under the 78 lighting conditions. Measured chromaticity values of the face were transformed into their respective RGB values using the calibration data of an LC-display used in this experiment. Each generated image of the woman's face was presented on the display. Participants observed the lower half of the woman's face, especially the lower cheek, and evaluated "naturalness," "activity", "sophistication" and "preference" with a numerical scale from -10 (bad) to +10 (good) in each visual image. The eighteen participants were all female in their twenties, and all had normal colour vision.

According to the results in the linearly increasing distributions, the results of "preference" under the lighting with added components of medium and long wavelength, 494-637nm, were all negative evaluations. The evaluation of preference under the lighting with added component of 443nm was higher than that under the lighting with added 512-579nm, and also that the preference under the lighting with added component of 553nm was lower than that under the lighting with added 435-486nm (P <.05). In the case of the flat distribution, the results of "preference" under almost all lighting conditions were positive evaluations. The "preference" under the lighting with added component of 621nm was higher than that under the lighting with added 520-562nm whereas the evaluations under the lighting with added 528nm and 562nm were lower than that under the lighting with added 469-486nm and 595-637nm (P <.05). In the linearly decreasing distributions, the "preference" evaluations under the lighting with added component of medium wavelength were negative. The evaluation under the lighting with added component of 621nm was higher than that under the lighting with added 477-570nm whereas the "preference" under the lighting with added 536nm was lower than that under the lighting with added 435-469nm and 579-637nm (P <.05). These results showed that the facial skin with make-up did not look preferable by the lighting including components of medium wavelength, approximately 528-562nm, suggesting that the lighting excluding these components of medium wavelength makes the face preferable.

Next, we analyzed these evaluation results with a multiple regression; "preference" was used as the response variable, and "naturalness", "activity" and "sophistication" were used as the explanatory variables. As a result, it was derived that the standardized partial regression

coefficient of “naturalness” is 0.565, that of “activity” is 0.253, and that of “sophistication” is 0.299.

Furthermore, we examined the correlation between these evaluation results and *CCT*, *Duv* and other kinds of index or scale on the colour appearance; *Ra*, *CQS*, *GAI* and *PS*. As a result, there are high correlations between the evaluation of “naturalness” and *Duv* (R = -0.80, -0.006 ≤ *Duv* ≤ 0.016), *CQS* (R =0.83, 80.1 ≤ *CQS* ≤ 99.1), and *GAI* (R =0.76, 34.4 ≤ *GAI* ≤ 105.0). It was found that the evaluation of “activity” is correlated to *Duv* (R = -0.76, -0.006 ≤ *Duv* ≤ 0.016), and that the evaluation of “sophistication” is highly related to *CQS* (R =0.88, 80.1 ≤ *CQS* ≤ 99.1) and *GAI* (R =0.76, 34.4 ≤ *GAI* ≤ 105.0). Also, there are high correlations between the evaluation of “preference” and *Duv* (R = -0.84, -0.006 ≤ *Duv* ≤ 0.016), and *CQS* (R =0.78, 80.1 ≤ *CQS* ≤ 99.1).

In conclusion, the component of medium wavelength in the lighting deteriorates the appearance of women’s facial skin with cosmetic foundation. Also, preference of the women’s face can be evaluated by *Duv,* and *CQS*.

*This study was supported by JSPS KAKENHI Grant Number 25282006. We would like to thank Masuda M. who is a graduate student in YNU for generating the visual images.

PO07

INFLUENCE OF DIFFERENT ROOM SURFACE COLOURS ON THE MELANOPIC FACTOR

Knoche, S.[1], **Kirsch, R.**[2],
[1] ITZ Innovations- und Technologiezentrum GmbH, Arnsberg, GERMANY
[2] TRILUX GmbH & Co. KG, Arnsberg, GERMANY
[1] s.knoche@tx-itz.com, [2] raphael.kirsch@trilux.com

Abstract

Objective

Current research in the field of non-visual lighting effects recently resulted in the standardisation of the relative melanopic spectral sensitivity function s_{mel}, (cf. DIN SPEC 5031-100:2015-08 (DIN, 2015)) and derived figures such as the melanopic factor $a_{mel,v}$. Both factors describe the melanopic efficiency of different light source spectra and can be used in lighting design by determining a “melanopically weighted” irradiance at the observer’s eye level.

In a real-world lighting application, only parts of the luminous flux of a light source directly reach the observer’s eye. Depending on the light distribution and orientation of luminaires, a considerable amount of light is first reflected by different room surfaces before actually contributing to any melanopic effect at eye level. If the reflectances of all room surfaces are spectrally non-selective, this does not lead to changes in $a_{mel,v}$. However, if room surfaces are coloured or consist of natural materials, this significantly changes the spectral composition of the indirect part of the illumination, and thus, $a_{mel,v}$.

Methodology

To quantify the effects of different paints and materials of room surfaces on $a_{mel,v}$, spectral reflectances of different colour samples were simulated under different light spectra. CIE-1974 test colour samples 1-14 (CIE, 1995) and samples of the MacBeth Colorchecker (McCamy, Marcus, & Davidson, 1976) were used to cover a wide range of standardised colours. Spectra of two typical phosphor-converted LEDs (ccT=2700 K and 6500 K) were used in the simulations. To estimate the proportion of indirect and thus, spectrally altered illumination in a relevant working environment, three typical office lighting applications were simulated using direct, direct/indirect and solely indirect lighting solutions.

Results

As expected, the results showed a strong dependency of $a_{mel,v}$ on the spectral characteristics of the reflecting colour sample. While red, yellow and brown tones significantly decreased $a_{mel,v}$, purple, cyan and blue tones were able to increase the melanopic factor by up to more than 300 %. For different shades of green the results were more diverse depending on the tone. While a yellowish green decreased $a_{mel,v}$ by around 30 %, a more blueish green has the opposite effect (~+35 %). In general, the change in $a_{mel,v}$ also depends on the light source spectrum. This effect, however was observed to be relatively small overall, but more noticeable in the cyan and blue tones, where the increase of $a_{mel,v}$ was greater for the 2700 K spectrum.

While the office lighting application with purely direct luminaires provided a direct to indirect ratio of about 1:0.6, the ratio for the direct/indirect solution was closer to 1:1.5. Of course, the indirect installation provided indirect light only.

Conclusions

The colour of room surfaces has a strong influence on the melanopic factor of the indirect part of the illumination. Thus, it is not sufficient to use the spectrum of the light sources and the illuminance at eye level in an investigation of the non-visual efficiency of a lighting installation.

Spectral characteristics of large surfaces within the space and the proportion of indirect light at the observer's eye level also have to be considered to obtain meaningful estimates of $a_{mel,v}$.

References

CIE 13.3-1995 Method of Measuring and Specifying Colour Rendering Properties of Light Sources. CIE: Vienna, A.

DIN SPEC 5031-100:2015-08 Optical radiation physics and illuminating engineering – Part 100: Melanopic effects of ocular light on human beings – Quantities, symbols and action spectra. Beuth: Berlin, D.

McCamy, C., Marcus, H., & Davidson, J. (1976). A color-rendition chart. *Journal of Applied Photographic Engineering*, *2*(3), 95–99.

PO08

CHARACTERIZING COLOURFULNESS AND GAMUT AREA OF WHITE LIGHT SOURCES, IN ADDITION TO COLOUR FIDELITY

Teunissen, K.
Philips Lighting Research, Eindhoven, NETHERLANDS
kees.teunissen@philips.com

Abstract

The objective of this paper is to present the importance of selecting appropriate test-colour samples for reporting variations in colourfulness and gamut area index for white light sources, in addition to colour fidelity. Also the impact of the reference illuminant on the reported colour quality attributes will be evaluated for a wide variety of white-light sources.

Since the last update of CIE publication 13 (CIE 13.3, 1995), many proposals have been published for updating the general colour rendering index (R_a). CIE TC 1-90 (Colour Fidelity Index) and TC 1-91 (New Methods for Evaluating the Colour Quality of White-Light Sources) are reviewing alternatives for the CIE general colour rendering index and aim at publishing their reports in this year (2016). Unfortunately, TC 1-90 only addresses colour fidelity, whereas TC 1-91 addresses new methods for evaluating colour quality of white light sources, explicitly excluding colour fidelity. Light quality, however, is defined by several perceptual attributes and their combination into light quality is application dependent and task specific (Teunissen *et al.*, 2016a, 2016b). A good description of the perceptual attributes together with models that predict the sensory strengths from the physical characteristics are essential for predicting the light quality for a specific application. To determine the contribution of individual perceptual attributes to colour quality, it is necessary that visual models are based on the same physical parameters (e.g. test-colour samples) and the same calculation methodology (e.g. colour space, colour matching functions and chromatic adaptation models).

There are examples of white-light quality evaluation proposals that use a combination of index values based on the principles listed above (e.g. Rea *et al.*, 2008; Houser *et al.*, 2013). A recently published proposal (IES TM-30-15, 2015) has been developed by David *et al.* (2015). This proposal includes 99 colour evaluation samples (CES) and a uses more recent colour space and chromatic adaptation function from which a fidelity index, a gamut area index and a colour vector graphic are computed. A statistical process was used for selecting the CES with the requirement to obtain a uniform distribution in the 3-dimensional CAM02-UCS (Luo *et al.*, 2006), within the NCS gamut boundary, and an equal contribution of all wavelengths to the fidelity index. A disadvantage of this selection process is that the resulting individual CES are scattered in the two-dimensional colourfulness space and consequently the individual CES cannot easily be used to calculate changes in gamut area between the reference illuminant and the test light source. To overcome this problem, the CES are distributed over 16 hue-angle bins in which an average colourfulness value is computed, for both the reference illuminant and the test source. However, four new problems are introduced by clustering the CES into 16 hue-angle bins. The first problem is that the average colours do not represent the changes for the individual CES (some CES in a hue-angle bin may show large colour shifts whereas other CES may show small colour shifts), the second problem is that the number of samples in a hue-angle bin depends on the correlated colour temperature (CCT) of the test source (a small change in CCT may have a relatively large impact on the obtained gamut area index), the third problem is that not all CES within a hue-angle bin have the same lightness value (although perceived colour differences may be equal at different lightness levels, samples that appear lighter may be perceived as more important), and the fourth problem is that the average colours for the hue-angle bins do not necessarily all have the same average colourfulness (and average lightness) values. For the latter, CAM02-UCS is a perceptually uniform colour space where absolute distances should be considered (a change in colourfulness from 30 and 33 should be equally visible compared to a change in colourfulness from 5 to 8). A gamut area index, as computed with the IES-method, represents a relative change in colourfulness, where the same increase in colourfulness for low or moderately saturated CES will yield a larger

relative gamut area index than for highly saturated CES. It is important to consider how absolute changes in colourfulness, for the individual CES, or relative changes in colourfulness, expressed by a gamut area index, contribute to perceived light quality. Another important question is whether colour quality is best described by an average value, e.g. the average change in colourfulness or the gamut area index, or if colour quality mainly depends on a hue-specific maximum change in colourfulness. It is well-known that different applications have different requirements, which are not easily captured in average index values.

The full-paper will address the impact of using several sets of test-colour samples with, within each set, approximately the same lightness and colourfulness values and with samples distributed with different hue-angle intervals in the CAM02-UCS colourfulness space. The resulting variations in colourfulness and gamut area index for the different sets will be carefully evaluated for a wide range of white-light sources. Subsequently, the impact of the reference illuminant on the index values will be explored by using a reference illuminant with the same CCT (similar to CIE 13.3) and by using a fixed reference illuminant. Finally, the stability of the positions of the test-colour samples in the colour space, as a function of CCT, will be explored.

References

CIE 13.3:1995, Method of measuring and specifying colour rendering properties of light sources.

David A, Fini PT, Houser KW, Ohno Y, Royer MP, Smet KAG, Wei M, Whitehead L, 2015. Development of the IES method for evaluating the colour rendition of light sources. *Optics Express* 23(12), 15888-15906.

Houser KW, Wei M, David A, Krames, MR, Shen, XS, 2013. Review of measures for light-source color rendition and considerations for a two-measure system for characterizing color rendition, *Optics Express* 21(8), 10393-10411.

IES TM-30-15, 2015. IES Method for evaluating light source color rendition.

Luo MR, Cui G, Li C, 2006. Uniform colour spaces based on CIECAM02 colour appearance model, *Color Research and Application* 31(4), 320-330.

Rea MS, Freyssinier-Nova JP, 2008. Colour rendering: A tale of two metrics. *Color Research and Application* 33, 192–202.

Teunissen C, 2016a. A framework for evaluating the multidimensional colour quality properties of white LED light sources. *PROCEEDINGS of CIE 2016 "Lighting Quality and Energy Efficiency", 3 – 5 March 2016, Melbourne, Australia*, 185 – 194.

Teunissen C, van der Heijden FHFW, Poort SHM, de Beer E, 2016b. Characterising user preference for white LED light sources with CIE colour rendering index combined with a relative gamut area index, *Lighting Res. Technol.* 0, 1–20, doi: 10.1177/1477153515624484

PO09

DISCOMFORT GLARE OF NON-UNIFORM LUMINAIRES – A LITERATURE REVIEW

Geerdinck, L.M.[1], Vissenberg, M.C.J.M.[1], Funke, C.[2], Schierz, Ch.[2]
[1] Philips, Eindhoven, NETHERLANDS, [2] Technische Universität, Ilmenau, GERMANY
Leonie.Geerdinck@philips.com

Abstract

For indoor lighting, it is generally agreed that discomfort glare produced by an individual source basically depends on four main parameters: the source luminance in the direction of the observer (L_s), the solid angle subtended by the source at the observers eye (ω), the angular displacement of the source from the observers line of sight (p) and the general field luminance controlling the adaptation level of the observers eye (L_b). Moreover, it is also generally agreed that L_s must be greater than 500 to 700 cd/m^2 for discomfort to exist[1]. In 1995 the CIE Technical Committee 3-13 developed a practical discomfort glare evaluation system for indoor lighting, including the four above mentioned parameters, which resulted in the Unified Glare Rating, UGR[2].

With the introduction of LED's in general lighting, research on the topic 'discomfort glare' was growing again. The possibility of using LED`s in general lighting allows for many new luminaire types. However, the high luminance contrasts and high local peak luminance in the exit window of some of these luminaires seem to provoke more discomfort glare than expected based on calculated UGR values. This discrepancy between the calculated UGR and the subjective discomfort glare experience of these luminaire types, gave rise to an increasing number of published studies on this topic, recently.

Many studies show that for the same average luminance, there is a significant difference in discomfort glare experience between uniform and non-uniform luminaires, and subsequently imply that UGR, using the average luminance for L_s, is not always a reliable measure for discomfort glare perception of those non-uniform luminaires. In 2014 the CIE Joint Technical Committee 7 *("Discomfort caused by glare from luminaires with a non-uniform source luminance"*) was established, in order to propose a correction to the UGR formula that takes into account this non-uniformity of glare sources. Gathering all relevant literature on this topic was the first shared activity of JTC7. This paper will give a summary of this literature review.

More than 50 papers were reviewed, of which about 60 % conference papers. Although the first papers on discomfort glare from non-uniform light sources date from the seventies, the majority of the reviewed articles are from a more recent date (2012-2016). Papers origin from many different regions in the world; Asia, America as well as Europe are represented.

The concept 'non-uniform' is approached in many different ways. Some studies compare a completely uniform light source with a pixelated matrix light source, with bare LED`s, with variations in pitch between LED's, the density of the LED's, and the size (surface area) of the light source. Besides comparison of completely uniform luminance with bare LED matrix light source with extreme high luminance contrasts, also other variations of non-uniformity are studied. Some studies vary the luminance ratio (peripheral/source), or the luminance gradients between LED and its surrounding, or the percentage luminous surface (luminance area ratios).

Many studies performed glare perception research in a laboratory set-up, with prototype luminaires, with the possibility to vary lighting parameters in a systematic way, but also studies with commercially existing luminaires are done, as well as studies in simulated office environments. In a laboratory set-up different viewing angles can be investigated separately, which is not possible in a more field-study like set-up, where participants have the freedom to

[1] CIE 55-1983

[2] CIE 177-1995

look into more directions. However, generalization is probably more reliable in the latter, as it is to a larger extent comparable with a realistic situation.

Most studies evaluate discomfort glare using a subjective (semantic) scale, but we also found studies that assessed the effects of non-uniform light sources on objective physiological visual fatigue measures or even on visibility, approaching the field of disability glare.

Besides studies demonstrating that the Unified Glare Rating is not always a reliable predictor for glare experience, and investigating which factors and parameters are of influence, also studies exist that try to capture the applicability boundaries of the Unified Glare Rating. Many papers make suggestions for alternative ways to predict discomfort glare, with improved reliability for both uniform and non-uniform luminaires. These proposals vary between a whole new way to approach glare perception prediction, and a small modification of the currently used UGR formula.

In this paper all proposed alternatives for the prediction of discomfort glare are discussed. The focus of this literature review however, is on the papers with suggestions for an easy to implement UGR modifications, which can serve as input for JTC7.

PO10

DISCRIMINATION THRESHOLDS FOR SKIN IMAGES

Chauhan, T.[1,2,3], Xiao, K.[1], Wuerger, S.[1]
[1] University of Liverpool, Liverpool, UK, [2] Université de Toulouse-UPS, Centre de Recherche Cerveau et Cognition, Toulouse, FRANCE, [3] Centre National de la Recherche Scientifique, Toulouse Cedex, FRANCE
research@tusharchauhan.com

Abstract

AIM: The objective of the present series of experiments was to estimate discrimination surfaces in 3-D colour space for simulated images of human skin under three illumination conditions – dark, simulated daylight or D65 and cool-white-fluorescent or TL84. Representative patches from two ethnicities – Caucasian and Oriental, were used.

METHODOLOGY: The stimuli were 5 cm × 5 cm patches subtending a visual angle of ≈1.65° at the observer's retina (the diagonals subtended ≈2.3°). They were displayed on a calibrated EIZO ColorEdge CG243W monitor using the ViSaGe system (CRS Ltd.), while the observers were seated 175 cm. away. When the stimuli were displayed under the illumination from the luminaire, the screen was covered by a grey cardboard sheet with cut-outs such that only the four patches remained visible. The reasons for doing this were twofold. First, doing so occluded the self-luminous background, forcing the observer to further adapt to the ambient illumination. Second, it made the patches appear less like images presented on a self-luminous screen, akin to what is often described as an object-mode[1] of stimulus presentation. We believe this is a more ecologically valid method of presenting stimuli such as natural or known textures and surfaces on a computer screen. In the dark condition, the stimuli were displayed against a grey background of the same chromaticity as the simulated daylight from the luminaire (x=0.32, y=0.34) at 20 cd/m^2. This was done in order to avoid adaptation to an arbitrary unpredictable source (the self-luminous stimuli) in the Dark condition. It also ensured that the condition would be comparable to the luminaire-illuminated condition (D65).

In all experiments, thresholds were estimated using a 4-AFC (4-Alternative Forced Choice) task. Four skin patches were simultaneously displayed on the screen, of which three were copies of the *reference image*, while one – the *test patch* – differed in colour. The observer's task was to indicate the odd-one-out by pressing the corresponding button on a response box. The *test patch* was generated by adding a *test vector* in 3-D CIELAB colour space to each pixel of the original patch. The *test vectors* were added along 14 directions such that the space was sampled evenly. Six of these coincided with the cardinal ±L*, ±a, and ±b* directions while the other eight directions were along the centres of the eight octants. During the experiment, the length of the *test vector* in each direction was controlled by the QUEST adaptive algorithm, leading to 14 interleaved staircases. The results were analysed in a Y-u'v' space which, unlike CIELAB, does not depend on a white-point normalisation. Ellipsoids were fitted to the 14 thresholds estimated for each session. The analysis of these ellipsoids was done primarily along the luminance and the chromatic projections as the elevation angles were found to be very close to 90. Results from 18 observers are presented.

RESULTS: An analysis of the volumes of the discrimination ellipsoids using a repeated-measures two-way ANOVA reveals a main effects of the illumination condition ($F(2,34) = 4.65$, $p = 0.016$) and the patch-ethnicity ($F(2,17) = 38.78$, $p < 0.001$), and a significant interaction between the two ($F(2,34) = 11.36$, $p < 0.001$). Bonferroni corrected post-hoc comparisons show larger discrimination volumes for the TL84 condition compared to the D65 condition ($p < 0.001$ for both Caucasian and Oriental patches). They also suggest that the main effect of the patch-ethnicity is found in the Dark ($p < 0.001$) and D65 ($p = 0.013$) conditions, but not in TL84 ($p = 0.21$).

A similar analysis of the luminance projections shows a main effect of illumination condition ($F(2,34) = 106.7$, $p < 0.001$), and a strong interaction between the illumination condition and the patch-ethnicity ($F(2,17) = 11.33$, $p < 0.001$). No main effect of the patch-ethnicity is

observed. Post-hoc tests reveal higher luminance thresholds in TL84 compared to D65 ($p < 0.001$) for both patch types and a higher threshold for TL84 than the Dark condition ($p < 0.001$) for the Caucasian patch.

When analysing the area of the chromatic projections onto the u'v' plance, a repeated-measures two-way ANOVA reveals a marginal main effect of the illumination condition interaction ($F(2,34) = 3.21$, $p = 0.053$), a significant main effect of the patch-ethnicity ($F(2,17) = 99.25$, $p < 0.001$) and a significant interaction ($F(2,34) = 8.99$, $p < 0.001$). Bonferroni corrected post-hoc comparisons show that the area of the chromatic projections is higher for the Oriental patch than the Caucasian patch ($p < 0.001$ for Dark and D65, and $p = 0.005$ for TL84). For the Oriental patch, we also observe that the area of the Dark condition ellipse is higher than that of the D65 ($p = 0.034$) and the TL84 ($p = 0.012$) conditions.

DISCUSSION: The discrimination volume is larger in TL84 compared to D65 for both patch-ethnicities. In other words, irrespective of the ethnicity of a given patch, human observers are better at discriminating small differences in simulated skin under daylight than under artificial fluorescent lighting of identical luminance. This increased volume of the discrimination ellipsoids (reflecting poor discrimination performance) is primarily due to increases along the luminance dimension rather than the chromatic dimensions. While the area of the projected chromaticity ellipses remains roughly the same, the luminance projections of the ellipsoids seem to follow the overall changes in the discrimination volume.

Our analysis is useful for predicting the visibility of small skin tone changes when skin images are simulated under different illumination conditions.

REFERENCES

[1] Tangkijviwat, U., Rattanakasamsuk, K., & Shinoda, H. (2010). Color preference affected by mode of color appearance. Color Research & Application, 35(1), 50–61. Retrieved from http://dx.doi.org/10.1002/col.20536

PO11

STUDY OF VISIBILITY UNDER COMPLEX LUMINANCE CONDITIONS FOR THE VISUALLY CHALLENGED PEOPLE USING LUMINANCE-IMAGE FILTERING

Iwata, M.[1], Kato, Y.[2] and Nakamura, Y.[3]
[1] Setsunan University, Neyagawa, Osaka, JAPAN, [2] Tokyo Institute of Technology, Yokohama, JAPAN, [3] Tokyo Institute of Technology, Yokohama, JAPAN
michico@led.setsunan.ac.jp

Abstract

In considering of a visibility under lighting conditions, the targets were printed letters or shapes on a uniform luminance background and the lighting environments were steady in practical studies. However, walking in public spaces, visual targets and backgrounds are non-uniform and non-steady, and it is very difficult to predict the visual effectiveness under the conditions. Thus, Professor Nakamura Y. suggested for using luminance contrast calculation filter (N filter) to predict the visual effectiveness as a contrast profile quantitatively under a complicated luminance distribution. This calculation method using N filter matches the calculation of luminance contrast (C level) for every object size and every target's environment of complicated luminance distribution.

The purpose of this study is to provide the visually challenged people with a safe and easily navigable environment. In this study, the authors examined and evaluated the visibility by the N filter calculation under complex backgrounds and various conditions using PC monitor (EIZO Colour Edge CG277). Therefore, the authors clarified the data of visibility using oval targets on 4 complex backgrounds: concrete, grasses, crumpled paper and paper textile, and a uniform background under 3 luminance backgrounds. The subjects participated in the experiment were 10 visually challenged people and 5 young students. The experiment was carried out from January 2015 to February 2016.

The authors calculated the C level (luminance contrast) of oval targets and A level (logarithm contrast average) of backgrounds, so the subjects' answers were plotted on figures with A for horizontal axis and C for vertical axis. As the result of this study, when the A level became higher the visibility became better so that the subjects could see the targets under lower C level condition. When the C levels of positive and negative luminance contrasts were equal, the visibility of the positive contrast (background luminance is higher than the target) was higher than the negative contrast. The tendency was same in all sizes of the targets.

PO12

INFLUENCE OF LUMINANCE LEVELS OF ILLUMINATION D65 ON EVALUATION OF HIGH CHROMATIC COLOURS

Pechová, M.[1], Kašparová, M.[1], Vik, M.[1], Viková, M.[1], Štefl, J., Čandová, J.[1]
[1] Technical University of Liberec, Faculty of Textile Engineering, Liberec, CZECH REPUBLIC
marcela.pechova@tul.cz

Abstract

High chromatic colours are used largely in various industrial sectors (e.g. textiles, emergency) in last years. Aim of research was observation of influence of decreasing luminance level on evaluation of observers and verification of adaptation mechanisms in mesopic and photopic level human vision.

The perception and discrimination of colour affect many aspects. These aspects are illumination, mental and physiological condition of observer, viewing conditions, position of samples, work place and also transmission of light through of human eye, photoreceptors (rods and cones) and processing the nervous system. According different of luminance level we can talk about photopic, mesopic and scotopic vision. Change of the spectral sensitivity of the human eye at change of luminance levels is named as the Purkinje shift, when change of luminance level is shifted the maximum luminous efficiency to the shorter wavelengths. Therefore the evaluation were carried in viewing box with fitted a daylight simulator D65. For achieving different luminance levels are used plates. On one side of plates were applied the tint foil with light transmittance 16 % or 6 %.

For evaluation of group of observers were selected high chromatic colours of blue from CIELAB colour space. All samples were measured on the spectrophotometer. The samples had with distance dE=1 to dE=5 from central sample.

Results of experiment were evaluated with using formulae for evaluation of colour differences – CIELAB, CIE2000 and CIECAM02, COQ, PF/3 factor and STRESS index. From the evaluation of the observers were obtained visually perceived colour differences. The dependence visually perceived colour difference and calculated colour difference were contained the dependence visually perceived colour difference on the luminance level. Finally, the results were compared with the results of the MOVE and LRC laboratories.

Keywords: mesopic vision, luminance, high chromatic colours, CIECAM02

[1] FAIRCHILD, Mark D. Color Appearance Models Second Edition. 2.vyd. Barcelona, Spain: John Wiley and Sons, Ltd., 2005, ch 16. ISBN 0-470-01216-1.

[2] GARCÍA, Pedro A., Rafael HUERTAS, Manuel MELGOSA a Guihua CUI. Measurement of the relationship between perceived and computed color differences. Journal of the Optical Society of America A. 2007, vol. 24, issue 7. DOI: 10.1364/josaa.24.001823. Available from: http://www.opticsinfobase.org/josaa/abstract.cfm?uri=josaa-24-7- 1823.

[3] MORONEY, Nathan, Mark D. FAIRCHILD a Robert W. G. HUNT, et all.. The CIECAM02 Color Appearance Model. 20??n. l. DOI: 10.1.1.77.8398. Available from: http://citeseerx.ist.psu.edu/viewdoc/summary?doi=10.1.1.77.8398.

[4] VIK, Michal, Martina VIKOVÁ a Marcela PECHOVÁ. Color discrimination on the border of photopic/mesopic vision. *In Proceedings of the 21st International Conference LIGHT SVĚTLO 2015*. Brno, 2015(1.), 95-99. DOI: 10.13140/RG.2.1.2914.3521. ISBN 978-80-214-5244- 2.

[5] LUO, Ming Ronnier a Changjun LI. CIECAM02 and Its Recent Developments. *Advanced Color Image Processing and Analysis*. 1. Christine Fernandez-Maloigne. New York: Springer-Verlag New York, 2013, s. 19-58. DOI: 10.1007/978-1-4419-6190-7 2. ISBN 978-1-4419-6189-1. Ming Ronnier Luo and Changjun Li. Available from: http://link.springer.com/chapter/10.1007/978-1-4419-6190-7_2.

PO13

VISUAL EVALUATION HIGH CHROMA SAMPLES UNDER THE TWO TYPES OF DAYLIGHT SIMULATORS

Kašparová, M.[1], Pechová, M.[1], Viková, M.[1], Vik, M.[1], Štefl, J.[1], Ulmanová, M., Čandová, J.[1]
[1] Technical University of Liberec, Faculty of Textile, Liberec,460 01, CZECH REPUBLIC
marketa.kasparova@centrum.cz

Abstract

Nowadays it is a trend to use high chroma colours. These colours are using in many application such as: warning clothes, fashion design and decorative cosmetics. Many companies were focusing on these colours due to high market potential. Therefore, it is important to study these colours and small difference between these colours. In many cases, the light sources are changed into LED light source due to it having the ecological and economical aspect. These changes bring lots of problem; discrimination of small colour differences is one among the problems.

International Commission on Illumination (CIE) defined a space called CIELAB, which isn't visual uniform. Based on the previous studies, the data for development and testing of new colour difference formulas and colour spaces are limited in chroma. In this work, we were used high chroma dataset for testing and prediction the performance of known colour difference formulas. For testing we used grey scale and source emitted daylight simulator (D65) and full spectral LED light source. This work has been compared with visual colour difference form observers and calculated colour difference from spectrophotometer. From this study, we made a data set for yellow-green region with high chroma. Observer was compares these data set under D65 and LED light source. The data set was compared with spectrophotometer data. Present research is to evaluate the prediction ability for different colour-difference formulas in high chroma, particularly yellow-green region of CIELAB colour space. Various colour-difference formulae, such as CIELAB, CMC, and CIE94, have been developed in order to facilitate the determination of instrumental tolerances and the measurement of colour difference. These formulae have been developed by analysing the results from visual experiments that have been employed in a variety of techniques for determining the colour differences, which based on acceptability or perceptibility. Nevertheless, such optimization is limited in chroma value from the previous studies on visual experiments. Based on these results, centre of high chroma yellow-green colour is used as starting point of wide visual experiment related to high chroma colours. The grey-scale comparison method was used to determine the colour tolerances for high chroma yellow-green colour centre in the hue, chroma, and lightness directions in CIELAB colour space. The performance of the visual differences and of the calculated colour difference of four colour-difference formulas of CIELAB, CMC, CIE94 and CIEDE2000 is calculated by: Standardized residual sum of square (STRESS), performance factor (PF/3), correlation coefficient (COQ) and wrong decision criterion (WDC).

Key words:

High chroma, colour-difference, visual perception, daylight simulator

References

[1] FAIRCHILD, Mark D.: Color appearance models. Reading, Mass.: Addison-Wesley, 1998, ISBN 02-016-3464-3.

[2] GREEN, Phil and Lindsay MACDONALD. Colour engineering: achieving device independent colour, Wiley, 2002,. ISBN 04-714-8688-4.

[3] KUEHNI, R.G.: Color Space and Its Divisions: Color Order from Antiquity to the Present. 1. Ed., Wiley Inter-science, 2003. ISBN 0-471-32670-4.

[4] VIK, M., VIKOVÁ, M., KAŠPAROVÁ, M.: Color difference evaluation at high chromatic colors, *Vlákna a textil* (3) 2014, pp. 88-91, ISSN 1335-0617

PO14

USING A STANDARD GREY SCALE FOR COLOUR CHANGE IN A MULTI-ANGLE COLOUR-ASSESSMENT CABINET

Melgosa, M.[1], Gómez-Robledo, L.[1], Cui, G.[2], Li, C.[2,3], Ferrero, A.[4], Bernad, B.[4], Campos, J.[4], Richard, N.[5], Fernández-Maloigne, C.[5]
[1] Departamento de Óptica, Facultad de Ciencias, Universidad de Granada, Granada, SPAIN, Wenzhou University, Wenzhou 325035, CHINA, [3] School of Electronics and Information Engineering, University of Science and Technology Liaoning, Anshan 114051, CHINA,
[4] Instituto de Óptica, Consejo Superior de Investigaciones Científicas (CSIC), Madrid, SPAIN,
[5] XLIM Laboratoire, UMR 7252 CNRS, Université de Poitiers, Poitiers, FRANCE
mmelgosa@ugr.es

Abstract

In recent colour-difference experiments involving solid and effect samples [M. Melgosa et al. *Optics Express* 22, 3458-3467, (2014); Journal of Physics: Conference Series 605 (2015) 012006; Proc. AIC 2015, pp. 1180-1185 (2015)] the standard grey scale for colour change of the Society of Dyers and Colourists (SDC) has been positioned inside a multi-angle byko-spectra colour-assessment cabinet. In these experiments the grey scale was illuminated by a light source close to CIE illuminant FL11 at a fixed angle of around 45° with respect to the perpendicular to the sample, and observed at 6 different viewing angles of -15°, +15°, +25°, +45°, +75° and +110°, measured with respect to the direction of the specular reflection (ASTM E2194.01, 2011). In this situation, the colour differences of the 9 colour pairs of this grey scale exhibited some variability, which may be mainly attributed to the lack of uniform and directional illumination on the samples in this cabinet and the goniochromatism of the samples. This paper focus on the measurement of such variability and potential best practices for future experiments using this kind of multi-angle colour cabinets and standard grey scales.

First, we performed 3 independent spectroradiometric measurements of each sample in the SDC grey scale placed in the byko-spectra cabinet (plus a PTFE reference white placed on top of each sample) for the 6 viewing angles mentioned above. We employed a Konica Minolta CS 2000 spectroradiometer (1° visual field, CIE 1964 colorimetric observer) placed at the same position that the head of the observer performing visual experiments in the cabinet. On the average, for the 9 colour pairs, the standard deviation of the measured colour differences at the 6 viewing angles was 0.81 CIELAB units (range from 0.49 to 1.39 CIELAB units), around 4 times higher than the standard deviation of the 3 independent acquisitions made with our spectroradiometer, where it was found an average standard deviation of 0.22 CIELAB units (range from 0.12 to 0.43 CIELAB units). These results suggest that the lack of uniformity in lighting cabinets and the goniochromatism of the samples are relevant factors to be taken into account. In addition, we noticed that for colour pair #5 (two identical physical samples) the average colour difference for the 6 viewing angles was 1.60 CIELAB units (range from 0.79 to 2.07 CIELAB units), considerably higher than the expected null value. This result can be attributed to the lack of uniform illumination when the colour pairs are not positioned just in the center of the multi-angle cabinet, and the problem can be partly solved by using a chromatic adaptation transform to the average reference white of the two samples in each colour pair.

Second, in order to analyze only the goniochromatism of the samples, we decided to perform additional BRDF measurements for each of the samples in the SDC grey scale, and also for each of the samples in the grey scale provided by the American Association of Textile Chemists and Colourists (AATCC), which seems visually identical to the SDC scale. Such measurements were made using the gonio-spectrophotometer available at Instituto de Óptica, CSIC, Madrid (A. M. Rabal et al., Metrologia 49, 213-223, 2012). For comparison purposes, we only considered in our next analyses the illumination angle of 45° and the 6 viewing angles used in the spectroradiometric measurements described in previous paragraph. From the experimental measurements of spectral reflectance factors, we assumed the CIE FL11 illuminant and CIE 1964 colorimetric observer for the computation of colour coordinates and colour differences. On the average, for the 8 colour pairs (now the colour pair #5 with two

identical samples was not considered) in the SDC/AATCC scales, the standard deviations of the colour differences at the 6 viewing angles were 1.25/1.95 CIELAB units (range from 0.40/0.36 to 2.30/4.08 CIELAB units). As we can see this variability in colour differences is slightly higher than the one found in the spectroradiometric measurements, which can be explained by different experimental setups (e.g. a directional illumination in the gonio-spectrophotometer against illumination at different angles in the colour-assessment cabinet where we performed the spectroradiometric measurements). From these results, it can be concluded that just goniochromatism is very relevant in the colour pairs, both in the SDC and in the AATCC grey scale. More specifically, we found that, for the AATCC grey scale, the CIELAB colour differences for the 8 colour pairs had considerable anomalous values at the viewing angle of -15°, and enough similar values for the remaining viewing angles. The colour differences of the 8 pairs in the AATCC and SDC grey scales had a discrepancy which ranged from 4.62 CIELAB units (angle of -15°) to 0.59 CIELAB units (angle of +25°), with an average value of 1.44 CIELAB units. Using a pseudo-divergence bidimensional representation [N. Richard et al., “Pseudo-divergence and bidimensional histogram of spectral differences for hyperspectral image processing,” Journal of Imaging Science and Technology, vol. (to appear), pp. 1-13, 2016], additional analyses were performed to compare the spectral reflectance factors measured by the gonio-spectrophotometer for the samples with identical designation in the SDC and AATCC scales, considering the different viewing angles. Although both scales seem almost visually identical, these analyses show important differences between the samples in both grey scales, in particular for viewing angles close to the specular reflection.

In summary, it can be concluded that, using the SDC and AATCC grey scales, the viewing angle is a relevant parameter in the values of the colour differences of the different colour pairs, which is the most important parameter in practical applications. Similar results to those shown in previous paragraphs can be also found using the currently CIE/ISO recommended colour-difference formula, CIEDE2000. Therefore, when using grey scales in multi-angle colour assessments cabinets, we cannot assume the colour difference values provided by ISO 105-02:1993 and ASTM D 2616, 2003 for D65 illuminant and CIE 1964 standard observer. In this situation, we recommend to perform instrumental spectroradiometric measurements at the different viewing angles in order to obtain meaningful results comparable with those found in visual observations.

PO15

IMPACT OF SURFACE CURVATURE ON SPECTRAL BRDF OF EFFECT COATINGS

Ferrero, A.[1], Bernad, B.[1], Campos, J.[1], Perales, E.[2], Martínez-Verdú, F.M.[2], Šmíd, M.[3], Porrovecchio, G.[3], Strothkämper, C.[4]
[1] Instituto de Óptica, Consejo Superior de Investigaciones Científicas (CSIC), Madrid, SPAIN, [2] Department of Optics, Pharmacology and Anatomy, University of Alicante, Carretera de San Vicente del Raspeig s/n 03690, Alicante, SPAIN, [3] Czech Metrology Institute, LFM, V Botanice 4, Praha 5, CZECH REPUBLIC, [4] Physikalisch-Technische Bundesanstalt (PTB), Bundesallee 100, 38116 Braunschweig, GERMANY
alejandro.ferrero@csic.es

Abstract

The development of effect pigments (or flake pigments) by industry has allowed new eye-catching visual effect for products. Unlike the traditional absorption pigments, they generate colour perceptions extremely angle dependent, which are function of both the illumination and observation directions. As a consequence of their appealing appearance, the market of effect pigments is steadily increasing and has become very popular in automotive, cosmetics, coatings, packaging, printing inks, ceramic tiles, building materials, textile, etc.

Effect pigments known as metallic pigments consist of a metal or an alloy of metal and their optical properties are described essentially by geometrical optics. They display a **metallic effect** which is mainly due to the specular reflection at the surface of these pigments. When embedded in a material or binder, called hereafter effect coating, the effect is determined by the optical properties of pigments and material and by the pigments orientation in the material. In this case, due to the non-perfectly horizontal inclination of the flakes in the binder, the effect can be observed for directions close to the specular directions. Since this effect is mostly observable around specular directions, it must present variations in appreciable extent when the coating is applied on a curved surface, for which specular reflection is dimmed.

In the context of the EMRP Project “Multidimensional reflectometry for industry” (xDReflect), we applied the same effect coating with metallic pigments to three surfaces of different convex curvatures, with curvature radii of infinity (flat), 300 mm (moderately curved) and 150 mm (very curved), and their spectral BRDF was measured at different illumination and observation directions, both in and out of the incidence plane. The measurements of the spectral BRDF of the three surfaces with the same effect coating will be presented and discussed in this contribution. They were performed with the goniospectrophotometer GEFE at IO-CSIC. For normal illumination, the samples are illuminated with a uniform spot of 3 cm in diameter, but the measurement area is only of 7 mm in diameter. The apparent dimensions change for different geometries. The half-angle of the solid angles of illumination and detection was around 0.5º.

We found that, **at** specular directions, the higher the curvature of the sample the lower the spectrally-averaged BRDF, and that, **around** the specular directions, the higher the curvature the higher the spectrally-averaged BRDF. Both observations were expected as a result of the divergence introduced by the curvature in the reflection at the first surface (convolution by curvature). In terms of colour, it can be interpreted as a “lightness flop” between curved and flat samples, being lighter the flat sample **at** specular directions and the curved samples **around** the specular directions. But, in addition, we have found another effect of curvature, which is not spectrally neutral and hardly can be explained by simple convolution. It is observed at some in-plane geometries with high incidence angles, and it can be described as an increase of the spectrally-averaged BRDF and a variation in the spectral distribution when comparing flat and curved samples. We may say here that there is “colour flop” between samples. This suggests a different contribution of the effect pigments to the spectral BRDF at those geometries for flat and curved samples. In these cases, the colour of the curved sample

is slightly more chromatic, which points out that the effect pigments contribute in higher extent to the spectral BRDF.

A possible explanation might be that, when irradiating a curved surface, incident light is refracted into the coating not only in a single direction but in a bunch of directions, as a consequence of the broad distribution of inclinations of the elementary surfaces in the irradiated area. Then the contribution of the effect pigments to the spectral BRDF for certain geometries may vary, because, unlike flat samples, effect pigments at different inclinations would now contribute. If this is correct, the variation at a given geometry of the contribution of the effect pigments to the spectral BRDF of curved samples with respect to flat samples would depend on the number of effect pigments contributing for every sample.

However, this hypothesis must be experimentally tested yet, and will likely require to reproducing the same procedure with concave curvatures samples. We must notice that both curvatures are usually present in car bodies, with sharp and smooth curvature.

The methodology applied in this work could be an interesting starting point to systematically study the effect of surface curvature in effect coatings, which could give insight into the impact of curvature of the effect pigment types (metallic, interference, pearlescent or diffraction pigments), the number of coating layers, the application process, etc.

PO16

INVESTIGATION AND MEASUREMENT OF UNCERTAINTY CONTRIBUTORS FOR COLORIMETRIC CALIBRATIONS

Kruger, I.[1], Coetzee, E.M.[2]
[1,2] National Metrology Institute of South Africa, Pretoria, SOUTH AFRICA
[1] ikruger@nmisa.org; [2] emcoetzee@nmisa.org

Abstract

Various empirical tests, calibrations, verifications and validations were performed to define the uncertainty contributors for the colorimetric calibrations of surface colour standards and emitted colour sources (including colorimeters).

A standard spectroradiometer was calibrated for luminance, using an incandescent luminous intensity primary standard lamp (Illuminant A), to illuminate a diffuse reflectance standard. A range of luminance values was produced by positioning the primary standard lamp at various distances from the diffuse reflectance standard. The luminance of the diffuse reflectance standard was calculated from the luminous intensity of the lamp, the distance between the lamp and the illuminated diffuse reflectance standard. The spectroradiometer was used to measure the luminance of the diffuse reflectance standard and the readings were compared to the known luminance values. The uncertainty of measurement was found to be 2,5 %.

The standard spectroradiometer was also calibrated for correlated colour temperature and CIE 1931 chromaticity coordinates using a standard colour temperature lamp. The measured CIE 1931 chromaticity coordinates were compared with the known values of the Standard Illuminant A. In addition, the correlated colour temperature was calculated from the measured CIE 1931 chromaticity coordinates and the CIE 1931 chromaticity coordinates were calculated from the measured correlated colour temperature and compared. All values were found to be within the stated uncertainty.

Verification was performed for the spectroradiometer for various surface colours using an incandescent luminous intensity standard lamp (Illuminant A) to illuminate a set of matt colour tiles, at a distance of approximately 1,0 m. The spectroradiometer was used to measure the luminance and chromaticity coordinates of the set of matt colour tiles and a diffuse reflectance standard at an angle of approximately 45°. The diffuse reflectance standard's reflectance was used to determine the percentage luminance of each colour tile. The reflectance of the set of matt colour tiles was measured on a double beam spectrophotometer. The CIE 1931 chromaticity coordinates and percentage luminance was calculated from the measured reflectance using the CIE 1931 standard colorimetric observer values. The results obtained with the spectroradiometer were verified with those obtained using the spectrophotometer. The method of measuring luminance and chromaticity coordinates using the spectroradiometer was also validated in this way.

The software of the standard spectroradiometer for calculating CIE 1931 chromaticity coordinates from the measured spectral radiance was validated. This was done by measuring the CIE 1931 chromaticity coordinates and spectral radiance of various ceramic colour tiles at a geometry of 0º/45º with the standard spectroradiometer. A primary, glossy, white, reflectance tile was used as the standard for the measurement. The 1931 CIE chromaticity coordinates for Illuminant A were calculated from the spectral radiance data using the CIE 1931 standard colorimetric observer values. The calculated and measured CIE 1931 chromaticity coordinates were compared and found to be within the stated uncertainty.

The contribution of stray light to the standard spectroradiometer measurements was investigated. This was done using an incandescent luminous intensity primary standard lamp (Illuminant A), to illuminate a diffuse reflectance standard. The spectroradiometer was aligned at an angle of approximately 45° with the normal of a diffuse reflectance standard. The spectral radiance of the diffuse reflectance standard was measured with the spectroradiometer with and without an order sorting filter. This method dictates that if the signal drops to zero

when inserting the filter, the effect of scattering is insignificant. The stray light contribution was quantified for various colours.

Uncertainty contributors, such as uniformity, stability, distance and viewing angle were also measured for nine colours on a colour reference monitor used for emitted colour calibrations. The uncertainty budget for colorimetric calibrations was calculated and will be discussed.

PO17

CCT CHANGES OF THE LED'S DEPENDING ON THE ANGLE OF THEIR RADIATION

Bos, P., Novak, T., Sokansky, K., Baleja, R.
Faculty of Electrical Engineering and Computer Science, Ostrava, CZECH REPUBLIC
petr.bos@vsb.cz

Abstract

The aim of the report is a description of an issue connected with subjective perception of colours from the extensive lighting system stepped by LED, where it was possible to observe identical light source (LED) within various angles. Colour of the light of LED sources depends not only on a type of a luminophor but also on a length that has to be overcome by a ray coming through the luminophor. The length can be defined by means of an angle of the normal, i.e. from a ray coming through the luminophor upright and having the shortest track. If the length of the ray coming through the luminophor is longer, the wider differences in its colour are. This phenomenon can influence sensation visual in a negative way. As it results from the article, the size of colour change is also influenced by a luminophor type. If the lights produced by LED go through diffuser, there is a partial blending of light and the colour change is smaller. Additional optical systems redistribute primary luminous flux coming from light source (LED) and thus there is a blending of luminous flux radiated to a certain angle of the illuminated space from various directions of the luminous flux radiation itself.

PO18

VISUAL EVALUATION OF WHITE SAMPLES NEAR TO CIE LIMITS

Vik, M.[1]
[1] Technical University of Liberec, Faculty of Textile Engineering, Laboratory Colour and Appearance Measurement, Liberec, CZECH REPUBLIC
michal.vik@tul.cz

Abstract

The evaluation of whiteness of a product is dependent from the materials and the application it is used in. Natural materials for example tend to yield some yellowish tint e.g. cotton or wool, so the industry modifies the materials to compensate for this effect (yellowish tint of a product is most often seen as a quality flaw, e.g. yellowed due to aging or dirt) and make the appearance of a product whiter.

The intuitive interpretation of paper whiteness is a material with high light reflection for all wavelengths in the visual part of the colour spectrum. However, a slightly bluish shade is perceived as being whiter than a neutral white. Fluorescent Whitening Agents (FWA), dyes and pigmented inks are used extensively in the textile, pulp and paper industry. It was found that in some cases, calculated CIE whiteness values increased with increasing amount of colours in the whitened substrate appeared darker or redder to the observers. Small deviations in measured CIE tristimulus functions X, Y, and Z often caused significant changes in calculated CIE, and Ganz whiteness values.

A visual assessment study of the selected samples was carried out in order to relate the influence of the high tint to perceive white. The results show the deficiencies in the current measurement techniques for assessment of brightness and whiteness of textile fabrics containing optical brightening agents.

Keywords: Whiteness, tint, fluorescence, visual assessment, colorimetry

References

[1] CIE 15:2004, Colorimetry, Third Edition, 2004

[2] E. Ganz, “Whiteness Formulas: A Selection and whiteness perception: individual differences and common trends”, *Appl. Opt*., 18, 1073-1078, 2963-2970 (1979)

[3] Swenholt, B. K., Grum, F., Witzel, R. F., “Colorimetry of fluorescent materials: visual evaluation of fluorescent whites”, *Color Res. Appl*. Volume 3, (3), 141–145 (1978)

[4] Vik, M., Viková, M., Periyasamy, A.P.: Influence of SPD on Whiteness value of FWA treated samples, 21st International Conference Světlo Light 2015, September, 8 - 10, 2015; Brno University of Technology, Czech Republic, pp. 257-261, ISBN 978-80-214-5244-2

PO19

METHOD FOR THE TREATMENT OF WAVELENGTH-DEPENDENT VOLUME SCATTERING IN A HOMOGENEOUS, ABSORPTIVE MEDIUM

Marutzky, M.[1], Kleinert, B.[1], Bogdanow, S.[1]
[1] IAV GmbH, Gifhorn, GERMANY
michael.marutzky@iav.de

Abstract

For the calculation of radiance fields often raytracing-based methods are used. These methods consider very well the reflection and scattering properties at the interfaces between media, but not the multiple scattering in volumes with reasonable calculation efforts. An example from praxis where volume scattering has to be treated is the simulation of the illuminance distribution on a road caused by a headlamp during fog. Often this problem is solved by modelling the dissipative volume with an artificial interface. This solution is physically not correct.

We present a method which is based on physical principles. The rays are considered in momentum space in dependence of the run-time of light. Conducting like this, the scattering in dependence is formal similar to a diffusion process und thus can be described by the diffusion equation. The radiance field results from back-transformation into real space. The wavelength dependence of the process is determined by three aspects. The first is the wavelength dependence of the scattering rate. The second is that the optical path is ruled by the wavelength dependent complex refraction index which has to be considered when calculating the spatial dispersion. The third is that beside the spatial dispersion the light will dissipate during time in relation of the absorptive part of the complex refraction index.

In this contribution, we deduct the method from physical principles in detail. In order to examine the behaviour of the light scattering in the volume, we calculate radiance fields and variate the wavelength, i.e. the scattering rate, the dispersive, and the absorptive part of the complex refraction index. Finally, we come back to the mentioned traffic situation in fog and calculate the illuminance distribution on the road caused by vehicle headlamps in dependence of visibility range. Additionally, we determine the glare illuminance on the eye of an oncoming driver during a passing situation caused by scattering of the head lamps.

The method was developed within IAV's efforts establish a comprehensive tool in order to evaluate the glare caused by the vehicle headlamps in a very early stage of the industrial development process. This tool "CAGE" [Kleinert et al., ISAL 2015] takes into account the surrounding conditions, especially the state of the road since a wet pavement will cause a dominant indirect glare illuminance on an oncoming driver. Our intention is to extend this tool and to get able to optimize headlamps light distributions for fog and rain in regard to glare and perceptibility.

Although it was originally designed for this specific automotive application, the method can be used in general for the computing of radiation fields in diffuse and dispersive media. At least following an exciting scientific approach, it could be of interest for other optical applications. Thus we would like to present it to the broad community of CIE and put it for discussion.

PO21

PROBLEMS IN KINETIC MEASUREMENT OF MASS DYED PHOTOCHROMIC POLYPROPYLENE FILAMENTS WITH RESPECT TO DIFFERENT COLOUR SPACE SYSTEMS

Periyasamy, A.P.[1], Viková, M., Vik, M.
[1] Technical University of Liberec, Faculty of Textile Engineering, Liberec, CZECH REPUBLIC
aravinprince@gmail.com

Abstract

One of the most promising and flourishing field of the photochemistry is photochromism and it has been studied the photochromic behaviour of both organic and inorganic materials. Photochromism is defined as a reversible transformation in a chemical species between two forms having different absorption spectra by photo-irradiation. It is simply a light-induced rev-erasable change of colour. Textile materials are one of the basic needs for the human life after food and shelter. It can be applied in various forms from clothing to high tech applications such as protective textiles, medical textiles, geo textiles and sport textiles. Consequently, it give immense inspiration to prepare photochromic textile materials, in this regards we take more attention to prepare the mass dyed polypropylene filaments with photo-chromic pigments. Therefore the preparation of photochromic pigments incorporated polypropylene multifilament was done by laboratory level melt spinning machine. The spinning solution (dope solution) contains the mixing of polypropylene granules along with photochromic pigments. There are several concentrations of photochromic pigments such as 0.5; 1; 3 and 5 % (on weight of material) were used for this study.

As we discussed in earlier, photochromic is having significant colour change or reversible colour changing properties, therefore it is difficult to measure kinetic properties in normal (commercial) spectrophotometer, which is required controlled exposure by the selective irradiance level; also it required long time between the individual measurement (cca 5s) or a separate UV source is the time delay between irradiation and measurement, these delay can causes to thermal fading to the sample which affect the total results. Also the commercial spectrophotometer cannot measure the whole colour change during the UV exposure without interruption of illumination of the samples. To solve this issue it is required to integrating the sphere of spectrophotometer, which modifies to add the additional aperture for the UV irradiation. In this study, we carried out the kinetic measurement of produced photochromic pigment incorporated polypropylene filaments in the LCAM developed FOTOCHROM spectrophotometer, and analysed the problems occur in the colour strength values (K/S) were analysed with respect to the L,a,b colour space and CIE X,Y,Z colour space.

Keywords: Photochromic textiles, kinetic measurement, decay, colorimetry, mass dyeing, colour strength.

[1] Viková, M., Vik, M.: Description of photochromic textile properties in selected color spaces, *Textile Research Journal*, 2015, Vol. 85(6), pp. 609–620

[2] Viková, M., Vik, M.:The determination of absorbance and scattering coefficients for photochromic composition with the application of the black and white background method, *Textile Research Journal*, 2015, Vol. 85 (18), pp. 1961-1971

[3] Viková, M., Vik, M., Periyasamy, A.P.: Optical properties of Photochromic pigment incorporated Polypropylene (PP) filaments: - Influence of pigment concentrations & drawing ratio, Workshop Světlanka 2015, 22nd-25th September 2015, Rokytnice nad Jizerou, pp. 140-145, ISBN 978-80-7494-229-7

PO26

THE COMPARISON STUDY OF INSTRUMENTAL COLOUR MEASUREMENT AND VISUAL GRADING OF COTTON FIBER

Khan, N.[1], Vik, M.[1], Vikova, M.[1]
[1] Technical University of Liberec, Liberec, CZECH REPUBLIC
knayabrpm@yahoo.com

Abstract

Colour of cotton fiber is one of the very important property which actually plays important role in the cotton colour grading. Currently, used system in the cotton world for the colour classificationis not that much reliable if keeping in view the importance of fiber. Mostly before the buying of cotton fiber a professionally trained visual cotton inspector gives grade to the cotton which is later on confirmed in the mills by HVI which measures Rd and +b values to grade the cotton fiber. The grade given by visual inspection not only varies from the HVI grading but, also has contradiction with the cotton classers which are professionally trained. The main objective of the study is to introduce a novel method for the measurement of cotton fiber and the comparison of colour grading with the visual grading. LEDs are used in the instrumental grading as a light source. This new method is also compared with the other methods used for the colour measurement globally. The cotton colour parameters are Rd (Degree of reflectance) and +b (yellowness) are used for the comparison of these methods. The representation of the colour parameters on the Hunter colour diagram for cotton is performed by calculation the Rd and +b values. Cotton samples from the Central research institute from Pakistan are used in the experimental as well as the cotton standards from USDA are used for the grading of cotton. The HVI (High Volume Instrument) readings are given by the USDA department. A strong relationship is observed between the two methods compared for colour grading. The visual grading of cotton fiber is performed and shows good relationship with the instrumental grading. Also the the utilization of LED is confirmed in the cotton colour grading.

Keywords: Rd, +b, LED, HVI, Non-contact.

PO27

OPTIMIZATION OF WHITE LED SPECTRUM UNDER MESOPIC CONDITION BASED ON 3D COLOUR GAMUT

Li, H.C[1], Sun, P.L[2], Luo, M.R[3]
[1,2] National Taiwan University of Science and Technology, CHINESE TAIPEI, [3] University of Leeds, UNITED KINGDOM
D10222503@mail.ntust.edu.tw

Abstract

The luminous of night-time outdoor lighting and driving condition normally falls into mesopic range, where is between 0.001 to 3 cd/m^2. The mesopic spectral luminous efficiency could be described in terms of a linear combination of the photopic and scotopic spectral luminous efficiency functions but the results are influenced by background luminous and spectrum distribution. [1][2] In previous studies about mesopic visual appearance were mainly adopted for calculating mesopic luminous. X-model and MOVE-model are typical examples. The apparently differences among the two were the upper luminance limit of the mesopic region, which is considered too low for the X-model and too high for the MOVE-model. [3] Hence, a modified MOVE-model was proposed with an appropriate upper luminance limit. Although the models could adequately predict the luminous for monochromatic lights, the chromatic mechanisms appeared to contribute to visual performance weren't taken into account. [4] A CIE recommended mesopic photometric system, CIE TC 1-58 model, has been successfully used in LED outdoor lighting for better improve the problems on mesopic photometry.

With the rapid development of solid state lighting technology, light efficiency of white LED has been gradually increased in recent years. However, the majority of white LED spectrum is optimized based on luminous efficiency and colour rendering index in photopic vision where shows wider colour gamut than in mesopic vision. In order to obtain mesopic luminous, the S/P-ratio of light source and photopic luminous were needed. The S/P-ratio was applied to present the luminous condition in scotopic vision compared with that in photopic vision. With larger S/P-ratio, the higher luminous would be perceived in scotopic condition and enable to enhance visual performance. Nevertheless, the reduction of luminous in night time becomes more significant as the light spectrum shifting from long wavelength (red) to short wavelength (blue) which indicated that night-time vision condition involves colour perception and gamut variation. [5] Besides, due to the narrow colour gamut in mesopic condition, the conventional colour rendering index might be unavailable for colour accuracy. Therefore, an optimization of white LED spectrum based on 3D colour gamut was essential to raise the ability of colour recognition under constant contrast condition for lighting application.

The aims of this study are to optimize the white LED spectrum based on 3D colour gamut in mesopic viewing condition in both theoretical and practical ways. In the theoretical part, ISO standard object colour spectral database (SOCS) and a mesopic colour appearance model [6] were used to optimize the white LED spectrum based on principal component analysis of a white LED database to simulate the range of 3D colour gamut composed of the variety of possible white LED spectrum under same radiant quantity condition. The optimal white LED spectra with wider colour gamut was further used in the practical evaluation. In this study, a psycho-visual experiment was carried out for the practical evaluation. Twenty observers with normal vision including 10 males and 10 females participated in each experiment. Before starting the experiments, 20-minute dark adaptation was required. The colour appearance of saturate colours on ColorChecker chart was evaluated under a pair of multispectral LED light booths calibrated by measuring the spectrum distribution with a high-end spectroradiometer (Topcon SR-UL1R) for its accuracy. The multispectral light booths contain 16-type narrow band LEDs which can be used to simulate the reference white LED (typical cool white LED) in one booth and the optimal white LEDs in the other for side-by-side visual comparison under 0.1, 0.3, 1, 10 cd/m^2 four mesopic luminance levels.

The initial result shows that background luminous and spectral distribution significantly affect the luminous efficiency and the range of 3D colour gamut in the mesopic luminance levels. The white LED spectrum with higher S/P-ratio and higher correlated colour temperature presented peak spectrum response in short wavelength (blue) where the eyes are more sensitive could extend the range of colour gamut and also improve the luminous efficiency under different background luminous. The psycho-visual experiment conducted with Magnitude Estimation to obtain visual data from observers suggests that perceived brightness and colourfulness increased with the optimal white LED spectral under identical luminous level. The visual performance of the optimized white LED spectral to visual performance also should be estimated. A visual recognition experiment will be conducted next under both the typical white LED and the optimal white LEDs to make sure if the optimal ones can really improve the visual performance under the mescopic conditions.

1. Halonen, L., & Puolakka, M. (2010). CIE and mesopic photometry. *CIE NEWS*, 1-2.
2. Rooymans, J. (2009). Luminous efficacy of white LED in the mesopic vision state. *Optoelectronics letters*, *5*(4), 265-267.
3. Viikari, M., Ekrias, A., Eloholma, M., & Halonen, L. (2008). Modeling spectral sensitivity at low light levels based on mesopic visual performance. *Clinical ophthalmology (Auckland, NZ)*, *2*(1), 173.
4. Walkey, H. C., Harlow, J. A., & Barbur, J. L. (2006). Characterising mesopic spectral sensitivity from reaction times. *Vision research*, *46*(25), 4232-4243.
5. Purkinje J. E. (1825). Neue Beiträge zur Kenntniss des Sehens in Subjectiver Hinsicht. Reimer: Berlin,109–110.
6. Shin J., Matsuki N., Yaguchi H. and Shioiri S. (2004). A color appearance model applicable in mesopic vision, Optical Review, 11(4):272–278.

Poster Session 2

Wednesday, September 7, 13:45–15:15

PO33

ANALYSIS OF THE INTERPLAY OF THE PIGMENT SHAPE AND SIZE ON SPARKLE DETECTION DISTANCE BY DESIGN OF EXPERIMENTS

Gómez, O., Micó, B., Perales, E., Chorro, E., Viqueira, V., Martínez-Verdú, F.M.
Color and Vision Group, Department of Optics, University of Alicante, Alicante, SPAIN
omar.gomez@ua.es

Abstract

There are numerous factors that can influence when detecting the sparkle texture effect [1] such as the size, shape, thickness and orientation of the special-effect pigment, its chemical composition and number and thickness of layers, pigment concentration, hue, chroma and lightness of the coating sample, etc.

In this work we will focus on the type (morphology) and the size (D_{50}) of the pigment, and how they affect these variables when visually detecting sparkle (glint or glitter). The two types of metallic pigments extensively employed in industry are the “Cornflake” and “Silverdollar”. Cornflake pigments are characterized by having an irregular edge particle (caused during the milling process) instead the Silverdollar pigments, with a relatively flat surface and with very rounded edges [2]. About size, conventional pigments have sizes ranging from about 5 microns to a maximum near 50 microns, while the thickness ranges from about 100 nm and 1 micron.

The first hypothesis of this work is to study what kind of pigment shape is detected at a longer distance for the observer, and the second one is to evaluate how it affects the pigment size to the sparkle detection distance. Subsequently a comparison of the results of the visual experiment with the instrumental values provided by the BYK-mac multi-angle spectrophotometer is performed, being nowadays the only device on the market capable of measuring texture values, to study whether there is a correlation between what predicts the commercial device and our eye perceive.

It was not available a large number of samples with a varying pigments sizes, enough to cover the full range of sizes mainly used in industry. All the samples, in this case a selection is made of 18 in total, 9 for each type of pigment, and having similar colorimetry (achromatic background). This was done because it was of utmost importance that the background colour of the sample did not intercede when performing the visual assessments, for this, instrumental BYK-mac values were also obtained both colorimetric and texture.

For this experiment a (6500K) wLED lamp, installed in an own gonio lighting cabinet, with a 800 lx illumination level was used. The illumination angles studied were 15ºas15º and 45ºas45º, the same used by the BYK-mac instrument.

For this experiment, 12 observers were included (6 men and 6 women) with normal colour vision. Each measurement made by observers consisted of the evaluation of the maximum sparkle detection distance applying the adjustment psychophysical method. To perform the visual assessments a mask was employed to have an area of 7x7cm. In total 2304 visual assessments were realized.

The adjustment psychophysical method used here is easy for the observer, after understanding the ASTM definition of sparkle, because she/he can adjust or manipulate the stimulus intensity (sparkle) until it is able to sense, or in this case not be able to detect it, and balancing the influence of the particle intensity and area variables.

Upon psychophysical experiment ended and collected all data for both geometries and for each observer, we proceeded to analyze the inter and intra-observer variability to ensure that all the assessments have been mostly consistent. For this, the STRESS formula, usually applied on testing colour difference formula, was used [3].

In order to apply design of experiments (DoE) [4], we selected a 2^2 factorial design since there are two variables (size and shape, quantitative and qualitative) at two different levels. As for the design of experiments 4 samples described above were used: two samples with Silverdollar pigments and two different pigment sizes, and two samples with Cornflake pigments and two different pigments sizes. Once these initial results are obtained we proceeded to the parameterization with the remaining 14 samples to give consistency to the results obtained in the design of experiments.

For the design of experiments proposed the interaction of both variables were observed (size and shape) in addition to the optimum response values. The results of the design of experiments indicated that for a small size pigment there is no difference between selecting one type of pigment or other because sparkle is not detected. However, for a large pigment sizes the pigment type influences being the Silverdollar type which is detected at a longer distance. This trend can be observed by analyzing the data obtained from the design of experiments, in which it is clearly seen that for enough large pigment sizes to be detected by the observer, the Silverdollar pigment type which is detected at a greater distance.

Another important section to consider and that the design of experiments provides valuable information, it is the referent to the interplay of the studied variables. In this work it has been obtained that all involved factors (size and shape) and the interaction between them are significant.

Once you obtained these results, we proceeded to set the parameterization. They remained the same conditions described above for the psychophysical experiment with the remaining 14 samples and the same methodology was followed throughout the experiment to obtain results as consistent as possible.

The visual results show that has more relevance the pigment size than pigment shape because to very small particles sizes the sparkle is not detected, therefore we do not care the pigment shape because the sparkle texture effect will not be detected. Thanks to the design of experiments it has been possible to analyze the influence of these two variables and the interaction between them. The best regression model for these data was a second order polynomial also including the qualitative variable of pigment type.

The visual and instrumental correlation is not quite good because at small pigment sizes the majority of observers they did not detect sparkle instead the BYK-mac provides values for SG, so for small sizes there is a poor correlation.

In future, we will extend this method, also applying the statistical design of experiments (DoE), for understanding the relevance and interplay of structural (concentration, orientation, etc.), environmental (illuminance level, colour rendering, geometry, etc.) and colorimetric (dark vs. light background, chroma, etc.) factors on the sparkle detection distance.

1. Kirchner, E., et al., *Visibility of sparkle in metallic paints.* Journal of the Optical Society of America A, 2015. **32**(5): p. 921-927.
2. Klein, G.A., *Industrial Color Physics.* Industrial Color Physics, 2010. **154**: p. 1-497.
3. Melgosa, M., et al., *Notes on the application of the standardized residual sum of squares index for the assessment of intra-and inter-observer variability in color-difference experiments.* JOSA A, 2011. **28**(5): p. 949-953.
4. Rössler, A., *Design of Experiment for Coatings*. 2014: European coatings library.

PO34

CORRELATIONS BETWEEN CONCENTRATION OF EFFECT PIGMENTS, OPTICAL MEASUREMENTS AND VISUAL ASSESSMENT OF SPARKLE

Gómez, O.[1], Perales, E.[1], Chorro, E.[1], Viqueira, V.[1], Martínez-Verdú, F.M.[1], Ferrero, A.[2], Campos, J.[2]
[1] Color and Vision Group, Department of Optics University of Alicante, Alicante, SPAIN,
[2] Instituto de Óptica, Consejo Superior de Investigaciones Científicas (CSIC), Madrid, SPAIN
omar.gomez@ua.es

Abstract

Quantifying the visual appearance of automotive coatings is essential for efficient product development and product/quality control. There is a specific need to develop techniques to measure the total appearance of coatings based on special-effect pigments. The present study focuses on two key visual attributes of sparkle: sparkle contrast and density. In order to develop and validate methods to measure these attributes, it is necessary to design psychophysical experiments for assessing sparkle as perceived on coated panels.

The sparkle is an optical effect of texture which shows micro brightness, glint or a diamond effect when the sample is directionally illuminated with a light source, such as direct illumination from the sun in a clear day. Currently there is only one instrument on the market (automotive, cosmetics, plastics, etc.) to measure the typical texture effects of effect coatings: the multi-angle spectrophotometer BYK-mac of BYK-Gardner. Recently it was designed a new procedure based on well-defined sparkle measurands, image capture and calculation of sparkle descriptors by the CSIC Institute of Optics, as an alternative for sparkle assessment [1].

The main objective of this work is to measure, evaluate and corroborate whether the recently proposed algorithm correlates well with structural parameters of the sample [2], and, with visual measurements obtained by well-designed psychophysical experiments to determine the influence of certain variables (size, shape, concentration and type of pigments) in the sparkle detection distance and visual scoring [3-4].

To carry out this work a total of 36 samples from MERCK with known formulations have been employed, which have used different types of pigments (Stapa, Iriodin, Xirallic), different sizes of pigments ranging between 15 - 24 microns, various concentrations between 1 % to 26 % and two background colours sample (black and white).

All samples were measured by BYK-mac as by the Spanish gonio-spectrophotometer (GEFE), being a device able to measure the bidirectional spectral reflectance distribution function (sBRDF) for any combination of irradiation and observation directions, including real retroreflection [5], and also adapted for measurements of sparkle with a camera [6].

GEFE is composed of three independent systems: the irradiation system, the sample positioning system and the detection system. The irradiation system is composed of a Xenon lamp (Hamamatsu Super-QuietXenonLamp) connected to a stable power source. The sample positioning system is composed of a robotic arm and it can be positioned at the desired incidence angle. A CCD camera (Qimaging, Rollera XR) was used to capture information on the spatial detail of the coating panels. The dynamic range of the camera is 12 bits, the detector size is 695 x 520 pixels (2/3") and the pixel size is 13.9 x 12.9 µm. An image of each panel was captured under the same viewing conditions as used for the visual assessments (15as15, 45as45 and 75as75).

We selected the measurement geometries resulting from combining illumination angles with respect to the coated surface normal (θ_i) from 15º to 75º (with angular steps of 30º) and viewing angles (θ_s) from 0º to 70º (with angular steps of 10º), always within the incidence plane (φ_s - φi = 0º and 180º, where φ represents the azimuth angle). After acquiring high-dynamic-range images at those geometries with the GEFE, we proceeded to apply the

mathematical model developed by the IO-CSIC for sparkle measurement and sparkle coefficients, and descriptors were obtained. Afterward, we compared the output variables (contrast and density) with the structural and visual data. Contrast of the sparkle spots (C_{sp}) is the median of the contrasts of the sparkle spots with values higher than a contrast threshold (C_{th} = 0.5 for this work, but it is function of the luminance background) within a measurement area large enough to be considered a significant statistical value (more than 10 sparkle spots). Density of the sparkle spots (d_{sp}) is the number of sparkle spots by area with values of C_s higher than the contrast threshold. C_s is the contrast of a single bright spot on the image. According to the proposed model, the sparkle contrast and density are obtained from the measurements of the contrast of all sparkle spots in the image.

We studied the correlation between the measured density and contrast values with structural and visual data. On one hand, as structural data, we have three sets of samples with different types of pigments, each set containing a number of samples with different pigments concentrations but with fixed pigment sizes. On the other hand, we have data of the visual assessment of these samples for two measurement geometries (15as15, 45as45) and two illumination levels (800 lx and 2400 lx). They were obtained from a psychophysical experiment designed to determine the maximum distance at which an observer can appreciate sparkle. From only the comparison between structural and visual data, it has been concluded that the lower the pigment concentration, the longer is the minimum distance to observe sparkle, although there is dependence on the geometry and on the background luminance.

We observed that the higher the measured density of sparkles, the longer the minimum distance, although there are different trends depending on the geometry and background luminance. In addition, it has an inverse behavior compared to the pigments concentration. Similar conclusions were observed for the measured contrasts of sparkles.

1. Ferrero, A. and S. Bayon, *The measurement of sparkle.* Metrologia, 2015. **52**(2): p. 317.
2. Ferrero, A., et al., *A single analytical model for sparkle and graininess patterns in texture of effect coatings.* Optics express, 2013. **21**(22): p. 26812-26819.
3. Gómez, O., et al., *Influence of the Effect Pigment Size on the Sparkle Detection Distance.* Color and Imaging Conference, 2015. **2015**(1): p. 175-179.
4. Kirchner, E., et al., *Visibility of sparkle in metallic paints.* Journal of the Optical Society of America A, 2015. **32**(5): p. 921-927.
5. Rabal, A.M., et al., *Automatic gonio-spectrophotometer for the absolute measurement of the spectral BRDF at in-and out-of-plane and retroreflection geometries.* Metrologia, 2012. **49**(3): p. 213.
6. Bernad, B., et al. *Upgrade of goniospectrophtometer GEFE for near-field scattering and fluorescence radiance measurements*. in *IS&T/SPIE Electronic Imaging*. 2015: International Society for Optics and Photonics.

PO35

THE RIGHT LIGHT FOR PAINTINGS: AN AMBITIOUS CHALLENGE

Bellia, L.[1], Fragliasso, F.[1], Stefanizzi, E.[1]
[1] University of Naples Federico II/Department of Industrial Engineering, Naples, ITALY
laura.bellia@unina.it

Abstract

Light is fundamental in architectural design: spaces' and objects' perception is strictly influenced by luminous scenarios. This is especially true as regards museums applications. In these cases lighting is essential to assure the complete perception of colours and shapes of artworks, guaranteeing visual comfort conditions.

The choice of the most suitable source to light an artwork is not banal. In addition to source parameters (as emitted flux and photometry, Correlated Colour Temperature -CRI-, Spectral Power Distribution -SPD- and Colour Rendering Index -CRI-), optical characteristics of the lighted objects and of the environment must be accounted for.

Moreover all these aspects must be analyzed considering the human response, indeed physiological and psychological conditions of observers can affect artworks' perception.

Several previous researches evaluated how the colours' perception can be influenced when changing sources' SPD and luminous intensity, investigating human reactions to the changes in lighting characteristics thanks to the use of tests.

Authors focused these aspects in a previous work. In this study a reproduction of the painting "Dame en Bleu" by Matisse (1937) was lighted using LED light sources characterized by different CCT (3000 K and 4000 K). For each CCT, luminaires were dimmed in order to determine two different illuminance levels at the painting (50 lx and 300 lx). Moreover, cardboards of different colours (white, blue and red) were affixed on the wall to which the painting was hung up. 12 obtained light scenarios were shown to 21 subjects. Then people were asked about their preferences, in order to evaluate how different parameters (luminous intensity, CCT, colour of background) can affect artwork's perception.

The new study will deepen issues of the previous one. A new painting, a copy of “Te aa no Areois” by Paul Gauguin will be analyzed. It portrays a young Tahitian woman sit on a sarong and surrounded by the nature. The background of the painting is a vivid landscape represented by the use of bright and unrealistic colours. The painter used a large chromatic range and colours are characterized by wide shades.

On the contrary, the painting previously analyzed, The "Dame en Bleu", is an unrealistic portrait, characterized by sharp and easily identifiable colours: only 7 prevalent colours are used to represent both the girl and the elements of the environment.

The goal of the study is to repeat the experiment carried out in the previous work and to analyze how results can be affected by the complexity of the represented subject and of the chromatic composition of the artwork.

Different luminous scenarios will be set, changing sources' CCT, illuminance levels and background colour. Observers' preferences will be analyzed thanks to the use of tests.

PO36

CREATE COLOUR MODEL INSPIRED BY CONES SPECTRAL SENSITIVITY IN THE RETINA OF THE HUMAN EYE

Abd El-Magid, T.B., Gazl, M.M.
Scientific College of Design, Muscat, OMAN, AlZhra College for Women, Muscat, OMAN
tarek@scd.edu.om

Abstract

Many colour description models have appeared since the old Greeks through Davinci and Goethe reaching to the modern colour description models which are based on the studies of Newton and Maxwell on light such as the studies of Chevreul, and Munsell and others. Finally reaching to (Lab CIE) and (xyz CIE) colour models of the Commission Internationale de l'éclairage.

The problem of the current study aroused by the study of these systems as these models based only on the physical aspects of colours which caused insufficiency in the explanation of many colour phenomena such as sparkling and the increase of the visual perception of secondary colours on the expense of primary colours and the relationship between the violet, red and blue in the visible spectrum.

Thus, the aim of this research is to develop a three-dimensional colour description model basically depends on the spectral response curves of cones in the human eye retina, as it is considered the real tool for colour perception.

To achieve this, the researchers used the descriptive and the experimental analytical methods to study the colour phenomena that other colour models failed to explain through three-dimensional colour description model that depends on the spectral response curves of cones in human eye retina, such as the production of all colour grades that can be recognized by the human eye. Moreover, this research has clarified the reasons behind the increasing visual perception for some secondary colours on the expense of some primary colours that cones sensitive region differs for each primary colour. Additionally, the research tried to confirm the independence of violet colour as a separate wavelength. Finally, the research attempted to interpret saturation and sparkling phenomena in metallic colours through chromatic vision of the rods in the retina. The results confirm the hypothesis search and lead to the recommendations to expand on the study of the impact of visual perception in colour science and in particular the effect of colour constants.

PO37

APPEARANCE RESEARCH BASED ON SPECTRUM TUNEABLE LIGHTING SYSTEMS

Luo, M.R.[1,2]
[1] State Key Laboratory of Modern Optical Instrumentation, Zhejiang University, CHINA
[2] School of Design, University of Leeds, UNITED KINGDOM
*m.r.luo@leeds.ac.uk

1 Introduction

With the advance of LED technology, lighting industry is going through an industrial revolution. Incandescent light is almost phased out. Fluorescent lights are also quickly replaced by LED lights. There is no doubt future lighting will be LED. It has the advantages of low energy consumption, long life, small size and high intensity. Most importantly, it is spectrum tuneable. It is expected that the intelligent LED lightings will arrive and their SPDs can be adjusted in different environments, including office, home, shops, museum, for different purposes such as cosy, concentration, lively, or even healthy.

Lighting is also important for appearance research, which can be divided into 4 parts: colour, texture, gloss and translucency. A Spectrum Tuneable Lighting System (STLS) can have great advantages for appearance research. STLS includes a multiple LED channels, an electronic control board and a software to compute light formulation for different research and applications.

In this paper, the components of STLS will first be introduced. Many appearance studies using the system will be introduced including colour appearance, colour difference, whiteness, texture discrimination and multispectral imaging capturing.

2 Introduction of STLS

An STLS includes two components: hardware and software. The former includes multiple LED channels. They are the mixture of coloured LEDs and blue-phosphor LEDs. These are used to match illuminants of any spectrum. For some particular applications, additional LEDs in UV or IR region can be added. The lights of a STLS are controlled by software engine including database of photometric and colorimetric data of each channel. All the lights are characterised via a measuring instrument such as tele-spectoradiometer.

Some typical software functions in a STLS should be provided. One is to report the quality parameters of a light such as spectral power distribution (SPD), correlated colour temperature (CCT), Du'v' (deviation from the blackbody locus), luminance (cd/m^2) or illuminance (lux), colour rendering index, R_a, metamerism index in the regions of visible (MI_{VIS}) and UV (MI_{UV}), luminous efficacy ratio (LER).

The other function is to generate light of CIE daylight illuminants, D75, D65, D55 and D50. It can also be accurately reproduced a given CCT in blackbody or daylight locus. For SPD of any given light, they can also be generated according to one or more parameters such as SPD, CCT, Du'v', R_a.

For lighting design in a given application, the SPD can be optimised according to some measures such as colour quality (colour fidelity, colour gamut, colour preference, memory colour, colour harmony, colour discrimination), wellbeing quality (circadian stimulus, alertness, etc), colour emotion (warm, light, activity).

When the lights of STLS are off target, some systems can be recalibrated, or have feedback function to recover the light within a tolerance at all time.

3 Appearance Studies

Various studies on appearance research based on STLS have been performed. Some of them are described below.

Hong *et al* conducted *white perception of illumination in a room*. An STLS generates a wide range of chromaticity close to blackbody locus. Observers were asked to judge their whiteness. It was found a white locus, different from those in the blackbody locus.

Ma *et al* carried out experiment to evaluate *whiteness of object colours*. An STLS with 14 channels, having 3 LEDs in the UV region, produced 12 lights at 4 CCTs and 3 levels of UV contents each. The visual results were used to extend the current CIE whiteness index into non-daylight applications.

Gu *et al* conducted colour difference experiment to compare LED lights with the conventional lights (an F8 fluorescent and a tungsten source) as *CIE D50 and A simulators*. The LED lights were generated by STLS to match the CIE illuminants. Note that the SPDs between LED light and CIE A illuminant are largely different. The visual results showed that LED lights outperformed F8, and gave similar performance as tungsten. This means STLS can be safely used for industrial inspection.

Gu *et al* evaluated the performance of different *colour rendering metrics* in a colour difference study. An STLS was used to produce 9 pairs of light having the same CCT but varying in R_a. Experiment was conducted by comparing colour differences of xx test samples between two lights illuminated in two viewing cabinets. The visual results showed that all colour fidelity metrics including Ra gave similar performance and they outperformed colour preference or colour gamut metrics.

Wang *et al* designed a lighting for presenting *preferred skin colours*. An STLS was used to produce various light metamers to have same CCT but different colour quality values. The real models with different degree of makeup were assessed by a number of observers under different lights. Finally, a light was recommended for skin lighting.

Zhai *et al* conducted *preferred museum lighting* for viewing paintings. They found that lighting parameters of CCT, Lux, R_a and Du'v' all had impact on the atmosphere of museum lightings.

Xu *et al* used STLS to design a series of lights for *revealing coloured texture details* based on the criteria of colour difference, colour gamut, CCT. Finally, an SPD including three peaks was found for organ, stone, wood natural samples.

Safdar *et al* produced a *multispectral imaging system* based on multiple LED exposures or a single exposure. The system with no colour filters and gave a reasonable accuracy performance.

4. Conclusions

With the advance of LED technology, spectrum tuneable lighting systems have been developed.

A STLS was introduced. A range of appearance research based on the systems were given here. It demonstrated that the system opens a new dimension for appearance research.

PO38

MEMORY EFFECTS IN GOLD MATERIAL PERCEPTION

Horiuchi, T.[1], Zheng, Q.[1], Hirai, K.[1]
[1] Chiba University, Chiba, JAPAN
horiuchi@faculty.chiba-u.jp

Abstract

Humans discriminate gold from other materials by perceiving its surface appearance. Previous studies have indicated that gloss and colour information influence the perception of gold materials. These studies generally use computer graphic images instead of real materials as stimuli. In our previous study, we investigated the influence of surface physical properties and observation conditions on the material perception of gold using gold-like and gold-plated materials (Zheng et al., 2015). The results also confirmed that humans utilize gloss and colour information to identify real gold materials.

In this study, we investigated the influence of the memory effects on the material perception of gold. Memory refers to the mental process of encoding, retaining, and retrieving environmental information. In memory matching techniques, it is well known that the retrieved colour might differ from the original colour even if the viewing conditions are the same. In several situations, these memory shifts have been observed. Thus far, memory shifts have been confirmed to diffuse an object; however, memory shifts for gold objects have not been investigated. In addition, it is interesting to examine other memory effects for gold.

We conducted three experiments. In Experiment 1, we prepared a two-dimensional (2D) gold plate. Ten participants observed and memorized the real gold object under illuminant A. The average CIE chromaticity of the surface was (x, y) = (0.49, 0.43). A set of reproduced images consisted of a photograph of the real object and six types of luminance modulation images were prepared. The six modulation images (SD0, SD1, …, SD5) were generated by changing the standard deviation of Gaussian noise. The standard deviations of luminance for images (SD0, SD1, SD2, …, SD5) were (0.0, 3.5, 7.0, …, 17.5), respectively. Therefore, the image SD0 was a monochromatic image by (x, y) = (0.49, 0.43). In fact, the standard deviation of the luminance for the photograph of the real object was not 0.0 but 7.0, which was the same as image SD2. The reproduced images displayed on a calibrated monitor (Eizo ColorEdge CG221) were evaluated with regards to high-fidelity image production by paired comparison in the memory matching procedure. Therefore, participants observed 21 paired stimuli. For determining the reproducibility, each participant evaluated the 21 paired stimuli twice. The viewing distance between the participants and stimuli of the gold material or images was 150 cm, and the viewing angle of the stimuli was 2°, which was similar to that of the original gold plate.

Z-scores were calculated for the 21 paired stimuli. The z-scores of the photograph and SD2 were substantially similar, and were the highest. Z-scores from images SD0 to SD5 formed a unimodal and developed a peak at SD2. These results indicate that appropriate luminance modulation is an important factor to perceive a high fidelity gold image, and the fidelity was modified by the standard deviation of the Gaussian noise to the luminance component. In particular, the image SD0, whose surface was represented by the same colour, was not at all perceived as gold.

In Experiment 2, we prepared a three-dimensional (3D) gold statue. Ten participants observed and memorized the real gold object under illuminant D65. A set of reproduced images consisted of a photograph of the real object and six types of luminance modulation images were prepared. Three modulation images (SD2, SD4, SD5) were generated by changing the standard deviation of the Gaussian noise (7.0, 14.0, 17.5), as explained in Experiment 1. Another three modulation images (CNT2, CNT4, CNT5) were generated using a contrast enhancement processing. The standard deviation of the luminance component for the images (CNT2, CNT4, CNT5) was equivalent to the images (SD2, SD4, SD5), respectively. The reproduced images displayed on a calibrated monitor were evaluated with regards to the high-

fidelity image production by the paired comparison in a memory matching procedure. Therefore, the participants observed 21 paired stimuli. For determining the reproducibility, each participant evaluated twice. The viewing condition was the same that in Experiment 1.

The z-scores were calculated for the 21 paired stimuli. The z-score of CNT2 was the highest, and three contrast modulation images (CNT2, CNT4, CNT5) were evaluated as a high-fidelity image compared to the unmodulated photograph. In contrast, the z-scores of three Gaussian noise modulation images (SD2, SD4, SD5), which were effective for high-fidelity 2D gold reproduction, were lower than the photograph of the 3D statue. If there was no memory effect, the unmodulated photograph should have the highest z-score. This result suggests that luminance deviation is enhanced in the memory effect and contrast enhancement is effective for high-fidelity image reproduction of 3D gold objects.

In Experiment 3, we used the same 3D gold statue as in Experiment 2. A set of reproduced images consisted of a photograph of the real object and eight types of luminance and saturation modulation images were prepared. The eight modulation images were generated by combining the luminance modulation (CNT0, CNT2, CNT4) and saturation modulation (SAT0, SAT1, SAT2). The combination of CNT0 and SAT0 was equivalent to the original photograph. The images SAT1 and SAT2 were generated by multiplying 1.2 and 1.4 to the saturation component in HSV colour space. Ten participants observed and memorized the real gold object under illuminant D65. Then the nine reproduced images were displayed on a calibrated monitor, and participants selected the highest fidelity image. The viewing condition was the same as that in Experiment 2.

If there was no memory effect, the unmodulated photograph (CNT0 & SAT0) should have been selected. However, only two participants selected that photograph as the high-fidelity image production. Three participants selected the saturation modulation image (CNT0 & SAT1), and the other three participants selected the luminance modulation image (CNT2 & SAT0). This result suggests that colour shifts also occurred with the metallic gold objects, and the memory effect with the greatest advantage of luminance enhancement and saturation shift, depends on the participant.

References

Zheng, Q., Hirai, K., Hoshino, K. and Horiuchi, T. (2015). Analysis of the material perception of gold using real objects. Proc. ICVS2015, 84.

PO39

PHYSICAL INDEX FOR JUDGING APPEARANCE HARMONY OF MATERIALS

Tanaka, M.[1], Horiuchi, T.[1]
[1] Chiba University, Chiba, JAPAN
horiuchi@faculty.chiba-u.jp

Abstract

In visual design, harmony refers to the similarity among objects and their components that look as if they belong together. Harmony is often related to the body, mind, and emotions in how we relate to our living space, which means that the harmony of real objects is a major characteristic. Indeed, harmony might be affected by the shared traits between objects, such as their colour, shape, texture, and material. Colour harmony in various objects has long interested researchers in colour design studies. However, other traits related to harmony have not been investigated deeply in previous studies. When harmony among actual objects is examined, both harmony among colours and the appearance of harmony among materials are major considerations. According to colour harmony theory, the pair having similar colours harmonizes. However, the appearance of materials with harmonized colour and different texture and surface properties, does not necessarily harmonize. Although the appearance of harmony in relation to specific materials has been investigated, harmony among different materials has not received adequate attention. Recently, the analysis of material appearance has been studied. Most of these studies have focused on visual estimates of specific properties of materials, such as glossiness, translucency, or roughness. According to experimental studies of material harmony, most of our empirical knowledge of harmony is based on combinations of specific material in the actual field of industrial design, such as those of wood or stone used in architecture or of metals used in car production. However, to the best of our knowledge, no previous studies on the appearance harmony of materials have been conducted.

In our previous study (Tanaka et al., 2016), we investigated the appearance harmony among various materials by conducting three psychophysical experiments using the following real materials and their displayed images: stone, metal, glass, plastic, leather, fabric, paper, wood, ceramic, and rubber. In Experiment A, the subjects were allowed to tilt sample pairs to fully assess the harmony of the pairs based on the reflective properties of the actual surfaces and their surface appearance. In Experiment B, the samples were placed such that their surfaces and viewing directions were perpendicular to the subject. In Experiment C, static sample images were displayed on a calibrated monitor. We conducted experiments using 435 round-robin pairs of 30 samples composed of 10 types of materials. After dark adaptation for 2 min, subjects evaluated the pairs based on each experimental method using a forced-choice, 10-point scale to rate harmony and disharmony. The subjects assigned a suitable rating for each combination from 1 (disharmonious) to 10 (harmonious) and recorded them on answer sheets. ‘Harmony’ was defined as a pleasing combination based on colour, texture and reflectance properties obtained from the objects’ surfaces. The results indicated that the sample pairs having similar surface properties were viewed as harmonious even though the materials were different. Based on subjective assessments, we confirmed that sample pairs with similar surface properties were viewed as harmonious even though the materials were different. Indeed, the appearance harmony of the materials differed among static real samples, tilted samples, and static images. For industrial applications, an investigation of psychophysical evaluations and physical properties is critical. If the relationship between them becomes clear, we can judge the appearance harmony of arbitrary materials without evaluating them subjectively.

In this study, we analysed the psychophysical evaluations obtained from our previous experiments and physical properties. For a physical property, we focused on an anisotropy measure. The measure of anisotropy for an input image was defined by Ulichney (Ulichney 1988) to targeting halftoning results in particular and has been used as a quality metric in other

studies. The measure is defined as follows: (1) the radially averaged power spectral density (RAPSD) is calculated to each annulus that corresponds to a central radius in a 2D frequency domain; (2) the anisotropy for each radius is calculated in order to divide the variance of the power spectrum by the square of the RAPSD.

In our analysis, we first calculated the anisotropy for rendered images of 30 samples. The material samples were then classified into five groups based on the shape of the anisotropy histogram. Group A consisted of three samples that included a graph that showed an increase in high frequency. Group B consisted of seven different samples that had similar properties with comparative even and included some spikes in the histogram. Group C consisted of 10 samples that had a flat histogram for all frequencies. Group D consisted of nine samples with bumps in low frequency. One specific paper sample was separated from other samples and named Group E. The clusters may have been reflected by the surface texture properties of rendered images.

For each classified group, the averaged harmony ratings were calculated when the materials belonged to the same or different group. For the pairs within the same group, the average ratings were 5.1, 5.3 and 5.2 for Experiments A, B, and C, respectively. By contrast, for the pairs belonging to the different groups, the average ratings were 4.0, 4.0 and 4.1 for Experiments A, B, and C, respectively. Thus, the averaged ratings within the same group were significantly higher than those of the different group. This result suggests that the texture property represented by the anisotropy histogram is an important index to judge the harmony of static materials.

References

Tanaka, M. and Horiuchi, (2016). T. Appearance harmony of materials using real objects and displayed images. Journal of the International Colour Association, 15, 3-18.

Ulichney, R.A. (1988). Dithering with blue noise. Proc. IEEE, 76(1), 56–79.

PO40

ESTIMATION OF THE SPARKLE TEXTURE EFFECT BY VISUAL AND INSTRUMENTAL ASSESSMENTS

Perales, E., Gómez, O., Chorro, E., Viqueira, V., **Martínez-Verdú, F.M.**
Color and Vision Group, Department of Optics University of Alicante, Alicante, SPAIN
esther.perales@ua.es

Abstract

Special-effect pigments provide a change in colour with viewing and illumination direction. Besides this angular dependence on viewing/illumination direction, metallic finishes also exhibit a visually complex texture. Depending on the properties of the finish and the viewing and illumination conditions, the pigment flakes exhibit a sparkle like texture. The sparkle (glint or glitter) is observed only at close distances and it is seen only under direct bright illumination. On the other hand, under diffused illumination such as a cloudy sky, metallic finishes do not sparkle. Instead they may create a salt and pepper, light dark pattern. This effect may be referred to as graininess or diffuse coarseness.

Nowadays, there is only an instrument on the market to measure the effects of texture, the multi-angle spectrophotometer BYK-mac. However, there are no standards or normatives like ISO, ASTM or DIN to define or propose the mathematical and optical algorithms to measure and calculate the sparkle or graininess effects implemented by the BYK-Gardner company. Therefore, it is very important to visually validate the sparkle and graininess effects by psychophysical experiments since these texture effects are important for the visual discrimination of many materials and to apply the quality control. Then, the objective of this work is to study by a psychophysical experiment of magnitude estimation the visual and instrumental sparkle texture effect correlation in order to guarantee a good performance of the instrument regarding the visual system response.

To make the psychophysical experiment, a lighting booth was used (byko-spectra cabinet) previously characterized at spectral, photometric and colorimetric level. This lighting booth is designed to evaluate colour in six different measurement geometries and to evaluate sparkle in three different measurement geometries. A total of 11 observers participated in the experiment and it was used a set composed by 92 samples. The method used for the visual assessment was the method of magnitude estimation. Observers were asked to assign numbers in proportion to the magnitude of a stimulus taking into account two references (extreme anchors).

To validate the instrumental measurement of sparkle by the BYK-mac multi-angle spectrophotometer, the correlation between the sparkle magnitude assigned by observers and the sparkle magnitude calculated by the instrument was studied. It was found that sparkle grade (Sg) correlates very well with human visual perception. The performance is slightly better for 15ºas15º measurement geometry than for 45ºas45º measurement geometry. However, sparkle intensity (Si) and sparkle area (Sa) do not correlate well with visual perception for any measurement geometry. It could be because the psychophysical experiment was designed to evaluate the sparkle grade and not to evaluate the two independent variables, although relevant for the final sparkle value. Therefore, a new psychophysical experiment is required perhaps with two additional instructions: visual assessment only thinking about sparkle intensity and other one only thinking about sparkle area.

PO41

EVALUATION INDEX FOR THE VISUAL APPEARANCE AND THE TACTILE TEXTURE

Kitamura, S.
[1] Mukogawa Women's University, Hyogo, JAPAN
kitamura@mukogawa-u.ac.jp

Abstract

1. Introduction

Visual appearance is considered to be a comprehensive impression combined with several simple impressions. Each surface property that is the basis for simple impressions such as colour, gloss, texture, softness, etc., is able to show objectively by measurement. On the basis of each relationship, the whole visual appearance need to be clarified how it consists of surface properties.

The purpose of this study is to clarify the evaluation structure to describe the visual appearance of the surface of building materials. The visual appearance of building materials is one of the important factors for the total impression of a room. It is evaluated through the sense of vision, touch, smell and hearing. Among them, it is considered that the sense of vision contributes largely to the visual impression of a room. This study also is aimed to be a foundation for a suggestion of the objective evaluation index of visual appearance.

2. Method

2-1. Experiment on the evaluation index of visual and tactile impression

In this experiment, the visual impression, the tactile impression and the visual-tactile impression of the surface of a specimen were described by adjectives. Specimens were 11 kinds of interior and exterior finishing materials. Subjects were 7 women students. Subjects were asked to describe their subjective impressions of the surface by free description by use of adjectives.

2-2. Method to evaluate visual roughness

The second experiment to evaluate subjective visual roughness of the surface was held in a dark room. Visual roughness was evaluated by use of Magnitude Estimation method. Specimens were made of a uniform material, a uniform white and different texture. These textures were molded from 10 kinds of building finishing materials and 4 kinds of artificial materials. A specimen and a reference sample were presented simultaneously on the black table in the darkroom. The reference sample was a sand-coat paper. The specimen and the reference sample were illuminated by 45-degree angle, and subject observed them the opposite from 45-degree angle. Subjects were asked to answer the visual roughness of the surface quantitatively compared to that of the reference sample, keeping their hand off the specimen. Subjects were 6 women students, and they tried to evaluate 3 times for each specimen.

2-3. Measurement of surface properties

The surface roughness was measured. The depth of concavity and convexity were measured at 10 points per a specimen by use of a contact type roughness meter. The value of surface roughness was calculated from the peak to valley from these measurements.

The BRDF was also measured in a darkroom. The measuring device consisted of a specimen table at the center of device and two goniometric rotation arms. The light was irradiated towards the center of a specimen, and the luminance was measured at any angles. In this

measurement, the incidence angle was set at -60 degree. The measurement angle was -45 degree to 75 degrees in a 5-degree interval and 60±10 degree in a 1-degree interval.

3. Results and Analysis

3-1 Evaluation index of visual and tactile impression

By a classification of KJ method about the adjectives described in the first experiment on visual and tactile impression, five evaluation criterions were extracted, gloss, roughness, warmth, softness and dryness. The visual impression and the visual-tactile impression consisted of these five criterions, and tactile impression consisted of four criterions except gloss.

3-2 Visual roughness

The evaluation of visual roughness did not vary largely among different individuals with the exception of a flat and smooth surface. The surface without concavo-convex was estimated to be difficult to evaluate its surface roughness.

3-3 Relationship between surface properties and visual roughness

Specimens made from artificial texture had high surface roughness value. The surface of these specimens had deep concavo-convex texture. Specimens with flat and smooth surface showed notably low surface roughness value.

The feature of BRDF can be classified into two main groups. Fine and smooth texture like fabrics showed a tendency which has one slight increase toward the angle of specular reflection. It is considered that this tendency is caused by its orderly delicate texture. Bumpy texture like stuccos showed sharp increase at the specular angle. Specimens made from artificial texture showed the retro-reflection and the influence of masking by the concavo-convex shape of the surface.

3-4 Surface Roughness and subjective visual roughness

In similar concavo-convex shape specimens, the subjective visual roughness related to the measured surface roughness. This tendency was particularly true of different concavo-convex shape specimens. As an overall trend, the visual roughness had a tendency to correlate with the surface roughness. But this tendency was not enough high. The reasons included that the measurement method of the surface roughness in this study did not count the breadth-depth ratio of concavo-convex sufficiently.

4. Conclusion

Two experiments were held to clarify the evaluation index for the visual appearance and the tactile texture and to contribute for a suggestion of the objective evaluation index of visual appearance. The conclusion is as follows.

-In the experiment on the visual and tactile impressions, five evaluation index were extracted, gloss, roughness, warmth, softness and dryness.

-In the experiment on the evaluation of visual roughness, the visual roughness had a tendency to correlate with the surface roughness as an overall trend. And it is considered that the breadth-depth ratio of surface concavo-convex is important as an index for visual roughness.

PO42

SPECTROPHOTOMETRY OF DYNAMIC COLOURS

Viková, M.[1], Vik, M.[1]
[1] Technical University of Liberec, Faculty of Textile Engineering, Liberec, CZECH REPUBLIC
martina.vikova@tul.cz

Abstract

Dynamic colours are sensitive on different stimuli such as UV-VIS radiation, temperature, humidity, etc. Potential application of these systems in industry, fashion and other branches brings problem of its measurement. For example photochromic colours need to be exposed by external light source during measurement. Based on that the special device was developed allowing such kind of measurement

This unique device allows the measure colorimetric and spectral characteristics of colour changeable materials as photochromic sensors and also the fatigue test for the control of colour change stability. This measurement of colorimetric and spectral parameters in comparison together with intensity of UV irradiation allows finding the dependence of colour change on intensity of irradiation and the development the scale for individual visual observation and to evaluate dangerousness of UV irradiation. In this article is described possibility to use different light sources (Xe 450 W and LED 390) for this kind of measurement and also there influence of selected light sources on photochromic effect is discussed. Is evident, there is a problem for future standardization of colour changeable materials measurement.

Keywords: Colour changeable materials, measurement of dynamic colour, fatigue resistance, light sources

References

[1] Viková, M. 2010, in Somani, P.R., editor, *chromic materials, Phenomena and Their Technological Applications*, chapter 15: Methodology of measurement of photochromic materials, Aplied Science Innovation, pp. 137-163

[2] Vik, M. & Viková, M. 2007, *Equipment for monitoring of dynamism of irradiation and decay phase photochromic substances* (in Czech) Czech Patent no.: PV 2007- 858 PS3546CZ, pp. 2-10

[3] Viková, M. & Vik, M. 2007, *Accurate measurement photochromic materials*, 6th International Conference - TEXSCI 2007, June 5-7, Liberec

[4] Klukowska, A., Posset, U., Schottner, G., Jankowska-Frydel, A. & Malatesta, V. 2004, Photochromic sol-gel derived hybrid polymer coatings: the influence of matrix properties on kinetics and photodegradation, *Materilas Science-Poland*, vol. 22, no. 3, pp. 187- 199

[5] Cojocariu, C. & Rochon, P. 2004, Light-induced motions in azobenzene containing polymers, *Pure Appl. Chem.*, vol. 76, no. 7–8, pp. 1479–1497

PO43

A CORRECTION METHOD FOR SKIN REFLECTANCE OBTAINED WITH DIFFERENT SPECTROPHOTOMETERS AND ITS APPLICATION: LONG-TERM CHANGES IN THE SKIN COLOUR OF JAPANESE FEMALES

Kikuchi, K.[1], Katagiri, C.[1], Yoshikawa, H.[2], Mizokami, Y.[3], Yaguchi, H.[3]
[1] Shiseido Global Innovation Centre, Yokohama, JAPAN, [2] Shiseido Co., Ltd., Tokyo, JAPAN,
[3] Chiba University, Chiba, JAPAN
kumiko.kikuchi1@to.shiseido.co.jp

Abstract

It is important to understand the characteristics of a facial skin colour (e.g. the mean and distribution) of targeting population based on accumulation of those data and quantitative evaluation for product design and the provision of service in various fields including cosmetic, fashion, lighting, and imaging fields.

Some previous surveys reveal that the facial skin colour of Japanese females varies across the ages. Compared with that in the early 1990s, the brightness of the skin colour of Japanese females in the early 2000s is confirmed to increase. These long-term changes of facial skin colour are thought to be affected by people's preferences regarding the skin colour and social awareness of UV-induced skin damage in Japan.

However, in the decades after 2000, changes in facial skin colour have been hardly investigated by evaluating them quantitatively.

The aim of this study was to investigate change in the facial skin colour of Japanese females for 25 years by analysing difference in skin reflectance measured with two different types of spectrophotometers.

Firstly, the skin colour on a specific part of a face was measured with two different spectrophotometers (CM-1000RH and CM-2600d, KONICA MINOLTA, Tokyo, Japan), and a correction equation was established for comparing the skin colour data by confirming difference in the output spectral reflectance. Correction equation, which was constructed at each wavelength from 400 to 700 nm with a 10 nm interval, was a linear model to predict the reflectance output from the target spectrophotometer. By regression analysis, the coefficients of the linear model were determined.

Next, the cheek skin colours of approximately 2,000 Japanese females were measured in 2005 and 2015 with CM-2600d, and the data were compared with corrected 1991 data obtained in 1991 and 1992 with CM-1000RH, and 2001 data taken from 1999 to 2002 with CM-1000RH.

Then, two-way analysis of variance (ANOVA) was conducted on each Munsell hue, value, and chroma for understanding the contribution of two factors, which were measurement year and age group.

The results showed that the skin colour of Japanese females shifted to lower chroma and become reddish since 2000. Especially, changes in those of women in their 20s were remarkable.

These results were discussed in terms of changes in the amounts of haemoglobin and melanin components in the facial skin. By multiple regression analysis, the amounts of haemoglobin and melanin were calculated from the spectral reflectance of skin, and changes in those for 25 years were analysed. As possible changing factors for the skin colour, decreases in the amounts of haemoglobin as well as melanin were expected.

Moreover, as a social background, the uses of skin-brighten and UV-care products become more regular cosmetic activity, and it would explain this trend of the skin colour change.

PO44

CONVOLUTION AND DECONVOLUTION OF BSDF DATA TO ENABLE INTER-INSTRUMENT COMPARISON

Audenaert, J.[1], Hanselaer, P.[1], Leloup, F. B.[1]
[1] Light&Lighting Laboratory, Dept. of Electrical Engineering (ESAT), KU Leuven, Gebroeders De Smetstraat 1, B-9000 Gent, BELGIUM
jan.audenaert@kuleuven.be

Abstract

Surface scattering properties can be fully described and defined by the bidirectional scatter distribution function (BSDF), which encompasses both the bidirectional reflectance distribution function (BRDF) as well as the bidirectional transmittance distribution function (BTDF). BSDF describes the amount of light scattered by a surface as a function of the direction of illumination and viewing.

Due to the lack of any standardization with regard to the optical design of BSDF measurement devices, several instruments have been proposed, each of which has been optimized for one or more specific parameters, such as the measurement time, spatial and spectral coverage, absolute measurement capability, etc. In result, the instrument function, reflecting the intrinsic optical features of the device and obtained by scanning the incident light beam in the absence of any sample, can vary significantly.

Experimental BSDF data can be considered as a convolution of the intrinsic BSDF with the instrument function [1]. In practice, this convolution engenders reduced peak values and an angular broadening of the BSDF. For this reason, BSDF functions of the same sample but obtained with different measurement devices will be different. Subsequently, visual attributes of materials, such as gloss, haze and distinctness-of-image, which can be derived from the measured BRDF of the material [2, 3], will also be different depending on the measurement device employed.

Theoretically, a deconvolution can be performed to minimize the effect of the instrument signature in order to reveal the “true” BSDF. It was demonstrated that a Bayesian deconvolution on symmetric BTDF data, obtained under normal incident light yields very good results compared to a matrix deconvolution [4-5]. However, a Bayesian deconvolution requires an early stopping iteration, especially when noise is present in the signal (which is obviously always the case with real measurements). Finding an optimal stopping iteration for non-symmetrical BSDFs has proven to be difficult; as such the application of a deconvolution procedure to obtain the “true” BSDF is still questioned.

In this paper, a method to transform measured BSDFs in order to enable a comparison between BSDF data measured with different instruments is proposed. Assuming two measurement devices A and B, with instrument functions S_A and S_B, respectively, S_B being angularly broader than S_A. The transfer function T_{AB} to convert S_A to S_B can be found by performing a deconvolution on S_B with S_A; $T_{AB} = (S_B * S_A)^{-1}$, with $*$ the convolution operator. The transfer function T_{AB} can afterwards be used to convolve the BSDF obtained with measurement device A, denoted as $BSDF_A$, as if it was measured with measurement device B; $BSDF_{A->B}$. This convolution is expressed as: $BSDF_{A->B} = (BSDF_A * T_{AB})$.

The described method was applied to BRDF data, measured with a home-built BSDF measurement setup [6] in a near-field goniophotometer (NFG) system [7]. While the photometer of the NFG acts as the detector, the sample under test is positioned at the centre of the system. The sample is illuminated using a tungsten halogen light source in combination with a condenser lens and adjustable aperture. The aperture is imaged onto the detector plane using a secondary lens. By adjusting the size of the aperture, the instrument function can be angularly broadened. Three different aperture sizes were selected. The corresponding instrument functions were measured with an angular resolution of 0.1°; the full width at half

maximum (FWHM) of the instrument functions approximately equals 3.2°, 4.4° and 6.2°, for the small (S_s), middle sized (S_M) and large aperture (S_L), respectively.

A high gloss tile from PolyVision [8] was selected as test sample, of which the BRDF was measured with an angular step of 0.1° and light incident at an angle of 30°. The measurement was performed with the three different apertures in place. As such, three BRDFs ($BRDF_S$, $BRDF_M$ and $BRDF_L$) were recorded. Indeed, as the instrument function becomes angularly broader, the measured BRDF also broadens and the peak value diminishes. The FWHM and peak value of the measured BRDF equals 3.7°, 4.8° and 7.6°, and 10.76 sr^{-1}, 8.5 sr^{-1} and 5.3 sr^{-1}, for $BRDF_S$, $BRDF_M$ and $BRDF_L$, respectively.

Next, the transfer functions $T_{S->L}$ (from small to large aperture) and $T_{M->L}$ (from middle sized to large aperture) are calculated, by deconvolution of the instrument function measured with the largest aperture in place with the instrument function with the small and middle sized aperture, respectively.

Finally, $BSDF_S$ and $BSDF_M$ are convolved with $T_{S->L}$ and $T_{M->L}$, respectively, resulting in $BRDF_{S->L}$ and $BRDF_{M->L}$. The FWHM and peak values of $BRDF_{S->L}$ and $BRDF_{M->L}$ now equal 5.5° and 6°, and 5.4 sr^{-1} and 5.4 sr^{-1}, respectively. By performing the described method the difference between $BRDF_{M->L}$, $BRDF_{S->L}$ and $BRDF_L$, with regard to peak value, FWHM, and overall shape, is much smaller than for $BRDF_S$, $BRDF_M$ and $BRDF_L$.

In conclusion, a method has been presented and applied to measured BRDF data, which allows a comparison between measured BRDF data of the same sample obtained on different measurement devices, by performing convolutions on the measured data by aid of determined transfer functions. By applying this method the agreement between results becomes significantly higher.

Acknowledgement

This work has been partially funded by the European Metrology Research Programme (EMRP). The EMRP is jointly funded by the European Commission and participating countries within the European Association of National Metrology Institutes (EURAMET).

References

[1] Stover, J. C., Optical Scattering: Measurement and Analysis 2nd edn, (Bellingham, WA: SPIE Optical Engineering Press),pp. 133–75, 1995.

[2] ASTM D5767 - 95(2012) Standard Test Methods for Instrumental Measurement of Distinctness-of-Image Gloss of Coating Surfaces.

[3] Obein, G., Audenaert, J., Ged, G. and Leloup, F., "Metrological issues related to BRDF measurements around the specular direction in the particular case of glossy surfaces", in *Measuring, Modeling, and Reproducing Material Appearance 2015* (8-12 February 2015, San Francisco), Ortiz Segovia, M., Urban, P., Imai, F. Eds., 2015, art. nr. 12.

[4] Audenaert, J., Leloup, F., Durinck, G., Deconinck, G. and Hanselaer, P., "Bayesian deconvolution method applied to experimental Bidirectional Transmittance Distribution Functions", Measurement Science & Technology, vol. 24, no. 3, 2013, art.nr.035202.

[5] Ferrero A, Campos J., Rabal A. M., Pons A., Hernanz M. L. and Corrons A., “Deconvolution of non-zero solid angles effect in Bidirectional Scattering Distribution Function measurements,” Proc. SPIE 8083, Modeling Aspects in Optical Metrology III, 808315, 2011.

[6] Leloup, F., De Ketelaere, W., Audenaert, J. and Hanselaer, P., "Rapid determination of the photometric bidirectional scatter distribution function by use of a near-field goniophotometer", in *Measuring, Modeling, and Reproducing Material Appearance* , SPIE 2014, pp. 1-8.

[7] Bredemeier K., Poschmann R. and Schmidt F., “Development of luminous object with measured ray data,” Laser+Photonik, vol. 2, pp. 20-24, 2007.

[8] PolyVision: http://nl.polyvision.com/

PO45

ENTROPY VERSUS FRACTAL COMPLEXITY FOR COMPUTER-GENERATED COLOUR FRACTAL IMAGES

Ivanovici, M.[1], Richard, N.[2]
[1] MIV Laboratory, Department of Electronics and Computers, Transilvania University, BRAŞOV, ROMANIA, [2] XLIM Laboratory JRU CNRS 6852, University of Poitiers, 86962 FUTUROSCOPE, FRANCE
mihai.ivanovici@unitbv.ro

Abstract

The notion of *complexity* is shared between various scientific domains, including all the ones associated to the vision or assessment of surfaces, and more particularly of non-uniform surfaces. Nevertheless, it does not exist a unique definition allowing to compare experimentally the perception or sensation induced by the observation of a coloured and textured surface, the measure being available from the existing metrological tools or from digital image processing approaches.

There are various definitions for complexity, the notion of *entropy* being often used as a measure directly linked to the complex aspect of a signal, thus of a texture image or surface. On another scientific path, the notion of *fractal* is associated to the auto-similarity property of a set or signal and it is well adapted for mathematical developments in signal or image analysis as it corresponds to natural structures characteristic to the inner organization of the signal at specific analysis scales. In the context of the CIE TC 8-14 dedicated to the definition and assessment of the spatio-chromatic complexity notion, we are interesting by the theoretical and experimental comparison of the different ways to assess the complexity of a coloured and textured surface.

The goal of this present article is to analyze the dependency between the entropy, computed in various ways, and the fractal complexity of synthetic colour surfaces generated using a fractal model. The desired complexity of the synthetic (computer generated) colour fractal texture images was specified in the generation process.

The notion of entropy was introduced by Shannon [1], in the context of information theory, as a measure of the disorder in signals. The same definition was assimilated by Haralick as one of his thirteen features used for texture characterization [2]. Various other definitions exist. Rényi entropy [3] was introduced as a generalization of the Shannon entropy, Hartley entropy, colision entropy and min-entropy. The Kolmogorov entropy [4] is another generic definition of entropy.

Our experiments were triggered by the statement made by B. Funt & E. Ott in [5] saying that a particular type of entropy (topological or metric) can be used to formulate a generally aplicable defiinition of chaos. Because the standard definitions of these entropies are difficult to implement as numerical procedures, the authors of [5] propose an alternative entropy called expansion entropy. As our pursuit is to identify a general definition of complexity, in the context of colour texture images, we start by analysing various definitions of entropy and to assess their capacity in ranking the complexity of synthetic colour fractal images. We computed two of the most used entropies, i.e. the Shannon and Rényi definitions. We present the measure evolution as a function of the fractal dimension for nine synthetic colour fractal images of varying complexity.

In our experiments, the entropy showed to have a limited dynamic range. Moreover, its dependency with the fractal complexity is not linear, saturation occuring for high complexity colour fractal texture images. The saturation may be a drawback for metrology of texture images exhibiting fractal properties.

References

[1] C. E. Shannon, "A mathematical theory of communication," *The Bell System Technical Journal,* 1948.

[2] R. Haralick, S. K. and H. Dinstein, "Textural features for image classification," *IEEE Transactions on systems, man and cybernetics,* 1973.

[3] A. Renyi, "On measures of information and entropy," in *Proceedings of the fourth Berkeley Symposium on Mathematics, Statistics and Probability*, 1961.

[4] T. D. Pham, "The Kolmogorov-Sinai entropy in the setting of fuzzy sets for image texture analysis and classi," *Pattern Recognition,* vol. 53, pp. 229 - 237, 2016.

[5] B. R. H. a. E. Ott, "Defining chaos," *Chaos,* vol. 25, 2015.

PO46

PHOTOMETRIC AND COLORIMETRIC COMPARISON OF HDR AND SPECTRALLY RESOLVED RENDERING IMAGES

Amdemeskel, M.[1], Soreze, T.[1], Thorseth, A. [1], Corell, D.[1], Dam-Hansen, C.[1]
[1] Department of Photonics Engineering, Technical University of Denmark, Roskilde, DENMARK
mekwub@fotonik.dtu.dk

Abstract

In this paper, we will demonstrate a comparison between measured colorimetric images, and rendered results from a ray trace model. The images are high dynamic range (HDR) and taken with a luminance and colour camera which is mounted on a goniometer. For the comparison, we used a scene similar to the cornel box (CUPCG, 1998) with a spectrally controllable LED light source. Our scene features a colour checker board. The luminance value and colour information of the HDR camera and rendering images will be used for the comparison. The spectral irradiances of the light source, both for warm and cold white lighting conditions, in the box were measured at different locations. Based on these measurements, we have done spectrally resolved renderings. To calculate the colour difference between the camera and rendering images, the most recent CIE metric (CIE2000), was used.

Introduction

The need for accuracy of optical simulation software for rendering is increasing at a very high rate within the graphics industry and within appearance research. This accuracy depends mostly on the sampling of the light source and the modeling of material properties used in the rendering. Although many achievements were obtained regarding physically based rendering within computer graphics during the last couple of decades, challenges persists. Examples of these are: Getting a better representation of the light distribution and a better modeling of the material, and these require further study. Different light sources and materials data have previously been measured and modelled at different institutions for comparison (Greenberg, 1999). However, these generic models do not represent the exact lighting conditions specific to any location; thus creating high levels of uncertainty in the rendering validation processes. Moreover, due to a limited number of measurement points, the generic models do not have enough data to adequately represent luminance variations, such as the rapid changes around the boundaries of light source and at distances away from the light sources inside the box. The Cornel light models include only very limited spectral information (CUPCG, 1998).

Method

Our aim is to compare a model rendering of a limited and controlled scene, with actual measurements using an imaging luminancemeter and colorimeter. The scene consists of a light source in the roof of a cuboid space, with a colour checker on the floor. The walls of the enclosure, except the light source diffuser surface, were painted in the same colour as the neutral 8 (.23 D) of the colour checker board and the spectral reflectance of these surfaces were measured. The light source is a multichannel LED light engine. We have chosen two white lighting conditions: cold colour temperature and warm colour temperature. After setting these conditions, we measured the light output with a spectral irradiance probe. For this measurement, we have used a high end spectroradiometer which has a high signal to noise ratio. By using these measured spectral irradiance data and assuming a lambertian distribution, we have done the simulation of the scene in the absence of colour checker to obtain the total power of the light source on the entire area of the plane. After obtaining the lighting model, the material properties of colour checker board were taken from BabelColor spectral reflectance measurements. Here, we took a lambertian distribution assumption for spectrally resolved reflectance properties. Then, we designed the 3D model of the scene using CAD software and we assigned the material properties of the different parts of the box. The colour checker spectral reflectance properties were also assigned into the CAD software in the same way. Then, the 3D model of the demobox, with all the material properties and light

source, was rendered with the rendering software to compare this modeling with HDR images taken by our imaging luminance and color meter.

Results and Conclusions

The preliminary results of the comparisons between HDR and rendered images were done using colour – luminance difference for both cold and warm white lighting conditions. In the experiment, spectrally resolved rendering was investigated to show how photorealistic images can be obtained in relation to HDR images. The colour difference was calculated with the most recent CIE colour difference approach, CIE2000. These calculations were done by selecting an area of the colour patch first and computing the average of the values included in this area. We compared only colour patches of the same colour or walls of the same colour. It was seen that both lighting condition renderings showed a high similarity to HDR images. But as compared to the warm white illumination, the cold white gave a higher resemblance. The found colour differences were, however, much larger than expected, and we will investigate the sources of these discrepancies.

References

CUPCG, 1998. The Cornell Box [WWW Document]. Website Cornell Univ. Progr. Comput. Graph. URL http://www.graphics.cornell.edu/online/box/

GREENBERG, D.P., 1999. A framework for realistic image synthesis. Commun. ACM 42, 44–53. doi:10.1145/310930.310970

PO47

VISUAL FIDELITY ASSESSMENT OF ARTWORKS IN VIRTUAL REALITY

Pardo, P.J.[1], Cwierz, H.C.[1], Suero, M.I.[2], Felicisimo, A.M.[1], Polo, M.E.[1], Perez, A.L.[2]
[1] University of Extremadura, Merida, SPAIN, [2] University of Extremadura, Badajoz, SPAIN
pjpardo@unex.es

Abstract

Head Mounted Displays (HMD) are experimenting a great development during the last years. This type of device allows immersive experiences in virtual worlds and it would be expected to have many applications, in both fields: recreational and professional. One of the devices that are most strongly expected to enter the market are the Oculus Rift Virtual Reality (VR) glasses. The aim of this paper is to check the accuracy of the visual appearance of real objects captured through a 3D scanner, rendered in a PC and displayed in the latest development kit available (DK2) of the VR device.

Along with the development of HMDs, they have also produced significant advances in rendering techniques following physical models of lighting and shading. Some of these developments are incorporated into the programming platforms providing content to devices such as Oculus Rift. One of these platforms is Unity Game Engine. Unity supports different Rendering Paths and programmers can choose which one to use depending on the game content and the target platform: software and hardware. Different rendering paths have different performance characteristics that mostly affect visual appearance of the rendered scene.

So far, *forward rendering* was the standard rendering technique that most engines use. In this rendering path, the geometry is supplied to the graphics card and this hardware projects the geometry and breaks it down into vertices. Then those vertices are transformed and split into pixels, which get the final rendering treatment before they are passed to the screen. This process is fairly linear, and each geometry is passed down the pipe one at a time to produce the final image.

In *deferred rendering*, as the name implies, the rendering is deferred a short period of time until all of geometries have passed down the pipe; the final image is then produced by applying shading at the end. In Unity 5, this rendering path uses a physical BRDF model with four main components (diffuse, specular, normal, smoothness).

Since the objective of this work is to study the fidelity in the rendering of real artworks in a VR device, the first step has been capturing three dimension real artworks samples. We have used six high quality artworks replica corresponding to different styles and periods (roman bust, amphora, arrowhead, roman vessel, cretan vessel, ax). We have scanned them with a Creaform Go!Scan 20 3D scanner and processed the 3D object model with VXscan and VXelements 4 software.

We have recreated two scenes in Unity Game Engine 5. The first scene simulates a light booth equipped with two light tubes. Each light tube corresponds with a D50 simulator. The second scene simulates the illumination of a museum with spot lights tending a 45º angle. These same two lighting configurations have been used in our real laboratory over the real artwork samples.

Subjective evaluation has been carried out in both environments, real and virtual. Ten observers through a survey based on the Mean Opinion Score scale. This scale is used in subjective assessment of audio and video compression and it has 5 steps comparing the difference between two samples (5. Imperceptible, 4. Perceptible but not annoying, 3. Slightly annoying, 2. Annoying, 1. Very annoying). We have compared *forward rendering* versus *deferred rendering* in real-time computing.

The survey contains six items for each artwork: colour, shading, texture, definition, geometry, chromatic aberration. The first three are directly related to the visual appearance of the scene and the last two to the virtualization technique.

The results indicate greater fidelity in the lighting and shading using the deferred renderer that includes the BRDF model, reaching in some case a rate close to 4 points. Regarding the geometry the achieved score is close to 4. For colour and texture, the results are worse, but can still be considered acceptable, around 3 points. The worst results were obtained regarding the definition and correction for chromatic aberration, with rates close to 2 in some cases.

As conclusion we should indicate that the advances in Virtual Reality made in recent years are significant. The visual quality of the image generated is considerable but it must still be improved especially regarding the density of pixels to avoid the perception of pixelated scene. A higher density of pixels results in a better correction of chromatic aberration especially at the edges of objects.

PO48

GENERAL ASPECTS OF THE SPECTRAL OPTIMIZATIONS OF MULTICHANNEL HYBRID LED-LUMINAIRES ON COLOUR FIDELITY, COLOUR PREFERENCE, COLOUR MEMORY AND SATURATION ENHANCEMENTS

Trinh, Quang Vinh[1], Tran, Quoc Khanh[1]
[1] Laboratory of Lighting Technology, GERMANY
vinh@lichttechnik.tu-darmstadt.de

Abstract

The colour quality of solid state lighting is an interesting and necessary theme to research and develop. Herewith, there are two approached aspects, the desired colour quality and their realization in applications. The colour quality is approached nowadays not only on traditionally colour fidelity, but on essentially updated factors of colour preference, colour memory and colour saturation. Consequently, the realization with the channel number, the appropriate peak wavelength combination, LED type coordination, digital quantization and their optimization should be satisfied with philosophical studies and correspondingly experiential investigation. This paper will present the essential aspects of spectral optimizations and supply important optimized results for solid state luminaires.

PO49

DEFINING THE EFFECTIVE LUMINOUS SURFACES IN THE UNIFIED GLARE RATING

Scheir, G.H[1], Hanselaer, P.[1], Ryckaert, W.R.[1]
[1] KU Leuven – ESAT – Light&Lighting Laboratory, Ghent, BELGIUM
Gertjan.scheir@kuleuven.be

1 Objective

Discomfort glare is defined by the International Commission on Illumination (CIE) in the international lighting vocabulary as: “glare that causes discomfort without necessarily impairing the vision of objects” (CIE, 1987). In Europe, the CIE proposed the Unified Glare Rating (UGR) (CIE, 1995) for the assessment of discomfort glare in interior lighting.

The applicability of UGR for non-uniform light sources is under discussion, most recently in Tashiro et al. (2015). The UGR only includes an average luminance level obtained from the luminous intensity distribution ignoring any non-uniformity in luminance distribution. With a growing market share of highly non-uniform LED luminaires for interior lighting, a valid assessment of visual discomfort becomes essential.

The CIE addition for the UGR formula for small, large and complex sources (CIE, 2002) focus on extending the UGR formula and complicate the UGR method by introducing ambiguous parameters. As an alternative, the UGR calculation from luminance maps can elegantly be refined by grouping pixels according to their luminance level (Scheir et al., 2015).

The present study describes a luminance boundary to discriminate between background and light emitting part of a luminaire. Where the standard considers the total projected luminaire size, the refined UGR only includes the area with a luminance level above a luminance boundary. The refined UGR method is validated with a paired comparison experiment encompassing commercially available recessed office luminaires.

2 Method

2.1 UGR calculation

The UGR is the standard discomfort glare metric in Europe. Each luminaire in the field of view corresponds to a term in the UGR formula and is characterized by one average luminance level, one position index and one solid angle. The average luminance level is calculated by dividing the luminous intensity in the direction of the observer’s eye by the apparent size of the luminaire. The luminance distribution or luminaire shape is totally ignored

To define the luminous surface in a luminaire, a luminance boundary is introduced. According to the IES (IES, 1973), areas with a luminance level above 500 cd/m² to 750 cd/m² are considered as luminous elements. In the refined UGR, only the luminous pixels from a luminous map are considered. Pixels below the luminance threshold are classified as background and are omitted in the refined glare calculation. The luminous pixels are per luminaire collectively treated as one light source and one term in the refined UGR calculation, disregarding whether they are connected. The luminance level of the group is the average luminance of all luminous pixels in the group. The solid angle is the sum of solid angles of all pixels in the group. The group position index is a weighted average of each pixel position index with its luminance level.

2.2 Experimental setup

The refined UGR method is validated with a paired comparison (PC) experiment involving 8 samples of 60 cm by 60 cm recessed office luminaires. Visual discomfort was rated by 16 naïve observers for a total of 56 pairs with a background luminance level of 10 cd/m². Observers were asked to look directly into the luminaires.

Luminance maps were measured with a LMK Labsoft luminance camera from TechnoTeam with a total reported error of 2.8 %. Intensity distribution patterns for the standard UGR calculation were copied from the manufacturer's website or measured with a near-field goniometer.

3 Result

The coefficient of determination between the subjective comfort and the standard UGR is significant ($R^2 = 0.44$) but smaller compared to the refined UGR ($R^2 = 0.80$). By omitting dark areas in the refined UGR, the solid angle decreases and the average luminance level increases. The quadratic relation with luminance level dominates the linear relation with solid angle resulting in a higher refined UGR value compared to the standard UGR. Since non-uniform sources produce more discomfort glare than uniform sources (Tashiro et al., 2015), the systematic increase in refined value for non-uniform sources explains the higher correlation for the refined UGR compared to the standard UGR.

For the refined UGR calculation, contrary to previous extensions of UGR (CIE, 2002), there is no need for fitting nor adding of extra parameters. Only a reconsideration of the luminous area, as already proposed before the UGR was developed (IES, 1973) but apparently ignored in the standard UGR method (CIE, 1995), elegantly ameliorates the refined UGR method as prediction index for visual discomfort.

Although the refined UGR performs satisfactory better than the standard UGR, it is a phenomenological model and lacks any physiological or psychological justification. The refined UGR method should be perceived as a temporary but necessary step in anticipation of a more comprehensive physiological model for visual comfort.

4 Conclusion

The refined UGR has been elegantly calculated from a luminance map by grouping pixels according to their luminance level. Where the standard UGR takes the total projected area into account, a luminance boundary of 750 cd/m² defines the effective luminous surface in the refined UGR calculation. A PC test encompassing commercially available recessed office luminaires validated the refined UGR method. With a coefficient of determination of 0.44, the standard UGR fails. The refined UGR, with a coefficient of determination of 0.80, elegantly ameliorates the visual discomfort predictability in anticipation of a more comprehensive physiological model.

References

CIE 1987. *International Lighting Vocabulary,* Vienna, CIE.

CIE 117:1995. Discomfort Glare in Interior Lighting, CIE.

TASHIRO, T., KAWANOBE, S., KIMURA-MINODA, T., KOHKO, S., ISHIKAWA, T. & AYAMA, M. 2015. Discomfort glare for white LED light sources with different spatial arrangements. *Lighting Research and Technology,* 47**,** 316-337.

CIE 147:2002. Glare from Small, Large and Complex Sources, CIE.

SCHEIR, G. H., HANSELAER, P., BRACKE, P., DECONINCK, G. & RYCKAERT, W. R. 2015. Calculation of the Unified Glare Rating based on luminance maps for uniform and non-uniform light sources. *Building and Environment,* 84**,** 60-67.

IES 1973. RQQ Report No. 2 (1972). *Journal of the Illuminating Engineering Society,* 2**,** 328-344.

PO50

COLORIMETRIC PROPERTIES OF LED ILLUMINATED ROADS STUDIED BY IN-FIELD MEASUREMENTS AND SIMULATIONS

Hsu, S.-W.[1], Wu, K.-N.[1], Hung, S.-T.[1], **Chen, C.-H.**[1]
[1] Center for Measurement Standards, Industrial Technology Research Institute, Hsinchu, CHINESE TAIPEI
SWHsu@itri.org.tw

Abstract

Objective

LED road luminaire is rapidly maturing to be ready for new light source for expressway or freeway. For safety and comfort of drivers, it is important to understand the colorimetric properties of the LED illuminated roads, such as spectral irradiance ($E_r(\lambda)$), colorimetric coordinates (u', v'), correlated colour temperature (CCT), and colour rendering index (CRI or CQS). The distributions of these colorimetric parameters over the roads are especially concerned. In this work, in-field measurements and analysis of a LED illuminated expressway and an experimental road in Taiwan were carried out to study their colorimetric properties. In addition, simulated colorimetric parameters of the experimental road form the spectral radiant intensity of the LED luminaires were also obtained and compared.

Methods

The sampling and measuring processes for the in-field measurements were mainly referred to the CIE-140, CIE-194, and EN-13201 standards. The spectral irradiances of the LED illuminated roads were measured by a commercial spectrometer. The measured spectra were corrected to obtain more accurate colorimetric parameters. The images of tri-stimulus (X, Y, Z) of the roads were captured by a calibrated DSLR with 70 mm focal length, and were analysed according to the definition of calculation points in CIE-140 with acceptance angle of 0.1 degree. The corresponding parameters of (u',v'), CCT, CRI and CQS were calculated with the familiar formulae. To derive the colorimetric dispersion du'v', distribution of (u', v') of a road is used to calculate the covariance matrix (**S**), and then the eigenvalues (λ_1, λ_2) and vectors (V_1, V_2) of **S** are also obtained. The product of square root of sum of the eigenvalues with coverage factor k is defined as du'v'. In general, k is selected as 1.96 for level of confidence of 95 %. The ellipse with center at average of (u', v') and axes along the eigenvectors draws the range of the distribution of (u', v') of the road.

Results

The LED luminaires were mounted at a 4-lane expressway with staggered arrangement. The height of the luminaires, width of each lane, and distance between the luminaires are 12 m, 3.7 m, and about 60 m, respectively. The other experimental road is 2-lane with single-side arrangement of lightings. The height of the luminaires and distance between them are adjustable for farther researches, and the width of each lane is about 3.9 m. The luminous efficiency of the LED luminaires in this work are all higher than 110 lm/W, and the average CCT of them are around 3000 K within five MacAdam circle.

By calculations with their spatial and spectral radiant intensities, the du'v' of a model of luminaire is above 0.013, which seems unacceptable for used as road lighting. However, both measurements and simulations on the experimental road lighted by the luminaire show that the du'v' obtained from the spatial $E_r(\lambda)$ are around 0.006, which is relatively smaller and acceptable. The major axes of the ellipses of the (u', v') distributions are roughly parallel to v'-axis, that may be originated the yellow-blue dispersion of the white LED components. The average CCT of the experimental road obtained from the images of tri-stimulus is about 2900 K. It is smaller than that found by spectral irradiance of 3000 K. Because the spectral reflectance of the asphalt pavement is relatively higher in the long wavelength region, the

above feature is reasonable. The distribution of (u' v') of the reflected lights is also shifted to the yellowish region with relatively smaller du'v' of 0.0041.

For the LED illuminated expressway, the shapes and locations of the ellipses confining the distributions of (u', v') are quite dependent on the models of luminaire. The du'v' is varied from 0.005 to 0.011, which would be used to classify the colorimetric quality of these types of luminaire in practical applications. The spatial distributions of CRI and CQS of the tested expressway are all higher than 70, and the CQS is higher than CRI with value of about 2~3. Additionally, the Pearson's correlation coefficient of 0.88 between CRI and CQS of this expressway presumes that the preferred colour rendering index for LED road lighting may be any one of them.

Conclusions

In summary, we have evaluated the spatial dependent colorimetric parameters on a LED lighted expressway and an experimental road by both in-field measurements and simulations. Based on the theory of multivariate normal distribution, we have defined the colorimetric dispersion du'v' and corresponding ellipse to analyse the measured and simulated results. The du'v' is successively influenced by model, distance, and height of the luminaires. The highly correlated colour rendering indexes of CRI and CQS are above 70 for all measurements. These practical results were expected to provide as references for the design and construction of LED lighted roads.

PO51

ARTIFICIAL VISION: WHY IS COLOUR HDR VIDEO NEEDED?

Or, K.H.[1]
[1] Eye Surgeon, Private Office, Istanbul, TURKEY
hilmi.or@gmail.com

Abstract

Aim: To show the similarities and dissimilarities of HDR to human visual perception, and to discuss the advantages and disadvantages of HDR imaging for achieving optical data for prosthetic vision.

Materials and Methods. The two ways of HDR imaging to achieve high dynamic range, the human visual perception due to Yarbus, the comparison of human visual perception with machine vision, the lack of eye movements for vision enhanching in extraocular sensors for prosthetic vision are discussed.

Results. The HDR imaging is more close to human visual perception than traditional digital imaging. Similarities with human visual perception allow the HDR images to be used as basic data for electrical transmission to retina . The disadvantages of HDR are the highly software dependent system and its transmission HDR imaging have both sensitivity problems because the data of many megapixels in imaging are transmitted to a limited number of electrodes in retina. In addition to these the artificial sensors cannot change their sensitivity as much as the human retina.

Discussion. Using HDR technology results in images which are closer to human visual perception than traditional imaging. The knowledge of the techniques used in prosthetic vision by ophthalmologists may contribute to better understanding and further improvement of vision simulating techniques.

Acknowledgment. This work has no financial support from any institution.

PO52

COLOUR VISION PERCEPTION: A TRIAL TO UNDERSTAND HOW THE CHANGE IN COLOUR PERCEPTION HAPPENS IN "#THEDRESS" PHENOMENON

Or, K.H.[1]
[1] Eye Surgeon, Private Office, Istanbul, TURKEY
hilmi.or@gmail.com

Abstract

Aim: The visual perception is individual. Colour perception is also individual. “#thedress” is a digital photo of a dress, which is taken occasionally. Some people see the dress golden-white and the others blue-black on the screen. Science still couldn’t explain how this happens. There is also a change in the perception of some people, if they look at the dress for the second, third, fourth time etc. Methods: The visual perception explanation of Yarbus combined with the physiologic sharpness of the “normal” vision in the visual field results in tiny spots of visual perception with high visual sharpness. So one sees a small area which can be only seen in a certain colour. The enviromental colour contrast in the small areas of the six fixation points due to Yarbus, is dependent from the colour contrast of the pixels around the main six pixels. With the propable change of the fixation pixels due to Yarbus model, the contrasting pixels change also. So the entire colour perception may change. Results: The colour perception change in #thedress may be due change in fixation pixels after the first “look”, and the conrast around the fixation pixels change also. This may be the reason of the change in the colour perception of #thedress.

PO53

EFFECTS OF CHROMATIC COLOUR LIGHTING ON WORK EFFICIENCY

Takahashi, H., Uetsuhara, T., Kohama, S.
Kanagawa Institute of Technology, Atsugi, JAPAN
htakahashi@ele.kanagawa-it.ac.jp

Abstract

1 Introduction

The use of LED lighting has become widespread. LED light sources are manufactured in the primary colours of red, green, and blue, and are able to reproduce most chromatic colours. Chromatic colour lighting is considered to have physical and psychological effects on humans. Therefore, the aim of this study is to investigate the work efficiency affected by chromatic colour lighting.

2 Experiment

In this experiment, a 500 lx LED light source and various coloured films were prepared in order to illuminate an experimental work environment. White, red, green, blue, yellow lighting were used in this experiment. Eight male participants are asked to perform six different tasks. Thinking task 1 is solving a Sudoku puzzle, in which players input numbers from one to nine into a grid consisting of nine squares, subdivided into a nine smaller squares, with the goal of ensuring that every number appears once in each row, column, and square. The work efficiency is the measured time needed to finish the puzzle. Creative task A is creating a new application task. The participant is given a topic and is asked to suggest many ideas in 3 minutes. Creative task B is a “predict results” task, in which the participant is given an impossible situation as a topic and asked to suggest many ideas on the predicted results in 3 minutes. The concentration task is making a card tower. The participant makes a three-stage card tower and the time needed is measured. Thinking task 2 is a crossword puzzle. Work efficiency is measured by the number of answers per minute. Subjective evaluation tasks are evaluated by the semantic differential (SD) method.

3 Results and Discussion

One-factor analysis of variance (ANOVA) was performed in this study. The factor was light colour and multiple comparisons were performed by using Fisher’s least significant difference (LSD) method. Analyses were conducted to determine significant differences between the white light and the other colours. As a result of thinking task 1, the yellow light had the shortest finishing time of all the colours, including the white light. As the results of thinking task 2, the white light had the highest score among all the colours, and the yellow light also had a high score, which was almost the same as the score for the white light. These results suggest that white and yellow lighting are considered to be suitable for thinking work.

In this study, creativity is evaluated by fluency, flexibility, uniqueness, concreteness. The fluency was evaluated by the number of participant’s answers. The flexibility was evaluated by categorization. Each topic was divided into categories, and the answers of the participant were evaluated relative to the number of categories. The uniqueness was evaluated by the number of participant’s original answers. The concreteness was evaluated by the number of participant’s specific answers. The green light is suitable for creative task A (creating a new application task) because this colour had the highest scores of fluency, flexibility and concreteness among all the colours. This result suggests that green lighting is suitable for a meeting, such as a brainstorming meeting. Moreover, the white light might be suitable for creative task B (predict results task) because this colour had the highest scores of fluency, flexibility and uniqueness among all the colours. White lighting might be suitable for a meeting, such as a meeting to predict an outcome. Furthermore, red lighting might not be suitable for a concentrative work because this colour had the longest finishing time to make a card tower among all the colours. As the results of subjective evaluation tasks, all evaluation scores for

the white and yellow light were positive. Many of the evaluation scores for the red light were negative, and many of the evaluation scores for the green and blue light were positive. These results suggest that red lighting is impractical.

4 Conclusion

In this study, the effects of a chromatic colour lighting environment on work efficiency were investigated. The results are summarized as follows:

(1) White and yellow lighting are suitable for thinking work.

(2) Green lighting is suitable for creative work.

(3) White lighting might be suitable for predicting the outcome of work.

PO54

HUE PERCEPTION OF NEAR-WHITE LIGHTINGS AROUND 5000 K

Oh, S.[1], Kwak, Y.[1], Ohno, Y.[2]
[1] Ulsan National Institute of Science and Technology, Ulsan, SOUTH KOREA
[2] National Institute of Standards and Technology, Gaithersburg, Maryland, USA
yskwak@unist.ac.kr

Abstract

The colour of the lighting can affect the atmosphere of the space. Therefore, for the effective lighting design, colour appearance of the lights needs to be predicted, which will be changed by the adaptation condition of the human eye. In this study, hue perceptions of the near-white lightings were investigated after the subjects' eyes were adapted to 5000K.

The psychophysical experiment was carried out in a dark room using 5 channels LED lighting booth. The inside of the booth is painted in mid-grey colour as Munsell N7 and the channels consist of red, green, blue, warm white and cool white. Total of 48 test lightings around 5000K were generated using the LED lighting booth. Illuminance of the colours was fixed to 3450lx.

At first, each subject was adapted to the reference lighting having 5000 K. Then a test lighting was shown for hue judgement followed by the reference lighting for 10 seconds. For hue estimation, major colours were asked among red, green, yellow and blue. If a colour was seemed as the mixture of two, two could be selected and one was decided as a dominant colour. For each subject, the order of test lightings was randomized. In total, five subjects participated the experiment and all of them repeated the experiment twice. All subjects' responses were averaged for data analysis.

The experimental results showed that unique yellow-blue colours are closely located around the Plankian locus while unique red-green colours roughly follow the line orthogonal to the Plankian locus in u'v' colour space.

When the visual data is compared with CIECAM02 prediction, it is found that green-to-blue range colours in CIECAM02 are perceived as mostly blue colours.

This experimental result indicates that new colour appearance model for the lighting applications is needed.

EVERFINE

Make every customer more satisfied

Color and Visual Appearance Measurement Instruments

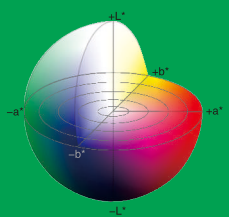

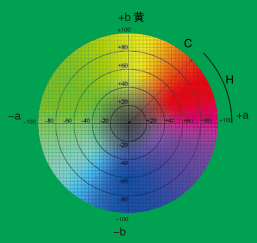

HACA-3000 High Accuracy Color Analyzer

EVERFINE is leading in the LED & lighting measurement instruments worldwide. Based on the accumulated technology in light detection, and through years of R&D, we are proud to promote series of color and visual appearance measurement instruments which feature high accuracy and repeatability. The products include fundamental systems for quantity generation & traceability, instruments for lab applications and portable ones for quick check.

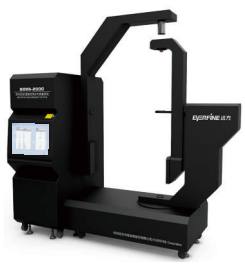

BBMS-2000 BRDF/BTDF measurement system

HAM-300 Spectral Haze Meter

TR-5000 UV-VIS-IR T&R Test System

PSC-20/30 spectrophotometer

More ☞ www.everfine.net

EVERFINE Corporation (Stock Code:300306)

Tel: +86 571 86698333 (30 lines) Fax: +86 571 86696433 E-mail: global@everfine.net Add: #669 Binkang Road, Binjiang National Hi-tech Park, Hangzhou, China